l'université nantes angers le mans
PÔLE DE RECHERCHE ET D'ENSEIGNEMENT SUPÉRIEUR

UNIVERSITÉ DE NANTES

Thèse de Doctorat

Kyle D. FINK

Mémoire présenté en vue de l'obtention du
grade de Docteur de l'Université de Nantes
sous le label de L'Université Nantes Angers Le Mans

École doctorale : Biologie Sante

Discipline : Neuroscience
Spécialité : Transplantation
Unité de recherche : *UMR791*

Soutenue le 28 août
Thèse N° : *2013*

Potentiel thérapeutique des cellules souches adultes pour le traitement de la maladie de Huntington

JURY

Rapporteurs :	**Roger ALBIN**, Professeur, University of Michigan **Kathy STEECE-COLLIER**, Professeur, Michigan State University
Examinateurs :	**Timothy COLLIER**, Professeur, Michigan State University
Directeur de Thèse :	**Laurent LESCAUDRON**, Maître de Conférence, Université de Nantes
Co-directeur de Thèse :	**Gary DUNBAR**, Professeur, Central Michigan University

Thèse en cotutelle entre l'Université de Nantes et Central Michigan University

UNIVERSITÉ DE NANTES
FACULTÉ DES SCIENCES ET DES TECHNIQUES

ÉCOLE DOCTORALE Biologie Sante

Année 2013

Potentiel thérapeutique des cellules souches adultes pour le traitement de la maladie de Huntington

THÈSE DE DOCTORAT
Discipline : Neuroscience
Spécialité : Transplantation

Présentée
et soutenue publiquement par

Kyle D. FINK

Le 28 août 2013, devant le jury ci-dessous

Rapporteurs Roger ALBIN, Professeur, University of Michigan
Kathy STEECE-COLLIER, Professeur, Michigan State University

Examinateurs Timothy COLLIER, Professeur, Michigan State University

Directeur de thèse : Gary L. DUNBAR and Laurent LESCAUDRON

ACKNOWLEDGEMENTS

I wish to thank the members of the committee: Drs. Dunbar, Lescaudron, Rossignol, Collier, Steece-Collier, and Albin. I also wish to thank the directors of the laboratory at Central Michigan University and at INSERM UMR1064, Drs. Dunbar and Anegon, respectively. I would like to thank the co-directors of my dissertation Drs. Dunbar and Lescaudron. I would like to extend my greatest gratitude to all of the undergraduate volunteers that have worked with me the past five years. Without their passion and dedication to the lab and research this dissertation project would not have been possible. I would also like to acknowledge the fellow graduate students that have assisted me on this work, specifically Andrew Crane who was a good friend and a great researcher to help design and execute these projects. I would like to give my sincere thanks to Dr. Julien Rossignol who taught me many of the techniques and truly jumpstarted my scientific career. Dr. Rossignol took a chance on me early in my graduate studies and gave me the freedom and independence when working with him to conduct interesting and meaningful research. Julien has been a great friend to me in and out of the lab and truly pushed me to succeed as a researcher. I would also like to thank Dr. Lescaudron for presenting me with the opportunity to study under him at the University of Nantes. The opportunities to live and work in a foreign country opened my eyes to the world of research and the requirements to excel in this field. I would also like to thank Dr. Gary Dunbar as he has been one of the largest influences on my career, he sets an unbelievable standard of hard work that I have spent the past five years trying to emulate. Dr. Dunbar has also shown me great deals of trust by allowing me to pursue challenging research projects, grants, publications, and allowing me to travel to many conferences to present our findings. Dr. Dunbar has also played a significant role in shaping the future of my career by consistently taking the time to offer advice and help guide me through my

graduate studies. I have been very fortunate, not only the past five years, but throughout my life to be surrounded by dedicated hard working individuals that set a clear example of how to excel in whatever career you pursue. Two of these major influences were my father and my grandfather. Both of these men taught me never to take shortcuts and to perform every task with due diligence and to truly take pride in my work. Both of these men shaped my life at an early age and were extremely supportive throughout my career. Sadly, my grandfather did not live to see me fulfil my goal of completing my Ph.D., but without his mentorship it is unlikely that I would be in the place I am today. Lastly, I need to acknowledge my loving wife, who understood the demands of graduate school, and appreciated the value of the research we were conducting. She served a very influential role of hearing me vent frustrations and bounce ideas and theories off her. Again, I would like to thank everyone that was involved in these studies over my graduate career. Finally, I wish to acknowledge the support of Central Michigan University and the University of Nantes in producing this work.

ABSTRACT

POTENTIAL OF ADULT STEM CELLS
FOR TREATING THE BEHAVIORAL AND
NEUROLOGICAL DEFICITS IN RODENT
MODELS OF HUNTINGTON'S DISEASE

by Kyle D. Fink

The goal of this doctoral dissertation was to compare the potential therapeutic effects of transplanting various types of adult stem cells into the striata of R6/2 transgenic mice or rats given 3-nitropropionic acid (3-NP), which are commonly-used rodent models of Huntington's disease (HD). It was observed that transplants of mesenchymal stem cells (MSCs), isolated from bone-marrow and, to a more limited extent, umbilical cord blood, reduced behavioral and neuropathological deficits in R6/2 mice. It was hypothesized that these stem cell transplants exerted their beneficial effects through the release of neurotrophic factors and/or anti-inflammatory cytokines, rather than via cell replacement. In addition, it was found that intrastriatal transplants of induced pluripotent stem cells (iPSCs) reduced behavioral and neuropathological deficits in 3-NP-treated rats. In this latter study, it was observed that the iPSCs were able to differentiate into cells with region-specific neuronal phenotypes. It was hypothesized that mechanisms, other than primarily providing trophic support, may underlie the recovery observed in this second group of studies. Taken together, the results from these five studies suggest that adult stem cells hold significant therapeutic potential for reducing behavioral deficits in HD.

L'objectif de ce travail de thèse dans le domaine de la Médecine Régénératrice a été d'étudier les effets d'une transplantation de 2 types de cellules souches adultes dans des deux modèles rongeurs de la maladie de Huntington. Pour se faire, des techniques de culture cellulaire et de biologie cellulaire et moléculaire ainsi que différents test comportementaux ont été mis en

œuvre. Les résultats ont révélé que les cellules souches mésenchymateuses (MSCs) obtenues à partir de moelle osseuse, ou de cordon ombilical (mais dans une moindre mesure), ont permis d'améliorer les déficits comportementaux et neuropathologiques observés chez des souris transgéniques modèle de la maladie de Huntington par rapport aux animaux non traités. Cependant, les effets bénéfiques des MSCs semblent plutôt être attribués à leur sécrétion de facteurs neurotrophiques dans l'environnement lésé qu'à leur trans-différenciation neuronale. Parallèlement, l'utilisation des cellules souches pluripotentes induites (iPSCs) dans le cadre d'une intervention thérapeutique dans un modèle de lésion toxique de la maladie de Huntington (3-NP) a également été étudiée chez le rat. Ainsi, après transplantation d'iPSCs, les animaux ont présenté une amélioration comportementale et neuropathologique significative. Le mécanisme de récupération de ces animaux après transplantation d'iPSC a été, cette fois-ci, attribué à la différenciation neuronale des cellules implantées, et non à leur production de facteurs neurotrophiques. Les résultats de ces deux études suggèrent de manière encourageante que les cellules souches adultes pourraient être utilisées comme traitement de la maladie de Huntington dans le futur.

TABLE OF CONTENTS

LIST OF TABLES

TABLE PAGE

LIST OF FIGURES

FIGURE PAGE

FIGURE PAGE

FIGURE PAGE

DEFINITION OF TERMS

HD-	Huntington's disease
HTT-	Human huntingtin protein
MRI-	Magnetic Resonance Imaging
mRNA-	Messenger Ribonucleic acid
GABA-	gamma-Aminobutyric acid
NMDA-	N-methyl-D-aspartate
ATP-	Adenosine Triphosphate
BDNF-	Brain-derived Neurotrophic Factor
UHDRS-	Unified Huntington's disease Rating Scale
NSC-	Neuronal Stem Cell
BM-	Bone Marrow
MSC-	Mesenchymal Stem Cell
ESC-	Embryonic Stem Cell
iPSC-	Induced Pluripotent Stem Cell
YAC-	Yeast Artificial Chromosome
KI-	Knock-in
3-NP-	3-Nitropropionic Acid
QA-	Quinolinic Acid
NMDAr-	N-methyl-D-aspartate receptor
BAC-	Bacterial Artificial Chromosome
htt-	rodent huntingtin protein

SORT-	Spatial Operant Reversal Task
WT-	Wild-Type
GDNF-	Glial-derived Neurotrophic Factor
EGF-	Epidermal Growth Factor
DMEM-	Dulbecco's Modified Eagle Medium
NGF-	Nerve Growth Factor
NeuN-	Neuronal Nuclei
DARPP32-	Dopamine and cyclic-AMP regulated phosphoprotein of 32 kDa
UCB-	Umbilical Cord Blood
HLA-	Human leukocyte antigen
RNAi-	Ribonucleic acid interference
shRNA-	Short Hairpin Ribonucleic acid
CNTF-	Ciliary Neurotrophic Factor
MSC Medium-	αMEM, 10% FBS, 10% HS, 1% Penicillin/Streptomycin
αMEM-	Alpha Minimum Essential Medium
FBS-	Fetal Bovine Serum
HS-	Horse Serum
ICC-	Immunocytochemistry
cDNA-	Complementary Deoxyribonucleic Acid
PCR-	Polymerase Chain Reaction
GAPDH-	Glyceraldehyde 3-phosphate dehydrogenase
TTF-	Tail-tip Fibroblast

HBSS-	Hank's Balanced Salt Solution
MWM-	Morris Water Maze
i.p. -	Intraperitoneal
GFAP-	Glial Fibrillary Acidic Protein
CYO-	Cytochrome Oxidase
DAB-	3, 3'-diaminobenzidine
TrkB-	Tyrosine Kinase receptor B
TNFα-	Tumor Necrosis Factor Alpha
LN-	Lentivirus
AD-	Adenovirus
OKSM-	Oct4, Klf4, Sox2, c-Myc
OKS-2A-	Oct3/4-2A-Klf4-2A-Sox2 shuttle vector
Fibroblast Medium-	DMEM, 10% FBS, 1% Penicillin/Streptomycin
dREF-	Deactivated Rat Embryonic Fibroblast
iPSC Medium-	DMEM, 15% FBS, 1% nonessential amino acids, β-mercaptoethanol , and 1%penicillin/streptomycin
SSEA3-	Stage-specific Embryonic Antigen 3
SSEA4-	Stage-specific Embryonic Antigen 4
Oct4-	Octamer-binding transcription factor 4
Neural Induction Media-	DMEM:F12 supplemented with 5% B27, 5% MEM non-essential amino acids, and 1mg/mL Heparin
NCAM-	Neural Cell Adhesion Molecule

ANOVA- Analysis of Variance

PLSD- Protected Least Significant Difference

CHAPTER I

INTRODUCTION TO THE PROBLEM

Huntington's disease (HD) is an autosomal dominant disorder caused by an expanded and unstable CAG trinucleotide repeat that causes a progressive degeneration of neurons, primarily in the putamen, caudate nucleus, and cerebral cortex (The Huntington's Collaborative Research Group, 1993). The HD locus was one of the first diseases to be mapped and characterized as a true dominant genetic disorder (Albin 1995). In the United States, there is estimated to be approximately 30,000 individuals with HD, while Europe has a slightly higher prevalence of individuals with symptomatic HD with an estimated 45,000 patients (Shoulson & Young, 2011). The symptoms of HD have been described as early as the fourteenth century, when it was also known as Saint Vitus's dance or dancing plague (Túnez, Tasset, Pérez-De La Cruz, & Santamaría, 2010). The disease was first described by Charles Waters as a convulsive disorder, but in 1872 George Huntingtin formally described it for the first time and referred to it as a hereditary chorea [(Huntington, 1872) reprinted in (Huntington, 2003)].

CHAPTER II

REVIEW OF THE LITERATURE

Neuropathology of Huntington's disease

HD occurs when the gene that codes for the huntingtin (HTT) protein, located on the short arm of chromosome 4, contains an increased number of CAG repeats (Estrada Sánchez, Mejía-Toiber, & Massieu, 2008). Mutant HTT contains an elongated N-terminal site characterized by numerous glutamine repeats. Typically, adult onset of HD occurs when there are more than 38 CAG repeats correlates with an onset of the illness in adulthood, although there is a more rare, juvenile form of the disease in which the glutamine repeats are greater than 60. The disease progresses slowly, with most patients presenting with clinical features in adulthood, and the remarkable clinical variation, even in affected members of the same family, stems directly from the size of the dynamic repeat expansion (Paulson 2011). HD in adults is characterized by cognitive impairment and psychiatric disturbances, such as irritability, aggressiveness and depression, which precede involuntary motor disturbances (Estrada Sánchez et al., 2008; Southwell, Ko, & Patterson, 2009), which eventually culminates in death around 15-20 years after the onset of motor symptoms.

Historically, the neuroanatomical changes in the striatum have been the focus of neuropathological and neuroimaging studies, but more recently, the presence of abnormalities throughout the cerebrum, including cortical thinning and decreased white matter volumes, especially in the prefrontal cortex, have gained significant interest (Stout et al., 2007). An area where some of the earliest anatomical changes can be observed is in the loss of striatal afferents in the globus pallidus, which degenerates in an age- and disease-dependent manner (Younes,

2012). Striatal atrophy as well as white matter loss, as measured by magnetic resonance imaging (MRI) studies, can detect HD-like degeneration 15 years prior to the onset of motor symptoms (Aylward et al., 2003; Tabrizi et al., 2009) suggesting that once the clinical onset of motor symptoms appear, significant striatal loss has already occurred. While the striatum seems to be the area most affected by the mutated allele, northern blot analysis has shown that HD messenger ribonucleic acid (mRNA) is expressed in non-neuronal tissue evenly throughout the body (Strong, 1993). HTT is ubiquitously expressed in the cytoplasm of neurons throughout the brain, a direct pathway from the genetic mutation to neurodegeneration has not been found. While the exact function of HTT is still unknown, it is thought to play a role in intracellular transport, autophagy, transcription, mitochondrial function, and signal transduction (J. Lee, Hwang, Kim, Kowall, & Ryu, 2013). The cause of specific sensitivity of neurons in the basal ganglia is still a major question in HD. If the sensitivity of these neurons to the genetic mutation is caused by purely intrinsic factors (cell-autonomous toxicity) or if the mutant HTT acts in other cell types (non-cell-automous toxicity) that contribute to the vulnerability of these neurons (C. Y. D. Lee, Cantle, & Yang, 2013). The mutant HTT inhibits fast axonal transport and destabilizes microtubules within the cell, which may play a role in why the mutant form triggers pathological cascades of cell loss through a "gain of function"(J. Lee et al., 2013). Loss of medium spiny neurons occurs early in the disease onset and is likely due to alterations of cellular pathways that make these neurons more susceptible to generic stresses, leading to neuronal damage and death (J. Lee et al., 2013).

Due to the discovery of the HD gene in 1993 (The Huntington's Collaborative Research Group, 1993), it became possible to test at-risk patients for expanded CAG repeats. DNA testing

is not required for individuals who have developed clinical symptoms of HD or for those who are at risk for HD, but adults may choose to have the testing performed after undergoing genetic counselling (Shoulson & Young, 2011). Testing for abnormal CAG expansion in exon1 of the huntingtin gene for HD is relatively easy, and provides reliable information on gene status, but not necessarily on disease state (O'Keeffe, Michell, & Barker, 2009). Genetic testing for HD has been available since 1993, but the emotional and psychological impact that a genetic diagnosis can have on the patient, as well as on their family members, can be devastating (Coustasse, Pekar, Sikula, & Lurie, 2009). Beginning in 1993, adults who are at risk for HD have had the option to have DNA testing for the disease, but fewer than 10% of at-risk subjects have participated (Shoulson & Young, 2011).

Although HD has a single genetic cause, it has a very complex pathology, with detrimental effects on a wide variety of cellular processes (Southwell et al., 2009). However, it is now recognized that all HD is familial and that only a small percentage of patients presenting with HD arise sporadically with newly expanded CAG alleles (Paulson 2011). The majority of sporadic cases of HD occur from CAG repeat instability when the paternal side is carrying between 27 and 35 CAG repeats, deemed intermediate alleles (Semaka et al., 2013) just below the disease threshold. It was found that new mutations of CAG repeat length occurred in the sperm of with intermediate alleles, with higher repeat lengths (i.e., 35) having the highest risk of a new mutation with expansions occurring more frequently than contractions (Semaka et al., 2013). The most striking neuropathological feature of HD-affected brains is the progressive atrophy of the caudate and the putamen, accompanied by a secondary enlargement of the lateral ventricles (Roos, Pruyt, de Vries, & Bots, 1985). The atrophy and loss of striatal projections in

HD patients occurs in a grade dependent manner (Reiner 1988). Grade 0 HD is characterized by a loss of cannabionoid, D2 dopamine and A2a adenosine receptors in the striatum and an increase in the gamma-aminobutyric acid (GABA) binding in the external globus pallidus, grade 1 HD is characterized by substantial loss of striatal projections to the external pallidal segment. Grade 2 HD is characterized by an 80-95% loss of the cannabionoid receptors and a 50% loss of striatal D1 receptors accompanied by an almost complete loss D2 and A2a adenosine receptors from the external globus pallidus. Grade 3 HD is characterized by an almost complete depletion of cannabionoid, D2, and A2a receptors with only 30% of striatal D1 receptors remaining. In grade 4 HD, the number of receptors and intracellular signalling markers are greatly reduced in the striatum and there is close to a total loss of all the striatal projection systems (Deng 2004). The time-dependant loss of neuronal tissue associated with HD is important to consider when designing therapeutic interventions. Post-mortem analysis of the brain tissue of HD patients reveals a distinct pattern of vulnerability in the striatum. Cholinergic interneurons, as well as somatostatin or neuropeptide Y-containing interneurons in the striatum are relatively spared during the disease progression, while the projection neurons, specifically those projecting to the external globus pallidus, are affected early in the disease progression (Albin, 1995; Albin et al., 1992). While it is known that the huntingtin mutation leads to widespread brain neurodegeneration, with cell loss in the striatum and cerebral cortex (Reiner et al., 1988), neuronal abnormalities are also found in many other brain regions (Conforti et al., 2008), and it has been discovered that the mutant huntingtin protein can cause changes in the physiology of neurons by interfering with their transcriptional mechanisms (Borovecki et al., 2005). While the degeneration within the striatum is the hallmark of HD, the rate of cell loss is also not equal for

all striatal neurons and is only relatively selective (Suzuki, Desmond, Albin, & Frey, 2001). Abnormalities in the density of striatal N-methyl-D-aspartate (NMDA) receptors are more prevalent during the course of the disease with presymptomatic HD patients displaying a intermediate decrease in the density of NMDA receptors (Albin et al., 1992). In addition, there is a progressive reduction in striatal binding of type-2 vesicular dopamine terminals over the course of the disease (Bohnen et al., 2000).

Different biochemical studies have also revealed the existence of major defects in the energetic metabolism of HD patients, characterized by mitochondrial dysfunction (Túnez et al., 2010). It is theorize that the mitochondria of HD patients are affected by alterations in electron transport chain function, in which complex II and III are affected, prompting a significant decrease in succinate oxidation and adenosine-5'-triphosphate (ATP) synthesis (Túnez et al., 2010). This phenomenon is associated with cellular damage and neuronal death and plays a crucial role in the neurodegenerative process of HD (Túnez et al., 2010). There are also hypotheses suggesting that disruption in neuronal calcium signalling may contribute to the pathogenesis of HD through mitochondrial disruption (Perry et al., 2010). However this hypothesis is controversial, as post mortem analysis of the striatal tissue in HD patients did not reveal these types of mitochondrial impairments (Powers et al., 2007). It has been discovered that the mutant HTT can cause changes in the peripheral blood by interfering with transcriptional mechanisms (Borovecki et al., 2005). However, the clinical symptoms depend mostly on degeneration of parts of the central nervous system, mainly the basal ganglia and the fronto-striatal loops (Klempír, Klempírová, Stochl, Spacková, & Roth, 2009).

The basal ganglia, the literal translation meaning the base nuclei, is a group of interconnected subcortical nuclei spanning the telencephalon, diencephalon, and midbrain. The seven specific nuclei of the basal ganglia are the caudate, putamen, internal globus pallidus, external globus pallidus, subthalamic nucleus, substantia nigra pars compacta, and the substantia nigra pars reticulata. The striatum is the primary structure of the basal ganglia and consists of two structures in the human brain, the medial caudate and the lateral putamen, plus the ventral nucleus accumbens and is composed primarily of projection neurons that are responsible for automatic execution of learned motor movements (Albin, Young, & Penney, 1989). One of the main functions of the basal ganglia is to provide for strategic planning of coordinated motor behavior and to receive behavioral feedback from the cortex. Many of the goal oriented behaviors involves the complex pathways of the basal ganglia. The different nuclei are connected by a series of direct and indirect pathways. The basal ganglia acts as a mediator of movements, either producing or preventing a planned movement by using opposing parallel pathways. The direct pathway is an inhibitory pathway from the striatum to the internal globus pallidus and substantia nigra reticulata which then project to the thalamus. The indirect pathway is an excitatory pathway from the striatum to the external globus pallidus, from the external globus pallidus to the subthalamic nuclei, and from the subthalamic nuclei to the internal globus pallidus and the substantia nigra reticulata and then to the thalamus. Projections from a set of medium spiny neurons, comprising the direct pathway, of the caudate and putamen to the internal globus pallidus and substantia nigra pars compacta serve to release motor neurons found in the supplementary motor cortices from tonic inhibition. A second population of medium spiny neurons, comprising the indirect pathway, project to the external globus pallidus and the

subthalamic nucleus that project back to the internal globus pallidus and substantia nigra pars compacta which modulate disinhibitory actions of the direct pathway.

Signs and symptoms of HD are dominated by chorea and other involuntary movements in the initial and middle stages of the disease, but it is becoming more evident that HD patients have cognitive deficits starting before clinical diagnoses of motor abnormalities. These cognitive deficits include slowing of psychomotor speed, with impairment of attention and memory, as well as executive and visuospatial functions, that eventually degrade into dementia (Klempír et al., 2009). Although only affecting a small subset of patients with HD, somatosensory deficits have been reported with symptoms ranging from aberrant sensations to shooting pains throughout the limbs (Albin & Young, 1988). The neurological symptoms may be linked to the reduced cortical-striatal trophic support in HD (Zuccato et al., 2001). The loss of motor control is hypothesized to be caused by the selective loss of striatal projections to the external globus pallidus (Albin, Reiner, Anderson, Penney, & Young, 1990) and it appears that there is a preferential loss of striatal neurons projecting to the external globus pallidus early in the course of the disease, followed by loss of neurons projecting to the internal globus pallidus (Albin et al., 1992) and is related to the choric movements observed in HD patients. In the absence of normal inhibitory input from the medium spiny neurons, the external globus pallidus becomes abnormally active, which in turn reduces the excitatory output of the subthalamic nucleus to the internal globus pallidus and the inhibitory effects of the basal ganglia are reduced. When this occurs, neurons found in the motor cortex can be activated by inappropriate signals, which then results in undesired movements (Purves, Augustine, & Fitzpatrick, 2001).

It was found that patients with symptomatic HD and lower levels of brain derived neurotrophic factor (BDNF) serum concentrations had significantly worse motor and cognitive performances than individuals with normal BDNF levels (Ciammola et al., 2007; Conforti et al., 2008). It is known that BDNF is very important for survival and differentiation of striatal neurons and lower BDNF may be a reason why these neurons deteriorate in HD (Conforti et al., 2008). Objective biochemical measures can allow one to monitor the progression of HD, and peripheral BDNF levels may become a potential marker to measure the state of the disease and/or the effectiveness of a given treatment (Conforti et al., 2008). While it has been reported in experimental models of neurodegenerative diseases that deep-brain stimulation, specifically in the subthalamic nucleus, can increase BDNF protein and mRNA levels in the striatum, functional recovery was only observed in the presence of the stimulation (Spieles-Engemann et al., 2011).

Current Treatments for HD

Currently, only symptomatic treatments of HD are available. Pharmacotherapy is difficult in HD, due to the complexity and amount of damage to the brain. Glutamate antagonists, such as riluzole, have gained significant interest as a treatment for the choreic movements associated with HD, but the ability of glutamate antagonists to slow the disease progression is unknown (Rosas et al., 1999). HD patients and the care given to their family members have improved due to the increased recognition of the disorder, better access to genetic counselling, and more availability to specialized care programs that utilize behavioral, neurological, and psychiatric rehabilitation programs (Shoulson & Young, 2011). However, most clinical treatments are aimed at suppressing the choreic movements and not in reversing or curing the disease. Patients

suffering from HD are generally treated with neuroleptics or anticonvulsants to help alleviate some of the symptoms (Sari, 2011). Treatment of HD by supressing catecholamine is widely used to supress the motor abnormalities as it is needed by the brain to initiate and execute movement.

Tetrabenazine is the only U.S. Food and Drug Administration-approved agent for the symptomatic management of HD (Venuto, McGarry, Ma, & Kieburtz, 2012). Tetrabenazine, which depletes vesicular store of catecholamine, has been demonstrated to suppress the severity of chorea and has been linked to an improvement in Unified Huntington's Disease Rating Scale (UHDRS; (Kenney, Hunter, & Jankovic, 2007; The Huntington's Collaborative Research Group, 2006), but the improvement was only observed short term (5-6 hours) correlating with the half-life of the drug. However, in a double-blind, placebo-controlled, dose-ranging trial, the patients receiving tetrabenazine displayed a worsening of chorea following a 1-week washout period (The Huntington's Collaborative Research Group, 2006). In addition to its potential for exacerbating the symptoms and the inability of this drug to prevent degeneration of striatal medium spiny neurons, administration of tetrabenazine involves a complicated prescribing process, specialty pharmacies for delivering the drug, strictly managed doses, and annual costs exceeding $70,000, which makes the drug prohibitively expensive for many patients (Venuto et al., 2012). Neuroleptic drugs, such as fluphenazine or haloperidol, which block postsynaptic dopamine receptors, may also be successful in suppressing chorea, but the long-term effectiveness has not been demonstrated, and their side-effects can be severe (Shoulson & Young, 2011).

Other drugs that target the expanded polyglutamine repeat fragment are also under consideration as a disease modifying therapy. Tetrathiomolybdate, a drug that has proven to be effective and tolerable in Wilson disease, has shown to reduce behavioral phenotypes and a trend towards neuroprotection in a mouse model of HD, but needs to be further validated for use in clinical trials (Tallaksen-Greene et al., 2009). Typically, HD is diagnosed in mid-life after the onset of motor symptoms (Venuto et al., 2012). While this is a reliable time point to diagnose the disease, motor symptoms typically appear after severe neuronal loss in the caudate and putamen. Due to the time and nature in diagnosing HD (following motor deficits and neuronal loss), restorative therapies should focus on creating a neuroprotective environment to slow the loss of endogenous neurons, in conjunction with replacing the lost neurons, either through stimulating endogenous neurogenesis or through transplantation of cells capable of differentiating, integrating, and replacing the lost cells.

Stem Cell Characterization

Over the last several decades stem cell transplantation has gained significant interest for the treatment of neurodegenerative diseases. Stem cells are defined by three characteristics: (1) they proliferate through cell divisions where at least one of the daughter cells remains a stem cell: (2) they can differentiate into multiple cells types: and (3) they must be able to repopulate a specific tissue *in vivo* (Verfaillie, 2009). All mammals are derived from a single totipotent stem cell, meaning a cell that can give rise to an entire organism. Then, during the very early phases of embryological development, totipotent cells differentiate into extra-embryonic endoderm (placenta and amniotic sack) or the inner cell mass, which are comprised of pluripotent cells capable of differentiating into all three germ layers but not extra-embryonic endoderm. The

pluripotent cells of the inner mass cell then differentiate into specific ectoderm, endoderm, or mesoderm lineages. With each step of differentiation, the cells become more limited in their ability to differentiate into multiple lineages. Cells that are limited in their ability to differentiate into tissue from their own lineage are referred to as multipotent cells (Verfaillie, 2009).

Neural stem cells (NSC) are cells in the developing and adult brain that are capable of differentiating into all neuronal cell types (Alvarez-Buylla & Lois, 1995). Cells that are isolated from specific areas of the fetal brain have the tendency to differentiate into mature cells of the same structures from which they were derived. For example, cells isolated from the ganglionic eminence (immature striata) have the tendency to differentiate into medium spiny neurons (Freeman et al., 2000), while cells from the ventral mesencephalon have the tendency to differentiate into dopaminergic neurons (Sawamoto et al., 2001), and cells isolated from the immature cortex have the tendency to differentiate into cortical neurons (Kallur, Darsalia, Lindvall, & Kokaia, 2006). However the use of fetal stem cells raises many ethical, logistical, and availability issues (for review see (Mathews et al., 2008; Pullicino & Burke, 2009). Apart from the ethical issues surrounding the use of fetal stem cells due to the need for aborted tissue, there are many logistical problems as well. For transplantation of fetal tissue to be successful the tissue typically needs to be surgically transplanted within a short period of time following access to the aborted fetus, because fetal tissue is very susceptible to damage and death if exposed to stress (Brundin, Barker, & Parmar, 2010). Isolating, purifying, and characterizing fetal cells in this short time frame, while keeping the cells viable for transplantation, has proven to be difficult (Brundin et al., 2010). There are also problems with contaminants and the availability of fetal tissue that further complicate these logistical issues. Typically, for ganglionic eminence

transplantation in patients with either Parkinson's or Huntington's disease patients, 3-5 aborted fetuses are needed for each patient (Brundin et al., 2010) and the efficacy of fetal cell transplantation often relies on the variable supply of donor material, limiting the ability to standardize these cells across multiple studies (Redmond et al., 2010).

To avoid some of these complications, use of adult, bone-marrow-derived (BM) stem cells have gained considerable interest. Cultured mesenchymal stem cells (MSCs) are characterized by plastic adherence, rapid proliferation, and multipotency (Dominici et al., 2006). Transplantation of BM MSCs into the striatum of rodent models of HD, has been shown to reduce behavioral deficits (Lescaudron, Unni, & Dunbar, 2003) and provide neurotrophic support [for review, see (Dunbar, Sandstrom, Rossignol, & Lescaudron, 2006)].

Given that MSCs are readily available and can provide functional efficacy following transplantation, they hold considerable promise as a source for an effective cell therapy. However, in order to expand BM MSCs in sufficient numbers for transplantation, *in vitro* passaging, which has shown to alter the properties of the cells (Ahmadbeigi et al., 2011), is necessary. Our previous work suggested that reducing the number of cell passages may increase transplant survivability in rats and increase their efficacy in reducing behavioral deficits in the 3-nitropropionic acid rat model of HD (Rossignol et al., 2009).

In a seminal publication, Takahashi and Yamanaka (2006) demonstrated that differentiated somatic cells could be reverted back to an embryonic stem cell (ESC)-like state by forced expression of four factors, Oct4, Sox2, Klf4, and c-Myc. Use of these cells, deemed induced pluripotent stem cells (iPSC), hold immense promise for tissue repair or replacement, while avoiding ethical, immunological, and availability issues that are inherent with the use of

ESCs (Yamanaka & Blau, 2010). Initially, iPSCs were met with scepticism, but several independent groups have shown that these cells have morphology, growth, and gene-expression that is similar to ES cells, and are capable of forming adult chimeras (Wernig et al., 2007) and functional germ cells (Okita, Ichisaka, & Yamanaka, 2007).

Since the initial creation of iPSCs, several groups have replicated their results using skin biopsies (Huangfu et al., 2008), liver (Aoi et al., 2008), bone marrow (Niibe et al., 2011) and neural stem cells (M.-Y. Chang et al., 2010) from mouse (Carey et al., 2009a), rat (W. Li et al., 2009), and human cells (Chin, Pellegrini, Plath, & Lowry, 2010). Several other labs have also discovered that other factors can be used in place of the original four that Yamanaka used, with certain groups publishing that, for some types of cells, the number of factors used can be reduced (Giorgetti et al., 2009; Huangfu et al., 2008; Kim et al., 2008).

Once iPSCs are formed, the transgenes are typically silenced and pluripotency is maintained and regulated by the activated endogenous genes (Yamanaka & Blau, 2010). Because the reprogramming factors are usually silenced after iPSC formation, research has focused on novel transfection methods to deliver the reprogramming factors in a safer and more efficient manner. The use of iPSCs that have been reprogrammed using integrative strategies are thought to be affected by phenotypic changes caused by genomic alterations through insertional mutagenesis or expression of oncogenic transgenes (Ho, Chronis, & Plath, 2011; Nakagawa et al., 2008; Okita et al., 2007; Wernig et al., 2008). Lentiviral transfection, using a single cassette containing four factors (Sommer et al., 2009), non-integrating polycistronic constructs (Gonzalez et al., 2009), four separate adenoviruses that each contain one of the four factors (Stadtfeld, Nagaya, Utikal, Weir, & Hochedlinger, 2008), non-viral single multiprotein expression vectors

(Kaji et al., 2009) and non-viral minicircle vectors (Jia et al., 2010), have all been used effectively for generating iPSC colonies that express pluripotent markers and that have the ability to differentiate into all three germ layers. However, the delivery system, combined with the reprogramming factors used, as well as the source of the starting cell, has a profound impact on the efficiency and differentiation capacity of the generated iPSCs [for review, see (Lowry et al., 2008)].

The goal of stem cell transplantation should focus on providing therapeutic benefit through two main mechanisms. Successful cell transplantation should be able to work synergistically with the endogenous microenvironment to up-regulate intrinsic cell proliferation or neuroprotection via trophic factor secretion and immune modulation, potentially enhancing the overall regenerative capacity of the transplanted tissue (Madhavan & Collier, 2010), or by being capable of integrating into the endogenous host network and replacing or repairing the lost neurons.

Clinical Transplantation of Embryonic Tissue in HD

Despite the issues surrounding fetal tissue, including ganglionic eminence transplantation, several long-term clinical studies have been conducted to assess the viability of fetal cells as a therapeutic treatment for HD (see Table 1). There have been varying results for the long-term viability of fetal cells for HD [for review, see (Dunnett & Rosser, 2011; Lindvall, Barker, Brüstle, Isacson, & Svendsen, 2012)]. Bachloud-Levi and colleagues (2009) found that 3 out of 5 patients with transplants of fetal ganglionic eminence showed metabolically active graft cells at 10 years following transplantation. These results correlated with a slowing of the progressive nature of the disease, with even some functional recovery observed at the early time

points. However, these trials were performed unblinded with no control group or sham surgery leaving the possibility of a placebo effect. Also, due to the large clinical variance in the progression of symptoms, it is difficult to confirm that the transplants delayed onset of symptoms. However, these initial tests serve as a proof-of-concept for the survival and engraftment of the cell transplantations in HD.

Table 1. *Clinical Transplantation of Stem Cells in HD*

Author	Clinical Size	Type of Cell	Clinical Outcome	Negative Side Effects
(Madrazo, Franco-Bourland, Castrejon, Cuevas, & Ostrosky-Solis, 1995)	2 Patients	Whole Ganglionic Eminence	Stability or improvement on functional capacity for up to 25 months following surgery when a slow progression of HD was observed	None Reported
(Philpott et al., 1997)	3 Patients	Lateral Ganglionic Eminence	Increased cognitive functioning 6 months following surgery.	None Reported
(Kopyov, Jacques, Lieberman, Duma, & Eagle, 1998)	3 Patients	Lateral Ganglionic Eminence	Clinical improvement for UHDRS for all 3 patients 12 months following surgery Graft survival and growth within the striatum without displacing host tissue	None reported
(Bachoud-Lévi et al., 2000; Bachoud-Lévi, 2009; Bachoud-Lévi et al., 2006)	5 Patients	Whole Ganglionic Eminence	3 of 5 patients showed stability of symptoms or clinical improvement for 4-6 years	One patient showed development of a putaminial cyst

Table 1. *Clinical Transplantation of Stem Cells in HD(continued)*

(Freeman et al., 2000)	1 Patient	Lateral Ventricular Eminence containing striatal primordia	Stability of UHDRS 15 months following transplantation Transplants integrated into the host tissue	None reported
(Hauser et al., 2002)	7 Patients	Ganglionic Eminence	Grafts developed striatal morphology, UHDRS improved significantly 12 months following surgery	3 subjects developed subdural hemorrhages, one patient died 18 months following surgery from probable cardiac arrhythmia
(Rosser et al., 2002)	4 Patients	Whole Ganglionic Eminence	Stability of UHDRS as well as cognitive ability up to 6 months following surgery Graft survival without overgrowth	None reported
(Furtado et al., 2005)	7 Patients	Ganglionic Eminence	Transplants failed to restore fluorodeoxyglucose uptake and D1 and D2 receptor binding in subjects	Possible technical issues with regards to the ganglionic eminence and in targeting the striatum
(Keene et al., 2007)	2 Patients	Lateral Ganglionic Eminence	Improved ambulation 3 months following transplant in 1 patient In both patients, transplanted cells displayed morphology of neurons and astrocytes	One patient reported chronic headaches following surgery and was treated for bilateral subdural hematomas Reported that transplants did not have an effect on the course of HD

Table 1. *Clinical Transplantation of Stem Cells in HD(continued)*

(Krystkowiak et al., 2007)	13 Patients	Fetal Neuronal Tissue	Pre- and Post-UHDRS were not reported 4 of the 13 patients had grafts that did not display signs of rejection	Biological, radiological, and clinical rejection of grafts in other subjects (reversible under immunosuppressive treatment)
(Reuter et al., 2008)	2 Patients	Whole Ganglionic Eminence	Clinical improvement for UHDRS over 5 year period for one patient Increased striatal D2 receptor binding, suggesting long-term survival and efficacy of grafts	None reported
(Capetian et al., 2009)	1 Patient	Whole Ganglionic Eminence	UHDRS score stability for 6 months Survival and differentiation of grafted cells	None reported (Patient died from unrelated causes)
(Cicchetti et al., 2009)	3 Patients	Lateral Ventricular Eminence containing striatal primordia	Improvement of UHDRS in 2 of 3 patients for up to 18 months before returning to pre-surgical levels	Grafts underwent disease-like neuronal degeneration Cortical hemorrhage, subdural hematoma following surgery
(Keene et al., 2009)	1 Patient	Fetal Neuronal Tissue	Clinical Improvement for UHDRS for 2 years Patient died 121 months following surgery from complications of advanced HD	Three mass lesions and one large cyst were present on the left caudate and putamen Five mass lesions and two cysts were present on the right caudate and putamen

Table 1. *Clinical Transplantation of Stem Cells in HD(continued)*

(Gallina et al., 2010)	4 Patients	Whole Ganglionic Eminence	Stability or improvement in motor, behavioral, and functional scores up to 24 months following surgery	None Reported

There have been mixed results following transplantation of fetal tissue into HD patients. Cicchetti and colleagues (2009) observed that when the ganglionic eminence is transplanted into HD patients, the cells undergo a neurodegenerative process similar to that observed in the endogenous cells. Reuter and colleagues (2008) noticed that these types of grafted cells begin to show aggregation of the mutant huntingtin protein and degenerate in a similar manner to endogenous HD neurons. Even in studies where the transplanted cells were still viable, their effect on behavioral recovery began to diminish between 2 and 4 years following the transplantation (Bachoud-Lévi, 2009; Gallina et al., 2010; Reuter et al., 2008). While HD patients with transplanted ganglionic eminence show some signs of improvement, there are many problems with the continued use of fetal cells for transplantation therapies that remain to be addressed. Even in situations whereby fetal striatal transplantation is targeted at the area where the most robust neuronal loss is observed, successful engraftment may actually provide only limited clinical benefits due to the global nature of degeneration in the HD brain (Albin, 2002). While fetal transplantation has proven to be efficacious in a limited number of patients, this technique is marred with biological and technical hurdles, thus prompting the need to explore sources of pluripotent cells [for review (Lindvall et al., 2012; Nicoleau, Viegas, Peschanski, & Perrier, 2011)].

Mouse Models of HD

Several animal models of HD have been used to study the progressive behavioral and histological decline observed in patients [for review (Heng, Detloff, & Albin, 2008)]. These models have also been invaluable for testing the efficiency and safety of stem cell transplantation for the therapeutic treatment of HD. At this time, there is no specific rodent model of that appears to be superior than other models, which underscores the importance of testing potential clinical interventions in multiple rodent models prior to clinical trials (Heng et al., 2008). Transgenic mouse models can be useful tools for the study of biochemical, morphological and functional changes associated with the mutant HTT (Estrada Sánchez et al., 2008; Tallaksen-Greene & Albin, 2011).

The R6/2 mouse model of HD expresses the N-terminal portion of human HTT, containing a highly expanded glutamine repeat (145-155), and develop progressive neurological phenotypes resembling HD (Murphy et al., 2000). At birth R6/2, mice are indistinguishable from littermates without the expanded glutamine repeat, and have a normal development, with little to no expression of HD-like symptoms until 6 to 8 weeks of age. At this point, R6/2 mice begin to express the HD-like phenotype, consisting of neurological signs of stereotypical hind limb grooming, dyskinesia, irregular gait, and motor dysfunction (DeMarch, Giampà, Patassini, Bernardi, & Fusco, 2008; Murphy et al., 2000). However, in the R6/2 model, neurodegeneration, defined as loss of medium spiny neurons in the striatum, is not detectable before 14-16 weeks, which is very late in the lifespan of this very aggressive mouse model of HD (Morton et al., 2005). Although the R6/2 model is still valuable for studying early deficits in synaptic physiology, cognitive deficits, or motor dysfunction (Morton et al., 2005), the early age of onset,

the lack of neuronal loss, and the aggressive nature of the disease make using R6/2 mice difficult for long-term behavioral assessments, pharmacological screening, and evaluations of neurological abnormalities. The R6/2 model also presents shortcomings in that the model does not reproduce all of the genetic regulatory sequence or protein content of the mutant huntigtin, but only a transgenic fragment with an expanded CAG repeat domain under a promoter sequence capturing the core pathogenetic mechanism (Tallaksen-Greene, Janiszewska, Benton, Ruprecht, & Albin, 2010).

In the yeast artificial chromosome (YAC) mouse model of HD, mice express the full-length human mutant htt gene, carrying 46-, 72-, or 128-CAG repeats (Estrada Sánchez et al., 2008; Southwell et al., 2009). These mice show several phenotypical alterations, resembling those observed in HD patients (Estrada Sánchez et al., 2008). Behaviorally, the YAC128 mice show early deficits in motor coordination on the rotarod, as well as biphasic hyperactive-hypoactive activity in the open-field (Van Raamsdonk et al., 2005), however these behavioral differences tend to plateau. In the brains of YAC128 mice, striatal and cortical atrophy develop around 9 months of age (Van Raamsdonk et al., 2005), which is a much longer timeline than that associated with the R6/2 mouse model of HD (Morton et al., 2005).

Knock-In (KI) mice are generated by the insertion of CAG repeats in the endogenous htt gene, with several models developed that mimic the phenotypic manifestations that differ, depending on the number of CAG repeats inserted (Estrada Sánchez et al., 2008). In general, KI mice show some degree of progression of clinical symptoms and associated neuropathological changes, but these symptoms emerge slowly, relative to the rapid progression of the phenotype observed, especially when compared to the R6/2 mouse model, which is atypical for the more

common adult-onset HD (Cao et al., 2006). However, in the Hdh CAG150 knock-in model, reductions in major brain regions or neuronal loss were not observed up to 90 weeks of age, but these mice did display a robust presence of ubiquitin- and huntingtin-positive nuclear inclusions in the basal ganglia, a common neuroanatomical phenotype associated with HD (Lin et al., 2001). An advantage to using knock-in mice is the ability to generate models with varying CAG repeat lengths. The use of knock-in mice has been able to effectively demonstrate the inverse correlation of onset of HD dysfunction with CAG repeat length (Heng, Detloff, Paulson, & Albin, 2010; Heng, Duong, et al., 2010). Knock-in mouse models have proven valuable in helping to study the role of NMDA receptors *in vivo*. A significant decrease in the number of neurons and in the volume of the striatum was observed when HDh150 KI mice were crossed with a mouse that over expressed NR2B receptors suggesting synergistic effects of the huntingtin gene and NMDA receptors (Heng, Detloff, Wang, Tsien, & Albin, 2009). Transgenic murine models of HD are indispensable, due to the large number of knock-in/knock-out gene protocols available making it possible to study gene mechanisms related to HD pathology by creating specific strains of transgenic mice.

Although useful in a variety of ways, transgenic mouse models of HD have several limitations. The relatively short life span and small size of the mouse brain limits the usefulness of these mouse models for longitudinal studies and for therapeutic approaches based on surgical intervention (Kántor et al., 2006). Progressive striatal degeneration generally has not been observed in transgenic mouse models of HD, except for one study by Slow and colleagues (Slow et al., 2003), who observed incremental cell loss in YAC128 mice. While these mouse models capture some of the phenotypes of HD, none of the mouse models recapitulates the substantial

striatal neuronal cell loss that is characteristic in HD patients, thereby limiting the effectiveness of translational research (Franich et al., 2008). Therefore, rat models of HD may offer advantages for examining learning and memory that more accurately recapitulates the time-course of HD (Nguyen et al., 2006).

Rat Models of HD

The rat has been the model of choice in biomedical research for over a century (Bugos, Bhide, & Zilka, 2009). The rat presents the best "functionally" characterized mammalian model system. However, the development of transgenic rats has lagged behind that of transgenic mice used as experimental models of neurodegenerative disorders (Bugos et al., 2009).

The neurotoxin 3-nitropropionic acid (3-NP) is synthesized by fungi and plants. 3-NP crosses the blood-brain barrier and can be administered systematically to induce cell death in the brain, through excitatory mechanisms closely correlated with HD [for review, see (Túnez et al., 2010)]. The evidence supporting the role of energy impairment in the pathology of HD has led to the increase use of mitochondrial toxins, such as 3-NP, in animal models to create the neuropathology and behavioral abnormalities of HD (Shear, Haik, & Dunbar, 2000). The exact mechanism of 3-NP is still not clearly understood, but the prime mechanism is due to irreversible, covalent binding of 3-NP with subsequent inhibition of succinate dehydrogenase, an enzyme of the citric acid cycle that transfers electrons to the electron transport chain via its complex II function (Kumar & Kumar, 2009). The resulting shortage of ATP causes systemic energy impairment and disturbs central nervous functions (Lukács, Szabó, Papp, & Vezér, 2009). Different animal species and strains can be used to develop this model, with neurological profiles that resemble those seen in HD brains (Túnez et al., 2010). Intoxication of 3-NP over several

days leads to selective striatal lesions, which begin in the dorsolateral quadrant of the striatum and later spread to the entire lateral striatum (El Massioui, Ouary, Chéruel, Hantraye, & Brouillet, 2001). Various protocols of 3-NP administration in rats have been developed that try to mimic the phenotype of HD patients. Intraperitoneal, subchronic administration induces mild behavioral abnormalities, depending on mitochondrial chain impairment (Cirillo et al., 2010). Although the 3-NP rat model presents the disadvantage of lacking the genetic pathogenesis of HD, it can be easily developed and used in laboratory animals to rapidly replicate many histological and motoric features of HD (El Massioui et al., 2001).

As with the 3-NP model, the use of quinolinic acid (QA) has been used to model the neuropathology of HD in rats. QA is an endogenous tryptophan metabolite that causes excitotoxicity by acting on the N-methyl-D-aspartate receptor (NMDAr) subtype, causing membrane depolarization and calcium influx in the neurons, which in turn, results in activation of proteases, lipases, generation of free radicals, constitutive nitric oxide synthase, disruption of mitochondrial oxidative phosphorylation and enhanced brain lipid peroxidation (Kalonia, Kumar, Nehru, & Kumar, 2009). QA has been reported to produce symptoms that mimic HD when injected into the striatum of rats (Ayalon, Doron, Weiner, & Joel, 2004; Bazzett, Becker, Kaatz, & Albin, 1993; Bazzett, Legnard, Bauter, & Albin, 1999; Edalatmanesh, Matin, Neshati, Bahrami, & Kheirabadi, 2010; Kalonia et al., 2009; Shear et al., 1998). QA administration recapitulates many histopathological and neurochemical features of HD neuropathy and also causes memory deficits, leading many researchers to use QA models to explore striatal neurodegeneration as well as to evaluate neuroprotective strategies against HD (Velloso et al., 2009). Chronic administration of QA to the striatum of rats has been shown to induce abnormal

contralateral limb use while acute administration typically results in disuse of the contralateral limb, suggesting different behavioral phenotypes dependent on the rate of neurodegeneration (Bazzett et al., 1999). Chronic administration of QA also results in spatial memory deficits that resemble working memory deficits in the human condition (Shear et al., 1998). Thus, intrastriatal of QA produce a useful model that can serve to emulate novel therapeutic strategies aimed at preventing, attenuating, or reversing the neuroanatomical and behavioral changes associated with HD (Emerich et al., 1997). The use of QA has also been beneficial for testing the excitotoxic hypothesis of HD as it is known to be a selective agonist of NMDA receptors (Bazzett et al., 1993).

However, like the 3-NP model, the shortcoming of QA models is the acute onset, which does not accurately reflect the progressive emergence of symptoms that is apparent with HD (Cao et al., 2006). The 3-NP and QA models of HD are useful tools for studying the motor dysfunction associated with clinical or late stage HD, but may not be appropriate to study the early cognitive deficits and presymptomatic pathology associated with HD patients. The number of transgenic rat models recapitulating key pathological hallmarks of HD is still limited, due to the fact that gene targeting technology is not yet established in rats (Bugos et al., 2009).

Currently, transgenic rat models of HD are limited. As to date there have been only two published reports of transgenic rat models of HD, the tgHD rat (von Hörsten et al., 2003) and the bacterial artificial chromosome (BAC) HD rat (Yu-Taeger et al., 2012). The tgHD rat, created by von Hörsten and colleagues (2003), utilizes a human HD mutation, containing an allele with 51 CAG repeats. This animal model exhibits progressive neurological, neuropathological, and neurochemical phenotypes that closely resemble the late-manifesting and slow progression of

symptoms found in HD patients (von Horsten et al., 2003). This transgenic HD (tgHD) rat expresses 727 amino acids of the huntingtin (htt) gene, corresponding to 22% of the full length, which are under the control of 886 base pairs of the rat huntingtin (htt) promoter and manifest neuropathological characteristics, such as neuronal cytoplasmic and intra-nuclear inclusions and enlarged lateral ventricles (von Hörsten et al., 2003 ; Winkler et al., 2006). Classic signs of HD, such as ophistotonus-like head movements, motor dysfunction, and cognitive decline, have been shown to emerge around 12 months of age and progressive impairments of hind- and forelimb coordination at 18 months of age (Winkler et al., 2006).

Several studies have reported that the tgHD rat closely resembles the human condition, suggesting that it is a good candidate to study behavioral, cellular, and molecular markers of the disease (Bode et al., 2009). This transgenic rat model accurately reproduces the neuropathological hallmarks of HD in a time dependent manner, namely the formation of intra-nuclear and neuropil polyQ aggregates (Nguyen et al., 2006). The mutant amino terminal portion of htt is expressed in the brain of these rats, especially in the frontal and temporal cortex, hippocampus, basal ganglia, and mesencephalon (Bauer et al., 2005) . Neuropathological examination reveals the presence of EM48-labeled aggregates in the striatum of these rats when they are greater than one year old (Bauer et al., 2005) . Similar to the situation in HD patients, the tgHD rats show striatal shrinkage and enlarged lateral ventricle in magnetic resonance images during adulthood (Kantor et al., 2006).

However, our lab has worked extensively with this rat model and has not observed the same robust behavioral or neuropathological deficits. We have shown that this transgenic rat model of HD does display cognitive deficits, prior to the onset of motor deficits, similar to what

is observed in the human condition (Fink et al., 2012). This cognitive decline was observed when these rats were 9-months of age and histological analysis revealed that these animals did not have any striatal loss, enlargement of the lateral ventricles, or striatal atrophy (Fink et al., 2012). A follow-up study was performed with rats at both 6- and 12-months of age and determined that this cognitive decline was age-dependent (Crane et al., in preparation). Briefly, tgHD rats at 6-months of age did not show any cognitive deficits in the spatial operant reversal task (SORT) when compared to wild-type (WT; non-HD gene carrying) rats, whereas 9- and 12-month old tgHD rats did. However, the cognitive dysfunction observed in the 12-month old rats was accompanied by motor dysfunction as well (Crane et al., in preparation). Due to the 9-month old tgHD animals displaying cognitive dysfunction, in the absence of motor deficits, this age group was selected for a subsequent drug study using a partial NMDA-agonist (Glyx-13) that has been reported as a cognitive enhancer and neural protectant (Burgdorf et al., 2011; Stanton, Potter, Aguilar, Decandia, & Moskal, 2009). However, the same cognitive deficits were not observed in these animals and treatment with Glyx-13 only had mild cognitive effects.

Our lab has also investigated the efficacy of adult stem cell transplantations using this model, as it was reported that the tgHD rats display robust motor deficits and neuronal loss. In our study, we successfully demonstrated that these rats do show progressive loss of motor function, as measured by a rotarod task, beginning at 14.5 months of age (Rossignol et al., in revision). While we were able to demonstrate that transplantation of either bone-marrow MSCs or a combination of bone-marrow MSCs and adult NSCs were able to prevent this decline in motor performance, we did not observe significant cell loss, striatal atrophy, or enlargement of the lateral ventricles in these rats even at 18-months of age (Rossignol et al., in revision).

Taken together, our data using this transgenic rat model suggests that, while it is possible to detect early cognitive dysfunction and decline in motor performance, this model does not show robust behavioral or neuropathological phenotypes of symptoms analogous to those observed in HD, making it less than an ideal model of this disease.

The BAC HD rat model is relatively new and little is known about its behavioral and neuropathological profiles, outside of those reported in the seminal publication (Yu-Taeger et al., 2012). Motor impairment are present at two months of age, hypoactivity at four months of age, and gait abnormalities at twelve months of age in this model of HD suggesting it may be valuable to study behavioral abnormalities in a rat model (Abada, Nguyen, Schreiber, & Ellenbroek, 2013). This model may prove to be beneficial in Huntington's disease research, but was not available to use in our studies.

While accurate animal models of the disease are vital for conducting research into potential treatments of HD, new *in vitro* models are now being created to gain a better understanding of the mechanisms underlying the disorder. Studies have shown that embryonic cells, differentiated into neurons and transfected with an expanded CAG repeat in the *Hprt* gene undergo abnormal neuronal differentiation, have aggregation of polyQ proteins, develop dystrophic neurites, and do not survive well in culture making them suitable models to study HD (Lorincz, Detloff, Albin, & O'Shea, 2004).

Embryonic and Fetal Stem Cell Transplantation in Animal Models of HD

Transplantation of fetal tissue has also been studied in a wide range of animal models of HD, producing results similar to those observed in clinical trials. Studies have shown that when the ganglionic eminence is transplanted into rodent models of HD, that the cells can differentiate

into mature neurons and astrocytes (Dunnett et al., 1998) and rescue some of the behavioral deficits (Ryu et al., 2004), but these effects are not long lasting (Bernreuther et al., 2006). Transplanted fetal striatal tissue has been reported to release beneficial trophic support when co-transplanted with other cells (Sortwell, Collier, & Sladek, 1998), suggesting that not only do fetal cells provide beneficial properties by neuronal differentiation, but also through trophic support. This short-term effect of the cells is likely due to a failure of the graft to successfully rebuild or replace the lost cellular connections, or due to the grafts being systematically rejected by the host immune system. However, in other disease models, transplantation of embryonic neurons resulted in graft survival and neurite outgrowth into the host brain (Redmond et al., 2009) with modest behavioral improvements (Collier et al., 2002). These behavioral improvements are not limited to rodent models, as fetal tissue transplantation into Parkinsonian non-human primates also provided functional recovery (Redmond et al., 2010). However, it was reported that the neurite outgrowth from the transplants remained limited, and grafted ventral mesencephalon cells were unable to extend their connections outside of the area of the graft (Redmond et al., 2009).

Even in the cases of successful engraftment of fetal tissue, a host of other issues may arise. The most troubling cases are when, following a successful fetal transplantation into animal models of Parkinson's disease, graft-induced dyskinesia may appear similar to what is observed following prolonged levadopa treatments. These graft-induced dyskinesia have been suggested to be related to the immune response following the transplantation, with cells that generate elevated immune responses also displaying an increase in aberrant behaviors (Soderstrom et al., 2008). In contrast, grafted fetal tissue can reduce dyskinesia if transplanted after chronic exposure to levadopa, an outcome which is likely due to denervation of striatal dopamine receptors (Steece-

Collier et al., 2003). If fetal tissue is transplanted prior to chronic exposure to levadopa, there is a there is a reduction in the prevalence of levadopa-induced dyskinesia, but graft-induced dyskinesia remain present (Steece-Collier, Soderstrom, Collier, Sortwell, & Maries-Lad, 2009). Taken together, fetal transplantation has proven to be therapeutically beneficial in several animal models of neurodegenerative diseases, but may not be the ideal cell type for regenerative therapies.

Due to advancements in technology in the early part of this century, it became possible to isolate pluripotent (i.e., non-lineage restricted) stem cells from the mouse embryos (Evans & Kaufman, 1981). Embryonic stem cells (ESC) have been tried in animal models of HD with limited success (see Table 2). Similar to the results that were obtained for transplantation of fetal tissue, transplanted ESCs were capable of differentiating into phenotypically mature striatal neurons and are able to decrease the striatal atrophy associated in animal models of HD. It has been observed that HD animals receiving ESCs show transient recovery of motor deficits, but this effect rarely extends beyond eight weeks (Bernreuther et al., 2006). Similar to what is observed in animals receiving transplants of fetal tissue, ESCs are either rejected by the host immune system or proliferate too extensively, disrupting the host cytoarchitechure and causing teratoma formation (Aubry et al., 2008). There is a concern with the ability of to control ESC differentiation, either prior to grafting or once the cells are in the brain (Soderstrom, O'Malley, Steece-Collier, & Kordower, 2006). In other disease models, it is reported that the grafted fetal neuron can have the mutant protein transferred from the host through retrograde transfer (Kordower et al., 2011). While transplantation of fetal and embryonic tissue has shown considerable promise in both clinical and experimental models, they are not ideal candidates for

large scale clinical applications, due to variable behavioral and histological results, in conjunction with issues of availability, tumor formation, ethical concerns, and logistical problems in preparing the cells.

Table 2. *Stem Cell Transplantation in Animal models of HD*

Author	Animal Model	Type of Cell	Behavioral Outcome	Histology
(Kordower et al., 1997)	QA Rat Model	Genetically Engineered Mouse Embryonic NSCs	No behavioral analysis was performed	Rats receiving grafts displayed sparing of striatal neurons after QA injection
(Dunnett et al., 1998)	R6/2 Mouse	Mouse Lateral Ganglionic Eminence	R6/2 mice receiving transplants demonstrated increased locomotion in the open field test	Grafts were capable of survival, integration, and differentiation into neurons
(Hurlbert, Gianani, Hutt, Freed, & Kaddis, 1999)	QA Rat Model	Human teratocarcinoma neural precursors	Rats receiving transplants exhibited reduced methamphetamine-induced rotational behavior and improved forelimb use in a staircase task when compared to untreated animals	Cells survived for 12 weeks and displayed markers of mature neurons but did not differentiate into medium spiny neurons (DARPP32)
(Armstrong, Watts, Svendsen, Dunnett, & Rosser, 2000)	QA Rat Model	Rat Embryonic NSCs	No behavioral analysis was performed	Grafted cells survived for 12 weeks following surgery and some differentiated into mature phenotypes expressing DARPP32 It was also observed that grafts exhibited neuronal fiber outgrowth

Table 2. *Stem Cell Transplantation in Animal models of HD(continued)*

(Ende & Chen, 2001)	R6/2 Mouse	Human Umbilical Cord Blood MSCs	Mice receiving transplants had a significantly longer life span and reduced weight loss when compared to untreated animals	No histological analysis was reported
(Lescaudron et al., 2003)	QA Rat Model	Rat Whole Bone Marrow	QA rats receiving bone marrow transplants demonstrated a reduction of cognitive deficits in the radial arm water maze when compared to untreated QA rats	No neuronal differentiation of transplanted cells
(Bosch et al., 2004)	QA Rat Model	Immortalized NSCs	Rats receiving transplants exhibited reduced apomorphine - induced rotational behavior when compared to untreated animals	Transplanted cells maintained a GABAergic phenotype, had elaborate neurite processes, and formed synaptic connections with endogenous neurons
(McBride et al., 2004)	QA Rat Model	Human Fetal Cortex	QA rats receiving cells performed better in a cylinder task than untreated QA rats	Grafted animals showed increases of striatal size when compared to untreated QA animals Grafted cells were capable of differentiating into neuronal and glial lineages

Table 2. *Stem Cell Transplantation in Animal models of HD(continued)*

(Ryu et al., 2004)	3-NP Rat Model	Immortalized Human Embryonic NSCs	Rats that received cell transplantation prior to administration of 3-NP demonstrated improved motor function on a rotarod task when compared to 3-NP animals not receiving cells	Transplanted cells expressed primarily immature neuronal markers with few cells expressing intermediate neurons or astrocytes
(Lee et al., 2005)	QA Rat Model	Intravenous delivery of Human NSCs	QA rats receiving transplants demonstrated a reduction in apomorphic rotations when compared to untreated animals	Grafted animals showed reduced striatal atrophy when compared to untreated animals NSCs were capable of differentiating into neurons and glial cells
(Lee et al., 2006)	QA Rat Model	Immortalized Human NSCs injected into the ventricle or tail vein	Behavioral recovery (apomorphic rotations) was not observed	Grafted cells migrated to the injured striatum Cell differentiation was not observed

Table 2. *Stem Cell Transplantation in Animal models of HD(continued)*

(Bernreuther et al., 2006)	QA Mouse Model	Mouse ESCs	Mice receiving transplants of cells exhibited reduced amphetamine-induced rotational behavior when compared to untreated animals up to 4 weeks following surgery, but returned to sham levels at 8 weeks	Transplanted mice showed an increase in the number of neurons in the striatum and differentiated into astrocytes and GABAergic neurons
(Roberts, Price, Williams, & Modo, 2006)	3-NP Rat Model	Immortalized NSCs	3-NP rats receiving transplants had spared motor movement in a beam walking test and intermediate recovery in a water maze task when compared to untreated animals	Transplanted 3-NP rats had a reduced rate of tissue loss when compared to untreated animals suggesting striatal sparing
(Vazey, Chen, Hughes, & Connor, 2006)	QA Rat Model	Rat Adult NSCs	Rats receiving transplants exhibited reduced apomorhine-induced rotational behavior and increased forelimb exploratory behavior when compared to untreated animals	Cells survived for up to 8 weeks following surgery, migrated throughout the striatum, and differentiated into astrocytes, mature neurons, and striatal medium spiny neurons

Table 2. *Stem Cell Transplantation in Animal models of HD(continued)*

Table 2. *Stem Cell Transplantation in Animal models of HD(continued)*

(Visnyei et al., 2006)	QA Rat Model	Rat Embryonic NSCs	No behavioral recovery was observed in QA rats receiving cells in apomorphine-induced rotation tests	Cells survived, migrated towards the lesion site and olfactory bulbs, and differentiated into astrocytes and neurons
(Johann et al., 2007)	QA Mouse Model, R6/2 Mouse	Mouse Embryonic NSCs	No behavioral analysis was performed	Cells differentiated into astrocytes and were rejected after 14- (QA Mouse) and 28-days (R6/2)
(Pineda et al., 2007)	QA Mouse Model	Genetically Engineered Mouse NSCs	Mice receiving transplants of cells exhibited reduced amphetamine-induced rotational behavior when compared to untreated animals	Cells were able to survive and proliferate in the mouse brain Mice receiving transplants showed less striatal loss when compared to untreated animals
(Song et al., 2007)	QA Rat Model	Human ESC Neural Precursors	Rats receiving transplants exhibited reduced apomorhine-induced rotational behavior when compared to untreated animals	Cells were positive for early neuronal markers and no tumor formation was observed at 3 weeks post transplantation
(Amin et al., 2008)	QA Rat Model	Rat Bone Marrow MSCs	No behavioral analysis was performed	QA rats receiving MSCs displayed less striatal atrophy than untreated animals
(Aubry et al., 2008)	QA Rat Model	Striatal Progenitors derived from Human ESCs	No behavioral analysis was performed	Cells transplanted at the ganglionic eminence stage were capable of survival, differentiation into striatal neurons, but resulted in tumor-like over proliferation

Table 2. *Stem Cell Transplantation in Animal models of HD(continued)*

(Bantubungi et al., 2008)	QA Rat Model	Rat MSC and Rat NSC	No behavioral analysis performed	8 week survival of grafts for both cell types
(Behrstock et al., 2008)	QA Rat Model	Genetically Engineered Human Cortical Neural Precursors	No behavioral analysis was performed	Cells were able to survive, migrate to the lesion site, differentiate into neuronal and glial lineages, and release Glial Derived Neurotrophic Factor
(Lim et al., 2008)	Cerebral Hybrid Neurons *in vitro*	Conditioned-Medium from Human NSCs	No behavioral analysis was performed	Conditioned medium reduced the levels of nuclear, cytoplasmic inclusions, and was neuroprotective
(Sadan et al., 2008)	QA Rat Model	Rat MSCs	No behavioral analysis was performed	Cells were capable of migrating towards the lesion site and aided in decreasing the lesion volume
(Lee et al., 2009)	QA Rat Model and R6/2 Mouse	Human Adipose Stem Cells	In QA rats receiving adipose stem cells, there was a reduction in apomorphine-induced rotation behavior In R6/2 mice receiving transplants, there was increased life-span, rotarod performance, and decreased limb clasping	Grafted QA rats had decreased lesion volume and striatal apoptosis Grafted R6/2 mice showed a decrease of striatal neuron loss and reduced huntingtin aggregation

Table 2. *Stem Cell Transplantation in Animal models of HD(continued)*

(Yang & Yu, 2009)	R6/2 Mouse	Mouse NSCs	R6/2 mice receiving cells had increased life spans and improved motor function on the beam walking and rotarod task when compared to untreated animals	NSCs transplanted into R6/2 mice differentiated into neurons, reduced striatal loss, and reduced ubiquitin-positive aggregation in the striatum
(Dey et al., 2010)	YAC 128 Mouse	Genetically engineered Mouse Bone Marrow MSCs	YAC 128 mice receiving bone marrow transplants demonstrated reduced clasping behavior and longer latencies on the rotarod task	YAC 128 mice receiving grafts had significantly more NeuN-positive cells in the striatum compared to untreated YAC 128 mice

Table 2. *Stem Cell Transplantation in Animal models of HD(continued)*

(Edalatmanesh et al., 2010)	QA Rat Model	Rat Bone Marrow MSCs injected *i.v.*	In QA rats receiving MSCs, there was a reduction in apomorphine-induced rotation behavior, increased performance in the cylinder test, improvement of motor function as measured by beam walking and hanging wire test, and memory improvement as measured in the Morris Water Maze when compared to untreated animals	Histological analysis was not performed
(Im et al., 2013)	YAC128 Mouse	HD Human Adipose Stem Cells	YAC128 mice receiving cell transplants showed a delay in motor deficits up to 4 weeks (measured on the rotarod) following transplantation	Normal adipose cells were able to reduce striatal atrophy while HD adipose cells were unable to prevent atrophy

Table 2. *Stem Cell Transplantation in Animal models of HD(continued)*

(Snyder, Chiu, Prockop, & Chan, 2010)	N171-82Q (Knock-In) Mouse	Human Bone Marrow MSCs	No behavioral analysis was performed	Human MSCs were rapidly rejected from the host However, mice receiving transplants had increased proliferation and neural differentiation of endogenous stem cells Mice receiving grafts also displayed decreased striatal atrophy and increased neurotrophic signalling
(Lin et al., 2011)	QA Mouse model, R6/2 Mouse	Human Bone Marrow MSCs	QA mice receiving MSC transplants demonstrated significantly motor recovery on the rotarod task and increased the survivability of the mice	QA mice receiving transplants showed partial striatal recovery in terms of striatal volume
(Jiang et al., 2011)	QA Rat Model	Rat Bone Marrow MSCs	Rats receiving transplants exhibited reduced apomorphine-induced rotational behavior and longer latencies on the rotarod when compared to untreated animals	Grafted cells survived for 8 weeks, significantly reduced the amount of striatal loss observed, and elevated the levels of NGF, BDNF, GDNF, and ciliary neurotrophic factor (CNTF) in the brain

Table 2. *Stem Cell Transplantation in Animal models of HD(continued)*

(Rossignol et al., 2011)	3-NP Rat Model	Rat Bone Marrow MSCs	3-NP rats receiving transplants showed reduction of deficits in paw placement, stepping test, and hind limb retraction when compared to untreated animals	Trend towards lesion size reduction in rats receiving transplants No neuronal differentiation of transplanted cells
(Shin, Palmer, Li, & Fricker, 2012)	QA Mouse Model	Mouse embryonic NSCs	No behavioral analysis was performed	Grafted cells survived for 28 days and differentiated into mature neurons expressing DARPP32
(Sadan et al., 2012)	QA Rat Model	Neurotrophic-factor-treated Human Bone Marrow MSCs	Reduction in apomorphine-induced rotations	Grafted cells survived for 28 days and reduced lesion size
(Moraes et al., 2012)	QA Rat Model	Rat Bone Marrow MSCs	No behavioral analysis	MSCs survived for 60-days and reduced striatal degeneration 7-days after transplantation
(El-Akabawy et al., 2012)	R6/2 Mouse	Human Striatal Neural Stem Cell	No behavioral improvement was observed following transplantation	50-70% of transplanted cells survived, but did not reduce striatal atrophy
(Im et al., 2013)	R6/2 Mouse	Adipose-stem-cell Extract	Delay in phenotypic weight loss and in motor function as measured on the rotarod	Treated R6/2 mice has reduced striatal atrophy and aggregation of mutant htt

Neuronal Stem Cells in HD

To avoid the issues of availability, logistical problems, and ethical concerns that fetal and ESCs present, other sources of stem cells need to be considered. In a seminal paper by Reynolds and Weiss (1992), it was reported that the striatum in the developing and adult brain contains self-renewing cells capable of differentiating into neurons and astrocytes. These cells, isolated from the subventricular zones, now referred to as neuronal stem cells (NSCs), grow in floating clusters, called neurospheres. Because of the stem cell properties of NSCs, the logistical and availability problems of using ESCs are avoided, due to the fact that NSCs are easily expanded *in vitro.* It has also been shown that NSCs can differentiate into mature neuronal phenotypes that have functioning synaptic connections *in vitro* (Wegner et al., 2008) and *in vivo* (Fu, Dai, Chiu, Chen, & Hsu, 2011). Transplantation of NSCs mediates neuroprotection and neurorescue through several mechanisms. There seems to be a reciprocal interaction between grafted NSCs and the host tissue resulting in an increase in endogenous NSC proliferation following transplantation (Madhavan, Daley, Sortwell, & Collier, 2012).

Due to their potential to form new neurons *in vitro*, NSCs have been transplanted into animal models of HD as a possible avenue for cell replacement therapy. Immortalized human- (Lee et al., 2005), mouse- (Yang & Yu, 2009), and rat- (Vazey et al., 2006), embryonic NSCs have all shown to have considerable promise when transplanted into various models of HD (Table 2). In both transgenic mice and toxic lesion rat models of HD, NSCs have been shown to survive up to eight weeks following transplantation, differentiate into mature neurons and astrocytes, and produce behavioral recovery, specifically in apomorphine-induced rotational tests (Bernreuther et al., 2006; Bosch et al., 2004; Pineda et al., 2007; Song et al., 2007; Vazey et al.,

2006), beam walking (Yang & Yu, 2009), and an increased latency to fall off a rotating cylinder (Ryu et al., 2004). However, Johann and colleagues (2007), found that NSCs were rapidly rejected after 14 days in a QA mouse model of HD and after 28 days in the R6/2 model of HD. This study also revealed that the majority of the NSCs differentiated into astrocytes and not into mature neuronal phenotypes, calling into question the feasibility of these cells to be used for cell replacement strategies. In other disease models, the time in which the NSCs are transplanted seem to have a profound effect on cell survival and neuronal protection. When neuronal precursors were transplanted prior to a Parkinsonian lesion, the cells were able to survive and stimulate significant endogenous NSC proliferation and to provide neuroprotection (Madhavan, Daley, Paumier, & Collier, 2009).

Despite the mounting evidence that NSCs have the ability to differentiate into mature neuronal phenotypes and integrate into the host tissue, our lab has studied long-term survival of NSCs in a transgenic rat model of HD and observed that when adult rat NSCs are transplanted into the striatum a large inflammatory immune response was observed and the grafts were significantly smaller 40 weeks after transplantation (Rossignol et al., in revision). While NSCs hold great promise for cell replacement therapies in HD, more work is needed to discover ways to direct these cells into a medium spiny neuronal fate and to ensure that these cells can form new and appropriate synaptic connections that are disrupted by the neurodegenerative processes associated with HD. The immune response elicited by the NSCs following transplantation also needs to be investigated further. While it is possible to globally suppress the immune system with cyclosporine A in order to enhance the graft survival, there are several side effects associated with long-term immunosuppressive treatments (Kawakami, Yoshimoto, Nakagata,

Yamamura, & Siesjo, 2011). For embryonic or adult NSCs to be a viable therapeutic option for HD, local immune suppression or genetically engineering the cells to avoid rejection from the host is needed, along with the ability to direct the cells into the correct lineage following transplantation.

Mesenchymal Stem Cells in HD

In 1976, it was observed by Friedenstein and colleagues (1976), that adult bone marrow contains proliferating MSCs capable of differentiating into multiple lineages. Subsequent to their discovery, these MSCs have been widely studied for their capacities to differentiate into mature cells of varying germ layers, their ability to release neurotrophic factors, and their ability to create a neuroprotective microenvironment through the release of specific interleukins and cytokines. Several groups have reported that MSCs have the ability to differentiate into neuronal lineages *in vitro* (Bae et al., 2011; Black & Woodbury, 2001; Sanchez-Ramos et al., 2000; Woodbury, Schwarz, Prockop, & Black, 2000) and following transplantation into the brain (Brazelton, Rossi, Keshet, & Blau, 2000; Hung et al., 2002; Yuehua Jiang et al., 2002; Kopen, Prockop, & Phinney, 1999; Mezey, Chandross, Harta, Maki, & McKercher, 2000; Muñoz-Elias, Marcus, Coyne, Woodbury, & Black, 2004). Many of the studies provided evidence that MSCs may have the capability to differentiate into neurons *in vitro* utilizing chemical compounds or trophic factors such as β-mercaptoethanol, retinoic acid, neurobasal medium, glial derived neurotrophic factor (GDNF), epidermal growth factor (EGF), or BDNF (Barzilay et al., 2008), but it has been recently suggested that when exposed to a lentivirus containing LMX1a, MSCs can be transdifferentiated into mature dopamine-producing neurons (Barzilay, Ben-Zur, Bulvik, Melamed, & Offen, 2009). However, the contention that MSCs have the ability to

transdifferentiate into mature neuronal phenotypes *in vitro* or *in vivo* remains controversial [for review, see (Hardy, Maltman, & Przyborski, 2008)]. Croft and colleagues (2006), suggest that while it is possible to culture MSCs in such a way that they form structures resembling neurons and express markers of neural proteins, these cells do not follow typical neuronal development. Furthermore, it has been suggested that the *in vivo* expression of neuronal markers may be due to spontaneous cell fusion and the *in vitro* neuronal phenotype observed is due to cellular stress of the culture conditions and not due to transdifferentation (Croft & Przyborski, 2006; Hardy et al., 2008).

Our lab has studied the properties of BM MSCs both *in vitro* and *in vivo* for the treatment of HD. Lescaudron and colleagues (2003), revealed that autologous transplantation of whole bone marrow in QA lesioned rats results in reduced working memory errors when compared to QA rats that did not receive transplants. However, there were no significant differences observed in the total lesion size between rats receiving bone marrow and rats with a sham treatment. The grafted cells were still present near the transplant site 37 days post transplantation, but less than 1% of these cells demonstrated differentiation into neuronal phenotypes. In this paradigm, the whole bone marrow was isolated and transplanted into the brain of rats that had received bilateral intrastriatal injections of QA. It is known that MSCs only make up 0.01% of the bone marrow and can be purified through a plastic adhesion selection (Pittenger et al., 1999). If the beneficial effect observed in this study is attributed to MSCs, finding only a modest reduction in behavioral and histological deficits may have been due to the low number of MSCs that were actually transplanted. It has been suggested that the beneficial effects that are observed following transplantation of MSCs into the brain may be due to the release of neurotrophic factors or other

chemokines that create a favorable microenvironment (Rossignol et al., 2009). Rossignol and colleagues(2009), also observed that MSCs express multiple anti-inflammatory cytokines *in vitro* that may be beneficial for providing a neuroprotective environment in an HD brain.

Rossignol and colleagues (2011), later tested whether purified MSCs or Dulbecco's modified eagles medium (DMEM; the medium in which the cells are cultured) could protect against neuronal loss and behavioral deficits associated with toxic 3-NP lesions of the striatum. Neuroprotection, in terms of lesion size, was observed in all 3-NP rats receiving transplantations of DMEM or MSCs. Behavioral sparing was observed in rats either receiving the MSCs and DMEM in several tests of motor ability and coordination. None of the transplanted MSCs displayed signs of neuronal differentiation, suggesting that the beneficial effects elicited by the transplantation were due to the release of neurotrophic factors or cytokines. To test the hypothesis that the beneficial effect of MSCs for HD was due to the release of neurotrophic factors Dey and colleagues (2010), by genetically modified MSCs to overexpress BDNF, nerve growth factor (NGF), or a combination of both factors. It was found that YAC128 mice that received transplantations of genetically modified and un-modified MSCs showed a reduction in the abnormal limb-clasping behavior, and that mice receiving MSCs engineered to overexpress BDNF had significantly longer latencies to fall off the rotarod, indicating that the genetically-engineered cells were capable of slowing the progression of behavioral deficits associated the YAC 128 mouse model of HD. It was also observed that YAC128 mice receiving MSCs engineered to overexpress BDNF had significantly more neuronal nuclei (NeuN; mature neurons)-positive and dopamine and cyclic AMP regulated phosphoprotein of 32 kDa

(DARPP32; medium spiny neurons in the striatum)-positive cells in the striatum than all other YAC128 groups, suggesting that BDNF plays a role in neuroprotection.

As observed previously (Rossignol et al., submitted), transplanted bone-marrow-derived MSCs, while capable of reducing behavioral and histological deficits in the R6/2 mouse, did not generate new neurons following transplantation in the mouse striata. However, stem cells from other sources, specifically from birth-associated tissues, are gaining interest because they may have a greater propensity to differentiate into neurons (Ende & Chen, 2001).

Umbilical-cord-blood (UCB) is an attractive source of MSCs, as they represent an intermediate link between adult and embryonic tissue, and can be isolated from a noncontroversial source and harvested at a low cost (Adegani et al., 2013; Weiss & Troyer, 2006). Human UCB MSCs have also been shown to have a higher harvest rate when compared to bone-marrow-derived cells, making it possible to isolate a substantial number of cells, while limiting the time and number of passages in culture to produce clinically-relevant numbers of cells for transplantation (Karahuseyinoglu et al., 2007; Manca et al., 2008).

UCB stem cells hold advantages over other types of adult stem cells, as they have been shown to survive in the absence of human leukocyte antigen (HLA) matching (Kurtzberg, Lyerly, & Sugarman, 2005; Laughlin et al., 2001). Further, cord-blood is easily cryopreserved, allowing for bio-banking and expansion for future use (Weiss & Troyer, 2006). It has also been reported that UCB MSCs express the pluripotent markers Oct-4, Nanog, and Sox-2, albeit at much lower levels than embryonic cells (Carlin, Davis, Weiss, Schultz, & Troyer, 2006). The expression of pluripotent markers may be due to the nature of the umbilical cord, which lies at an intermediate position between the embryo and the adult organism during development (although

the migration of fetal cells between the embryo and adult is not fully understood (Bongso & Fong, 2013). It is speculated that some of the fetal cells get "trapped" in the Wharton's jelly of the umbilical cord (Bongso & Fong, 2013).

With this potential for pluripotency, many researchers have explored the use of UCB MSCs as a cell replacement therapy in neurodegenerative disorders. Several groups have reported that human UCB MSCs express neuronal precursor markers and can differentiate into mature neurons *in vitro,* when exposed to the differentiation signals (Fong, Richards, Manasi, Biswas, & Bongso, 2007; Fu et al., 2006; Fu, Shih, Cheng, & Min, 2004; Mitchell et al., 2003; Wang et al., 2004; Weiss & Troyer, 2006). In the brain of a Parkinsonian rat, transplanted UCB MSCs survived, proliferated, and expressed phenotypical markers of dopaminergic neurons (Medicetty, Bledsoe, Fahrenholtz, Troyer, & Weiss, 2004). Several studies have also reported behavioral improvements following human UCB MSCs transplantations in experimental rat models of middle cerebral artery occlusion (Ding et al., 2007; Koh et al., 2008; Zhang et al., 2011).

Stem Cells as a Delivery System

Due to the ease in which MSCs can be genetically modified *in vitro* (Barzilay et al., 2008; Bauer et al., 2008; Dey et al., 2010; Joyce et al., 2010; Meyerrose et al., 2010), their potential as a delivery vehicle is being examined. One of the most promising treatments for HD consists of using RNA interference (RNAi). This technology uses small pieces of RNA that specifically target, bind to the mRNA and destroy the double stranded RNA. This method has proven to be effective in targeting the mutant huntingtin gene and in reducing behavioral and histological deficits in the transgenic knock-in mouse model of HD (Boudreau et al., 2009;

DiFiglia et al., 2007; Harper et al., 2005). However, there are many hurdles for RNAi to be clinically effective [for review, see (Dykxhoorn & Lieberman, 2006)]. The first is the *in vivo* delivery to the targeted organ of the short hairpin-RNA (shRNA) in a manner that will retain the ability to silence the RNA. Another hurdle is that the accessibility of the RNAi to the targeted organ. The shRNA requires uptake into the cytoplasm to effectively bind and silence the RNA (Dykxhoorn & Lieberman, 2006), which has proven difficult to the short half-life and the propensity of RNAi to be rapidly cleared and degraded in the body (Olson et al., 2012). MSCs have become an ideal candidate for the delivery of interfering RNA(Olson et al., 2012), due to their ability to survive (Rossignol et al., 2011) and migrate to the site of neurodegeneration in HD (Edalatmanesh et al., 2010). MSCs are capable of transferring RNAi specifically targeted to mutant huntingtin and were effective in lowering the levels of mutant huntingtin *in vitro* (Olson et al., 2012).

This new technology is especially promising for the treatment of HD, in that genetically engineering MSCs to release RNAi does not interfere with their growth, capacity to differentiate, or disrupt the normal karyotype of the cells. Theoretically, combining the beneficial effects of RNAi with the propensity of MSCs to create a favorable microenvironment through the release of anti-inflammatory cytokines and neurotrophic factors provides great therapeutic promise for the treatment of HD. However, while using MSCs for delivering RNAi for HD patients holds great promise for slowing or even stopping the progression of neurodegeneration, this strategy will not aid in replacing neurons lost during the course of the disease. As mentioned earlier, once the clinical onset of motor symptoms appear, there has already been significant loss of medium spiny neurons in the basal ganglia (Shoulson & Young, 2011). Due to the ethical concerns

surrounding presymptomatic testing of individuals at risk for HD (Coustasse et al., 2009), using RNAi delivered by MSCs may only stop the progression of HD at that time point and will fall short in rescuing or restoring the lost functions caused by neuronal loss. While RNAi treatment is an exciting new avenue for the treatment of HD, a new lineage of stem cells that can successfully replace the lost neurons is needed.

Induced Pluripotent Stem Cells

As described earlier, iPSCs are pluripotent cells that are isolated from adult somatic tissue and reprogrammed to a pluripotent state. However, before iPSCs can truly be considered a possible source for clinical purposes, the ability of the cells to survive in the brain following transplantation without the formation of tumors along with the ability of the cells to differentiate into functional neurons that can integrate into the host network needs to be examined. These cells hold great promise for the treatment of HD due to the fact that iPSCs can be created to be patient specific, meaning that it may be possible to transplant one's own ESC-like cell into their brain. This, in theory, would address issues of rejection (in that the iPSC would be 100% compatible with the host), issues of availability, and any ethical concerns that are associated with clinical fetal or ESC transplantation.

Summary of Background Information and Goal of Thesis Research

While cell replacement strategies for treating the neuronal loss of HD holds great promise, many issues need to be resolved before large-scale clinical trials can commence. It has been demonstrated in small, proof-of concept studies that transplantation of fetal ganglionic

eminence can be effective to slow the progression of the disease, but the beneficial effects are usually short-lived and the use of this type of cell raises many ethical and political issues.

The goal of this dissertation research was to examine the effects of transplanting several types of adult cells in both a transgenic mouse and toxic lesion rat model of HD. As mentioned above, the five sets of experiments were designed with the aim of assessing the potential of MSCs and iPSCs for reducing morphological and behavioral deficits in rodent models of HD. In Experiment 1, entitled "Reductions in Behavioral Deficits and Neuropathology in the R6/2 Mouse Model of Huntington's disease following Transplantation of Bone-Marrow-Derived Mesenchymal Stem Cells is Dependent on Passage Number," were designed to confirm and extend previous findings that indicated transplants of bone-marrow MSCs provide behavioral sparing and reduced morphological deficits in the 3-NP rat (Rossignol et al., 2011).

In Experiment 2, entitled "Transplantation of Umbilical-Cord-Blood-derived Mesenchymal Stem Cells into the Striata of R6/2 Mice: Behavioral and Neuropathological Analysis," were conducted to compare the efficacy of umbilical-cord-blood-(UCB) derived MSCs in the R6/2 mouse model of HD. As previously addressed, it was hypothesized that MSCs isolated from the UCB could possess a higher level of potency, as they are isolated from peri-embryonic tissue and are taken earlier in development than BM MSCs. UCB MSCs may offer an exciting avenue for transplantation therapies if they are able to exert beneficial factors similar to BM, while possessing the ability to differentiate into neuronal lineages. The same procedures as the BM MSC study were used, so a comparison between BM and UCB would be possible.

In order to transplant a type of cell that could differentiate into neuronal lineages, Experiment 3, titled "Adenovirus-Generated Induced Pluripotent Stem Cells," was performed to

generate and characterize induced pluripotent stem cells. As mentioned previously, induced pluripotent stem cells are somatic cells that have been reprogrammed to closely resemble embryonic-like cells, in terms of their expression of pluripotent markers and in their ability to differentiate into the three germ layers. The goal of the third set of experiments was to generate an iPSC that could be transplanted into the brain for cell replacement therapies.

In Experiment 4, entitled "Survival and Differentiation of Adenovirus-Generated Induced Pluripotent Stem Cells Transplanted into the Rat Striatum," involved transplanting the iPSCs, isolated from adenovirally-reprogrammed tail-tip fibroblasts, generated from experiment three into the striatum of adult, immune competent rats. The survival of the transplanted iPSCs, immune response from the host to the cells, potential tumor formation, and neuronal differentiation of the cells were assessed in this study.

In Experiment 5, entitled "Intrastriatal Transplantation of Adenovirus-generated Induced Pluripotent Stem Cells for Treating Neuropathological and Functional Deficits in a Rodent Model of Huntington's disease," were designed to test the ability of these newly-generated iPSCs to provide functional recovery in the 3-NP rat model of Huntington's disease. This model was chosen because 3-NP delivered intraperitoneally, over the course of several weeks with increasing concentrations of the toxin, results in reliable behavioral deficits and neuronal loss, specific to the medium-spiny neurons of the striatum. This model of HD was more suitable for examining the iPSCs as a cell replacement therapy, because rats receiving 3-NP display robust cell loss in the striatum, whereas many of the transgenic models of HD only show modest decreases of cells in the striatum. This experiment also examined the therapeutic time points in which cell transplantation is the most viable. The same iPSCs as used in experiment three and

four were transplanted into the brains of the 3-NP rats at time points representing early- (7-days following 3-NP administration), mid- (21-days following 3-NP administration), and late-stage (42-days following 3-NP administration) Huntington's disease.

CHAPTER III

STATEMENT OF THE PROBLEM

The use of adult MSCs in animal models of HD has been shown to produce beneficial effects by creating a neuroprotective microenvironment that helps slow the progressive striatal atrophy of the brain, but transplants of these cells have little, if any, capacity to replace any of the previously lost neurons. Induced pluripotent stem cells offer one of the most exciting avenues for cell replacement in HD, but the ability of the cells to differentiate into appropriate lineages, their safety, and their long-term survival in the HD brain needs to be addressed prior to their use in clinical trials.

CHAPTER IV

METHODOLOGY

Procedures

Experiment 1. *Reductions in Behavioral Deficits and Neuropathology in the R6/2 Mouse Model of Huntington's disease following Transplantation of Bone-Marrow-Derived Mesenchymal Stem Cells is Dependent on Passage Number*

In Vitro Cell Characterization

The extraction protocol for obtaining BM MSCs was adapted from previously published procedures (Rossignol et al., 2011). Briefly, bone marrow was aspirated from the fibia and tibia of adult (6-8 week-old) wild-type littermates of R6/2 transgenic mice (C57/BL6 background; Jackson Laboratory, Bar Harbor, ME) using a 25-gauge syringe. The cells were then suspended in 10 mL of MSC medium [Alpha Modified Eagles Medium (αMEM: Sigma, St Louis, USA) with 10% fetal bovine serum (FBS; Invitrogen, Carlsbad, USA), 10% horse serum (HS; Invitrogen), and 5 mg/ml streptomycin and 5 UI/ml penicillin (Sigma)]. Following incubation for 48 hours at 37°C, the medium was replaced with fresh MSC medium to remove non-adherent cells.

When cells reached 85% confluency, the cells were passaged. Briefly, the culture medium was aspirated, 0.25% trypsin-EDTA solution (Sigma) was added for 5 minutes to detach the cells, trypsin was then deactivated with 2 mL of FBS. The trypsin/EDTA solution and FBS containing the cells was collected and centrifuged at 1500 rpm for 7 minutes at 4°C. The supernatant was removed and the pellet was then re-suspended, counted, and replated at a density of 8,000 cells/cm^2, in a new 75 cm^2 flask (Phenix, Candler, USA) with fresh MSC media.

At passage 6 (low-passage) and at passage 50 (high-passage) BM MSCs were analyzed by immunocytochemistry (ICC). Briefly, BM MSCs were plated into 6-well-plates containing poly-L-Ornithine coated glass coverslips (25 mm #1; Fisher Scientific) and cultured in MSC medium. At 80% confluency, the cells were fixed with 4% paraformaldehyde in 0.1 M PBS at 4°C for ten minutes. To block non-specific binding sites, the coverslips were incubated for one hour at room temperature in phosphate buffered saline (PBS) with 0.1% Triton-X (Sigma) and 10% normal goat serum (Sigma). Following blocking, the coverslips were incubated in primary antibodies overnight at 4°C. Primary antibodies included CD45 (1/500; Abcam) and SCA1 (1/500; Abcam). After 24 hours, the coverslips were then rinsed and incubated for one hour at room temperature with the appropriately conjugated secondary antibodies. The secondary antibodies included AlexaFluor488 and AlexaFluor594 (1/300; Invitrogen). The coverslips were then rinsed and incubated in Hoechst 33358 (1/1000; Thermo Scientific) for 5 minutes at room temperature to visualize cell DNA and then mounted onto glass slides using Fluoromount (Sigma). Slides were imaged at 20x using a Zeiss Axiovert 200M inverted fluorescent microscope.

The low-passage and high-passage BM MSCs were analyzed by flow cytometry at passage 2 and 45, respectively, following previously published protocols (Lescaudron et al., 2012). Briefly, 200,000-300,000 cells were plated into each well of a round-bottom-96-well plate following a passage. The cells were rinsed in 0.1 M PBS containing 1% bovine serum albumin (Sigma) and 0.1% azide (Sigma) and centrifuged at 2500 rpm for 1 minute at 4°C. The cells were then re-suspended in 30 μL of primary antibodies for one hour at 4°C. The primary antibodies and dilutions were described above for ICC. The cells were then rinsed twice and incubated in

secondary AlexaFluor488 (1/300; Invitrogen) for one hour at 4° C. The cells were then rinsed twice and fixed using 4% paraformaldehyde for ten minutes on ice. The cells were then rinsed and stored at 4°C until analysis was performed using a LSR II (BD Bioscience, San Jose, CA).

Cell cultures were also analyzed for BDNF mRNA expression. RNA isolation was performed from BM MSC cell cultures using a Qiagen RNeasy system (Gaithersburg, MD). All procedures followed the manufactures guidelines. Briefly, two million cells were isolated following passaging, and stored at -80º C in 200 µL Trizol overnight. Then 300 µL of buffer RLT was added to the pellet/Trizol and transferred into a gDNA Eliminator tube and centrifuged at 8000 x g for 1 minute, at which point 350 µL of 70% ethanol was added to the flow-through and mixed thoroughly. All contents of the flow-through were then added to an RNeasy spin column and centrifuged at 8000 x g for 30 seconds. The flow-through was discarded, 700 µL of RW1 buffer was added to the RNeasy spin column, and the column was centrifuged at 8000 x g for 30 seconds. The flow-through was again discarded and 500 µL of RPE buffer was added to the RNeasy spin column and the column was centrifuged at 8000 x g for 30 seconds. The RNeasy spin column was placed in a new collection tube, 30 µL of RNase-free water was added to the spin column, and the column was centrifuged at 8000 x g for 1 minute. The purified RNA was analyzed using a NanoDrop2000 spectrophotometer (ThermoScientific), then stored at -20ºC.

A QuantiTect Reverse Transcription Kit (Qiagen) was used for complementary DNA (cDNA) synthesis following the manufacturers' guidelines. Briefly, RNA was incubated at 42ºC for 2 minutes in a genomic DNA elimination buffer. The solution was transferred to a reverse-transcription master mix and incubated at 42ºC for 30 minutes and then 3 minutes at 95ºC to

inactivate the reverse transcriptase. The cDNA was stored at -20ºC until used in quantitative polymerase chain reaction (PCR) experiments. Primers used for quantitative PCR were BDNF and NGF. All values were normalized to the housekeeping gene glyceraldehyde 3-phosphate dehydrogenase (GAPDH) and fold increase was calculated from control cDNA isolated from mouse tail-tip fibroblasts (TTF). Sequences are located in Table 3.

Table 3. *Primer Sequences in Experiment One.*

Primer	Sequence
GAPDH Forward	AAG AGA GGC CCT ATC CCA A
GAPDH Reverse	CAG CGA ACT TTA TTG ATG GTA
BDNF Forward	GAA GAG CTG CTG GAT GAG GAC
BDNF Reverse	TTC AGT TGG CCT TTT GAT ACC
TrkB Forward	CTC AAG TTG GCG AGA CAT TCC A
TrkB Reverse	AAT CCA GGC ACT TCC TCG TTC
NGF Forward	TAG CGT AAT GTC CAT GTT GT
NGF Reverse	CCC ACA CAC TGA CAC TGT CA
TNF-α Forward	GTT CGG ATC CCA CTG TGA CT
TNF-α Reverse	GTC CCC AGA GCC AAT GAC TA

GAPDH was selected as a housekeeping gene. BDNF was selected to measure the mRNA levels of Brain-derived Neurotrophic Factor. TrkB was selected to measure the mRNA levels of a receptor for BDNF. NGF was selected to measure mRNA levels of Nerve Growth Factor. TNF-α was selected to measure the mRNA levels of a protein associated with inflammation.

Animals

Male and female R6/2 and wild-type (WT; C57/BL6 background; Jackson Laboratory, Bay Harbor, ME) mice were housed at 22°C under a 12h light/12h dark reverse light cycle with

ad libitum access to food and water. The mice were separated into the following four groups balanced by gender and genotype: (1) sham-operated (Hanks Balanced Salt Solution; HBSS; Gibco, injection into the striatum) WT mice (WT; n = 19); (2) sham-operated R6/2 (R6/2; n = 10) mice; (3) R6/2 mice transplanted with low-passage BM MSCs (R6/2 BM Low; n = 7); and (4) R6/2 mice transplanted with high-passage BM MSCs (R6/2 BM High; n = 10).

BM MSC Transplantation

At 5 weeks-of-age, mice were anesthetized with isoflurane gas and O_2. The head of each mouse was shaved and cleaned using chlorhexadine (Molnlycke Healthcare). Prior to placing the mouse in the stereotaxic device, 2% lidocaine gel (Hi-Tech Pharmacal) was placed on the tip of the ear bars. Anesthesia was maintained with isoflurane gas and O_2 for the duration of the surgery. A midline incision was made on the scalp and the skin was retracted, exposing Bregma. Two burr holes (0.5 mm) were placed directly over the neostriatum (coordinates relative to Bregma: anterior +0.5 mm; lateral ± 1.75 mm; tooth bar set at -3.3 mm). Prior to transplantation, MSCs at either low-passage (P3-8) or high-passage (P40-50) were pre-labeled with Hoechst 33358 (5 µg/mL, Sigma) and re-suspended at a density of 200,000 cells/µL in HBSS. The cells were loaded into a 10 µL Hamilton microsyringe and bilaterally transplanted (2.5 mm ventral to dura) at a constant rate of 0.33 µL/minute, for three minutes. Following the first injection, the syringe was left in place for three minutes to allow cell diffusion, raised 1 mm, and injected a second time. After a second three-minute wait period, the microsyringe was withdrawn at a steady rate over a three-minute period. The same procedure was then followed on the opposite hemisphere, the burr holes were sealed with bone wax, and the wound was closed using sterile wound clips (7 mm).

The mice were placed in a recovery cage until fully mobile, at which point, they were returned to their home cage.

Behavioral Analysis

All mice were tested for baseline behavior at 5 weeks-of-age, prior to cell transplantation. Mice underwent 6 weeks of testing on all behavioral tasks, beginning the week following surgery, except for the Morris Water Maze (MWM), for which testing began two weeks following surgery and lasted 5 weeks.

The rotarod (SDI Rotor-Rod; San Diego Instruments) was used to assess motor coordination. The mice were required to maintain balance on a 3 cm diameter rotating rod for 60 seconds. The rod rotated at a constant speed of 10 rpm and each mouse was given 3 trials per day. If the mice were incapable of remaining on the rotarod for the full 60 seconds, they fell onto a foam pad placed below the apparatus.

The mice also had their limb-clasping response recorded. The mice were suspended by their tails from a height of 50 cm for 30 seconds, and a limb-clasping response was defined as the withdrawal of any limb to the torso for more than one second. Each testing session consisted of three trials with a clasping score ranging from 0 to 4 with 0 representing the absence of clasping, 1 representing a withdrawal of any single limb, 2 representing the withdrawal of any two limbs, 3 representing the withdrawal of any three limbs, and 4 representing the withdrawal of all four limbs. The limb-clasping response scores were averaged for each testing session for each animal.

The MWM was used to test cognitive function through spatial memory. Briefly, the MWM is a 142 cm diameter tank filled with opaque water (30.5 cm deep water mixed with non-

toxic white paint). A 14 cm platform was placed 1 cm below the surface of the water. Prior to baseline testing, each mouse was given a "cued" trial, where the platform was placed in the center of the MWM with a visible flag. The mice were given four training trials from four starting locations (North, South, East, and West) to shape the mice on the escape paradigm and to assess visual acuity and swimming ability. During each testing week, mice were placed in the water facing the south location and the hidden platform was subsequently altered each testing day between the Northwest and Northeast quadrant with the platform in the center of the quadrant. During baseline and the subsequent testing days, the mice were given five trials to find the hidden platform. Following a successful trial, the mice were left on the platform for 5 seconds, removed from the tank, dried, and given a forty-five second inter-trial interval. Mice who did not locate the hidden platform within 60 seconds were guided by hand to the platform and allowed to rest on the platform for five seconds. Swim speed, distance traveled, and swim time was tracked and recorded using Viewpoint VideoTrack version 1.75. Each trial was scored as "correct" if the mouse was capable of finding the hidden platform in less than sixty seconds and the probability of a "correct" trials was calculated at the end of each testing session (number of correct trials/number of total trials).

Histological Analysis

At the conclusion of behavioral testing, when mice were 11.5 weeks old, half of the animals from each group were deeply anesthetized with an overdose of sodium pentobarbital (*i.p.*), and transcardially perfused with 0.1M PBS, followed by 4% paraformaldehyde (diluted in 0.1M PBS at pH 7.4) to fix the brains. The brains were then rapidly removed, suspended in 4% paraformaldehyde for 24 hours at 4°C, and then transferred to 30% sucrose in 0.1 M PBS for 48

hours at 4°C. The brains were then flash frozen, using methylbutane (Sigma, St. Louis, MO) and stored at -80°C until they were processed.

Tissue was sectioned on a cryostat (Vibratome UltraPro 5000) at 30 µm, labeled using previously established free-floating fluorescent staining protocols (Rossignol et al., 2009) and were mounted on positive charged microscope slides (Globe scientific Inc, Paramus, USA). For immunohistochemical analysis, the tissue was labeled with antibodies for neuronal nuclei (NeuN; 1/500, Abcam) and glial fibrillary acid protein (GFAP; 1/500, Abcam). The tissue was first blocked using 10% Normal Goat Serum in PBS with 0.1% Triton-X for 45 minutes at room temperature. The tissue was then transferred to a well containing the primary antibodies and stored at 4°C overnight. The following day, the tissue was rinsed three times in PBS with 0.1% Triton-X and transferred to a well containing the appropriately conjugated secondary antibodies for one hour at room temperature. Secondary antibodies consisted of AlexaFluor488, conjugated with GFAP, and AlexaFluor594, conjugated with NeuN (1/300; Invitrogen). Images of the fluorescent labels were captured using a Zeiss Axiovert 200M inverted fluorescent microscope at 20x magnification.

Cytochrome oxidase (CYO) histology was used to determine metabolically active tissue and these same sections were used for subsequent morphological analysis. Briefly, the tissue was submersed in a solution of 800 mg sucrose, 4 mg of cytochrome C, and 1 mg of 3, 3'-diaminobenzidine (DAB) dissolved in 20 mL of phosphate-buffer for 4 hours at room temperature on an agitator. The tissue was then transferred to deionised H_2O, mounted onto positively charged glass slides, and coverslipped using Depex (Electron Microscopy, Hatfield, PA). CYO labeled tissue was scanned using Nikon ScanPro.

All images were analyzed using ImageJ (NIH; Bethesda, Maryland). Briefly, images of the transplants from each animal were captured from five levels, centred at 0.5 mm anterior to bregma (the transplant site) with two additional sections anterior and posterior to the transplant site, approximately 200 µm apart. Average intensity of the label, counts of positively labeled cells, as well as percent of co-localization between the transplanted MSCs and NeuN or GFAP, and were analyzed between all groups. Densitometric measures of CYO and GFAP were taken from the same sections as described above and the average intensities were normalized to the corpus callosum of each section. Cells were counted as positive cells if they showed: (1) antibody immunoreactivity within the cell body; (2) the nucleus of that cell was within the counting frame without touching the exclusion lines; and (3) the nucleus of that cell was in focus. For total brain area, 5 sections (at 100-, 300-, 500-, 700-, and 900 µm anterior to bregma) were traced using ImageJ and the total area was calculated.

RNA Isolation

Mice that were not used for immunohistological analysis were killed via cervical dislocation, when the mice were 11.5 weeks old, and striata of these mice were isolated, flash-frozen with liquid nitrogen, and stored at -80ºC. RNA isolation was performed using a Qiagen All-Prep system following the manufactures guidelines. Briefly, striatal tissue was homogenized using a lysis buffer and transferred to an All-Prep spin column and centrifuged at 8000 x g for 1 minute. The contents from the flow through was then transferred to a protein clean-up spin column and centrifuged at 240 x g for 3 minutes. The flow-through, containing purified protein, was stored at -80ºC. The All-Prep spin column was then placed in a new collection tube, 300 µL of buffer RLT was added, and the sample was centrifuged at 8000 x g for 1 minute. Then, 350

μL of 70% ethanol was added to the flow-through and mixed thoroughly. All contents of the flow-through were then added to an RNeasy spin column and centrifuged at 8000 x g for 1 minute. The flow-through was discarded and 700 μL of RW1 buffer was added to the RNeasy spin column, and the column was centrifuged at 8000 x g for 30 seconds. The flow-through was again discarded and 500 μL of RPE buffer was added to the RNeasy spin column and the column was centrifuged at 8000 x g for 30 seconds. The RNeasy spin column was placed in a new collection tube and 30 μL of RNase-free water was added to the spin column before the column was centrifuged at 8000 x g for 1 minute. Purified RNA was collected in the collection tube and was analyzed using a NanoDrop2000 spectrophotometer (ThermoScientific) and stored at -20ºC until used for cDNA synthesis. A QuantiTect Reverse Transcription Kit (Qiagen) was used for cDNA synthesis following the manufacturers' guidelines. Briefly, RNA was incubated at 42ºC for 2 minutes in a genomic DNA elimination buffer. The solution was transferred to a reverse-transcription master mix and incubated at 42ºC for 15 minutes and then 3 minutes at 95ºC to inactivate the reverse transcriptase. The cDNA was stored at -20ºC until used in quantitative PCR experiments. The primers used for gene expression were brain derived neurotrophic factor (BDNF), nerve growth factor (NGF), neurotrophic tyrosine receptor kinase, type 2 (TrkB), and tumor necrosis factor alpha (TNF α). All values were normalized to the housekeeping gene GAPDH. The sequences for each primer can be found in Table 3.

Experiment 2. *Transplantation of Umbilical-Cord-Blood-derived Mesenchymal Stem Cells into the Striata of R6/2 Mice: Behavioral and Neuropathological Analysis*

In Vitro Cell Characterization

The extraction of UCB MSCs was performed from day 15 gestation pups of wild-type (WT; C57/BL6 background; Jackson Laboratory, Bay Harbor, ME). Briefly, the placenta was discarded from the distal end of the umbilical cord and the fetus and held above a sterile Petri dish with sterilized forceps. The UCB was then pushed out of the umbilical cord using a separate set of sterile forceps. The UCB was then diluted in 10 mL MSC medium [Alpha Modified Eagles Medium (αMEM: Invitrogen, Carlsbad, USA) with 10% fetal bovine serum (FBS; Invitrogen), 10% horse serum (HS; Invitrogen), and 5 mg/mL streptomycin and 5 UI/mL penicillin (Sigma)] and collected in a 15 mL Falcon tube and centrifuged at 1500 rpm for 7 minutes at 4°C. The cells were then counted and plated in a 75 cm² flask containing 15 mL of MSC medium.

Following incubation for 48 hours at 37°C, 5% CO_2, UCB MSCs were allowed to attach and non-adherent cells or debris was removed and replaced with fresh MSC medium. When the UCB MSCs reached 85% confluency, the cells were passaged. Briefly, the culture medium was aspirated, 0.25% trypsin-EDTA solution (Sigma) was added for 5 minutes to detach the cells, then the trypsin was then deactivated with 2 mL of FBS. The trypsin/EDTA solution and FBS containing the cells was collected and centrifuged at 1500 rpm for 7 minutes at 4°C. The supernatant was removed and the pellet was then resuspended, counted, and re-plated at a density of 8,000 cells/cm^2, in a new 75 cm^2 flask (Phenix, Candler, USA) with fresh MSC media.

The UCB MSCs were analyzed with ICC and flow cytometry as described in Experiment 1. The experiment was conducted in the same manner as in Experiment 1, with the expression

levels of SCA1 and CD45 in low- and high-passage UCB MSCs being examined. The mRNA expression of BDNF in low- and high-passage UCB MSCs was examined using the same techniques as describe in Experiment 1. The same protocol was used for RNA isolation, cDNA synthesis, and RT PCR experiments. The primer sequences used can be found in Table 4.

Table 4. *Primer Sequences in Experiment Two.*

Primer	Sequence
GAPDH Forward	AAG AGA GGC CCT ATC CCA A
GAPDH Reverse	CAG CGA ACT TTA TTG ATG GTA
BDNF Forward	GAA GAG CTG CTG GAT GAG GAC
BDNF Reverse	TTC AGT TGG CCT TTT GAT ACC

GAPDH was selected as a housekeeping gene. BDNF was selected to measure the mRNA levels of Brain-derived Neurotrophic Factor.

Animals

All procedures were carried out under the approval of Central Michigan University Animal Care and Use Committee. Male and female, R6/2 and wild-type (WT) mice, were housed at 22°C under a 12h light/12h dark reverse light cycle (lights on at 0900) with *ad libitum* access to food and water. The mice were randomly assigned to one of the following four groups, with the exception of having the groups balanced by gender and genotype: (1) sham-operated (Hanks Balanced Salt Solution; HBSS; Gibco, injection into the striatum) WT mice (WT; n = 17); (2) sham-operated R6/2 (R6/2; n = 12) mice; (3) R6/2 mice transplanted with low-passage UCB MSCs (R6/2 UCB Low; n = 9); and (4) R6/2 mice transplanted with high-passage UCB MSCs (R6/2 UCB High; n = 8).

UCB MSC Transplantation

The same protocol for MSC transplantation in experiment one was followed for experiment two. Briefly, at 5 weeks of age, mice were anesthetized with isoflurane gas and O_2 and prepared for surgery as previously described. Pre-labeled UCB MSCs were transplanted in the same location as experiment one (coordinates relative to Bregma: anterior +0.5 mm; lateral + 1.75 mm and -1.75 mm; tooth bar set at -3.3 mm; and -2.5 mm ventral to dura) at either low passage (P3-8) or high passage (P40-50) and resuspended at a density of 200,000 cell per microliter in HBSS. Two injections were performed as previously described for a total of 400,000 cells per hemisphere.

Behavioral Analysis

All mice were tested for baseline behavior at 5 weeks of age, prior to cell transplantation. Following a one-week resting period after transplantation, the mice were tested weekly for 6 weeks, on all behavioral tasks, except for the Morris Water Maze (MWM), for which testing started at two weeks post-transplantation. The experimental design and timeline for the rotarod task, MWM and limb-clasping was performed in the same manner as in Experiment 1.

Histological Analysis

At the conclusion of behavioral testing, when the mice were 11.5 weeks old, they were deeply anesthetized and overdosed with sodium pentobarbital (delivered i.p.), and transcardially perfused with 0.1M PBS, followed by 4% paraformaldehyde (diluted in 0.1 M PBS at pH 7.4) to fix the tissue of the animal. The brains were then rapidly removed, suspended in 4% paraformaldehyde for 24 hours at 4°C, and then transferred to 30% sucrose in 0.1M PBS for 48

hours at 4°C. The brains were then flash frozen, using methylbutane and stored at -80°C until they were processed. Coronal sections were cut on a cryostat (Vibratome UltraPro 5000; Sim Co Ltd, Denizli, Turkey) at 30 µm, and were mounted on positive charged microscope slides (Globe Scientific Inc, Paramus, USA).

The same procedures for fluorescent and CYO labeling in Experiment 1 were used in Experiment 2. The images produced from these labels were analyzed in the same manner as well. Briefly, images of the transplanted cells were captured from five sections of each animal, starting at 0.5 mm anterior to bregma and 2 sections, approximately 200 µm apart, anterior and posterior to the transplant site. Average intensity of the label, counts of positively labeled cells, as well as percent of co-localization between the transplanted MSCs and NeuN or GFAP, and were analyzed between all groups. Densitometric measures of CYO and GFAP were analyzed from images taken in the striatum and the average intensities were normalized to the corpus callosum. Cells were counted as positive if they showed: (1) antibody immunoreactivity within the cell body; (2) the nucleus of that cell was within the counting frame without touching the exclusion lines; and (3) the nucleus of that cell was in focus. For total brain area, 5 sections (at approximately 100-, 300-, 500-, 700-, and 900 µm anterior to bregma) were traced using ImageJ and the total area was calculated.

Experiment 3. *Adenovirus-Generated Induced Pluripotent Stem Cells*

Virus Construction

A single cassette lentivirus (LN) and a combination of adenoviruses (AD) were created using Oct4, Sox2, Klf4, and c-Myc (OKSM, (Takahashi & Yamanaka, 2006). The construction

of the single cassette lentivirus described previously (Carey et al., 2009b). The lentiviruses were then produced using 293T packaging cells (Clontech) (T. H. Nguyen et al., 2005). Titers were 5.10^8 TU/ml as determined by quantitative PCR following transduction of HeLa cells using a serial dilution of the vectors. The recombinant adenoviruses were developed in our lab at Central Michigan University. First, to construct the shuttle vector, the Oct3/4-2A-Klf4-2A-Sox2 (OKS-2A) gene fragment was released from pCX-OKS-2A (Addgene, plasmid 19771) and the c-Myc gene from pCX-cMyc (Addgene, plasmid 19772) at the cloning sites of *EcoR*I [Addgene, previously published by (Okita, Nakagawa, Hyenjong, Ichisaka, & Yamanaka, 2008)]. The pacAd5 CMVK-NpA shuttle Vector from RAPAD CMV Adenoviral Expression System (cat# VPK-252, Cell Biolabs) was linearized with *EcoR*I at the multiple cloning sites (Figure 1). Each of the four genes were treated for dephosphorylation and then ligated into the respective *EcoR*I sites of the vector. The clones with correct gene orientation were selected and further confirmed via sequencing. The recombinant adenovirus, Ad-OKS or Ad-Myc, was generated, amplified and prepared according to the manufacture's instruction. The titer of each adenovirus was determined with QuickTiter Adenovirus Titer Immunoassay Kit (Cell Biolabs).

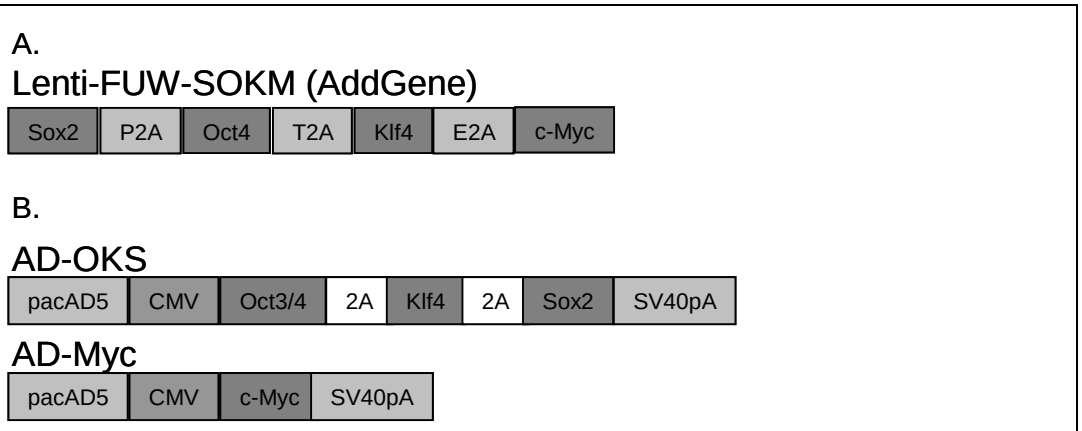

Figure 1. *Single Cassette Lentivirus (A) and Adenovirus pair (B) used for iPSC induction.*

MSC, TTF and REF Culture

Mesenchymal stem cells (MSC) were isolated from the femur of an adult Sprague-dawley rat (Charles River, Rouen, France) according to previously published protocols (Rossignol et al., 2009). Briefly, the rat was anesthetized with ketamine and rompun (PanPharma, Fougeres, France) and the femur and tibia were isolated and placed into ice cold sterile 0.1 M PBS. Using an 18 gauge needle, a hole was drilled in the head of the femur and tibia and bone marrow was aspirated using a 25-gauge needle and syringe. The bone marrow was collected and placed into a sterile 15 mL falcon tube with 10 mL of MSC medium consisting of alpha-MEM (Life Technologies, CA), 20% fetal bovine serum (FBS; Life Technologies, CA), and penicillin streptomycin (Life Technologies, CA) and the tube was centrifuged at 1500 rpm for 7 minutes at 4º C. Cells were counted and plated at a density of 600,000 cells per cm^2 in a 75 cm^2 flask containing 20mL of MSC medium. Following 24 hours of incubation at 37° C with 5% CO_2, the MSC medium was aspirated and replaced with fresh MSC medium. After 7 days MSCs were

passaged following previous protocols (Rossignol et al., 2009). At passage 5, MSCs were used for transfection protocols.

Tail-tip fibroblasts (TTF) were cultured from the tails of adult Sprague-Dawley rats (Charles River, Rouen, France). Briefly, the donor rat was anesthetized with ketamine and rompun and had the tip of the tail (approximately 3 cm) removed using sterile scissors. The tail was washed twice with sterile PBS under a chemical safety hood. A lengthwise incision was made down tail and the superficial dermis was peeled away only leaving the inner white skin of the tail. The tail was minced into 3 mm pieces using a sterile scalpel blade and placed into 60cm Petri dishes that had been coated with 0.1% gelatin. Then, 15mL of fibroblast media (DMEM, 10%FBS, and penicillin/streptomycin, Life Technologies, CA) was added to the TTFs and incubated at 37° C for 5 days, at which point fibroblast cells were visualized migrating from the tail pieces. At day 5, the tail pieces were removed and the TTFs were allowed to grow until 85% confluency. The TTFs were passaged between 2 and 5 times using the procedures applied to the MSCs and these cells were then used for transfection protocols.

The iPSCs were grown on deactivated rat-embryonic-feeder (dREF) cells that were derived from 15-day rat embryos. The embryos were isolated from a pregnant female rat and placed into sterile PBS and separated from their placenta and surrounding membranes with forceps. The head, visceral tissues, and gonads were removed and the remaining tissue was transferred to a clean dish and washed twice with sterile PBS. This tissue was then minced, transferred to a 50 mL falcon tube containing 0.25% Trypsin/EDTA (Life Technologies, CA) and incubated at 37°C for 20 minutes. The Trypsin/EDTA was deactivated with equal parts of fibroblast medium and the tissue was manually dissociated by gentle pipetting. The 50 mL tube

was then left at room temperature for 5 minutes to allow the debris to settle and the supernatant was transferred to a separate 50 mL falcon tube and centrifuged at 1000 rpm for 5 minutes. Following centrifugation, the supernatant was discarded, the cells were re-suspended in 1mL of fibroblast medium, counted, and plated at 200,000 cells per cm^2 in a 75 cm^2 flasks containing 15mL fibroblast medium. The next day the media was replaced and any remaining debris or floating cells was removed. Cells were allowed to grow to 80% confluency, at which point they were passaged.

Prior to use in iPSC cultures, the rat-embryonic fibroblasts were deactivated using mitomycin C. Briefly, mitomycin C (Sigma, MO), at a final concentration of 6 µg/mL, was added directly to the culture medium and incubated at 37°C for 3 hours. Following deactivation, the medium containing mitomycin C was aspirated and the cells were rinsed twice using sterile PBS. The cells were then passaged and 100,000 dREF per well were plated into 12-well plates or 500,000 dREF per well were plated into 6-well plates and incubated at 37°C with 5% $CO_2$for 24 hours. On the next day, the medium was replaced, removing any non-adherent cells, with the residual dREFs being used for iPSC culture within 48 hours.

Transfection

TTF and MSC were grown in 12-well culture dishes until 90% confluent. When the cells reached 90% confluent, the culture medium was aspirated and the cells were washed with sterile PBS. One mL of medium (DMEM with 10% FBS) containing either both adenoviruses (1.44 µL/mL AD-OKS and 1.07 µL/mL AD-Myc) or the single cassette lentivirus (0.8 µL/mL Lenti-OKSM) was added to each well and was incubated for 4 days, at which point morphological changes were observed. After four days of incubation, half of the virus-containing medium was

aspirated and replaced with iPSC medium [DMEM, 15% FBS, 1% nonessential amino acids (Life Technologies), β-mercaptoethanol (Sigma), and penicillin/streptomycin]. This process was repeated every 48 hours until the colonies were large enough to be selected (typically between 18 and 25 days). To select the colonies, the iPSC medium was removed and 250 µL of 0.25% Trypsin/EDTA was added to each well for approximately 30 seconds. Using a sterile pipette, each colony was selected and pipetted into a 96-well plate containing iPSC medium. This process was repeated for each colony in the 12-well plate. The 96-well plate was centrifuged and the colonies were re-suspended in iPSC medium and transferred into a 12-well plate containing deactivated feeders.

Passage

The iPSC were passaged every 5-6 days into a new 6-well plate containing deactivated feeders. During passaging, the medium was carefully removed and discarded, and the cells were rinsed twice with sterile PBS. Then, 500 µL of 0.25% Trypsin/EDTA was added to each well for 2-3 minutes at 37° C to allow the iPSC colonies to detach. Following incubation, the Trypsin/EDTA was deactivated with equal parts FBS. The solution containing Trypsin/EDTA, FBS, and detached cells was collected in a 15 mL tube. The 15 mL tube was then centrifuged at 1200 rpm for 5 minutes at 4° C. The supernatant was discarded, the cells re-suspended in 1 mL of iPSC medium, counted, and plated at a density of one million cells per well in a 6-well plate containing dREF. During each passage, a small number of dREFs would detached and be replated with the iPSCs. This small number of dREFs was accounted for in all *in vitro* analyses.

Flow Cytometry

After 4 passages, the iPSC colonies were analyzed via flow cytometry for markers of pluripotency. The pluripotent panel, provided by Abcam, included Tra-1-60, SSEA3, SSEA4, Nanog, and Oct4. The preparation of iPSC for flow cytometry followed a standard lab protocol (Lescaudron et al., 2012). Briefly, iPSC were plated into a 96-well plate and incubated in the primary antibody for 30 minutes on ice. The cells were then rinsed and incubated with the corresponding secondary fluorescent antibody (Life Technologies). AlexaFluor488 was used for Tra-1-60, stage specific embryonic antigen 3 (SSEA3) and stage specific embryonic antigen 4 (SSEA4). AlexaFluor568 was used for Nanog and octamer-binding transcription factor 4 (Oct4). The data collection and analysis was performed on a Becton Dickinson Biosciences (New Jersey) LSRII with FACSDIVA. Approximately 10,000 cells were analyzed for each label.

Immunocytochemistry

The same pluripotent markers used for flow cytometry were also used for immunocytochemistry. The cells were grown on poly-L-Ornithine-coated, 20-mm glass coverslips for 4 days. The cells were then fixed using 4% paraformaldehyde for 10 minutes at 4°C and analyzed within 48 hours. Then, the coverslips were placed in a blocking solution containing 0.1% Triton X-100 (Life Technologies) and 10% normal goat serum (Jackson ImmunoResearch, PA) in PBS for 1 hour. The blocking solution was then aspirated and the primary antibodies were added according to the manufacturer's recommended dilution in 0.1% Triton X-100 and PBS. A double labeling was performed with Rat SSEA3-Mouse SSEA4 and Mouse Tra-1-60-Rabbit Nanog. Rabbit Oct4 was analyzed using single labeling. The primary antibodies were incubated at 4° C overnight. The primary antibodies were then aspirated and the

coverslips were rinsed 3 times. Secondary antibodies were then added according to the manufacturer's recommended dilutions. The SSEA3 was conjugated to AlexaFluor488 (Invitrogen) and SSEA4 was conjugated to AlexaFluor568 (Invitrogen). The Tra-1-60 was conjugated with AlexaFluor488 and Nanog was conjugated with AlexaFluor568. The Oct4 was conjugated with AlexaFluor568. The coverslips were incubated with the secondary antibodies at room temperature for 1 hour. The secondary antibody was then aspirated and the coverslips were rinsed 3 times. For cellular localization, Hoechst 33258 (Sigma) was added to each coverslip at a dilution of 1/1000 for 5 minutes at room temperature. The Hoechst was then aspirated, the coverslips rinsed 3 times, and then the coverslips were mounted onto glass slides using Prolong Gold Antifade reagent (Invitrogen). Imaging was done using a Zeiss Axioskop 2 *plus* and analyzed using Axiovision 4.7 (Zeiss, Oberkochen, Germany). Images were taken at 20x magnification from at least 12 locations per coverslip. Exposure time for each secondary antibody (Hoechst, 488 and 594) was held constant for each label examined across all groups.

In Vitro Differentiation

The TTF-AD, TTF-LN, MSC-AD, and MSC-LN iPSCs were differentiated into neuronal lineages, using a modified neural rosette protocol (Ma, Liu, & Zhang, 2011). Briefly, iPSCs were plated into a 6-well plate at a density of 415 cells per mm^2. Cells were allowed to adhere to the plastic and expand over 48 hours in iPSC medium. After 48 hours, iPSC medium was removed and replaced with neural induction medium (DMEM:F12 supplemented with 5% B27, 5% MEM non-essential amino acids, and 1mg/mL Heparin; Life Technologies, CA). Half of the medium was replaced with fresh neural induction medium every 3 to 4 days. Differentiated iPSCs were visualized using ICC for neuronal marker Neural Cell Adhesion Molecule (NCAM), and neural-

progenitor marker Nestin (Abcam) conjugated with either AlexaFluor488 or AlexaFluor594 (Invitrogen).

Quantitative RT PCR

The iPSCs were also analyzed *in vitro* using quantitative RT PCR to delineate levels of pluripotency. RNA isolation followed the protocol of Ohnuki and colleagues (2009). Briefly, RNA from each cell line was isolated using Trizol (Invitrogen) and purified with the RNeasy kit (Qiagen, Hilden, Germany). The cDNA was synthesized using QuantiTect Reverse Transcription Kit (Qiagen). Primers consisted of pluripotent markers Oct4, Sox2, Klf4, and c-Myc (Integrated DNA Technologies, Coralville, USA). The RNA and cDNA quantity was measured using a NanoDrop 2000 (Thermo). Analyses of transcripts were performed by quantitative PCR using 2x QuantiTect SYBR Green RT-PCR Master Mix (Qiagen). The glyceraldehyde 3-phosphate dehydrogenase gene (GAPDH) was used as an endogenous control gene. Primers consisted of Oct4, Sox2, Klf4, and c-Myc (Table 5). Quantitative-PCR was performed on MyiQ (BioRad), using the following cycling conditions: 10 minutes at 95°C; then 40 cycles of 10 seconds at 95°C; 10 seconds at 50°C; and 30 seconds at 72°C; a melt curve analysis was ran starting at 65°C for 10 seconds, then increased by 1°C for 10 seconds and repeated 30 times to an end temperature of 95°C. The fold change of each iPSC lineage was calculated using the ΔΔCT normalizing the cycle threshold of each primer pair to GAPDH and then comparing this value to the normalized cycle threshold of the TTFs.

Table 5. *Primer Sequences in Experiment Three.*

Primer	Sequence
GAPDH Forward	GTA TGT CGT GGA GTC TACT G
GAPDH Reverse	GAG TTG TCA TAT TTC TCG TGG T
Oct4 Forward	GAA CAT GTT TCT GCA GTG
Oct4 Reverse	GGT TAC AGA ACC ACA CTC
Klf4 Forward	CCC ACA CTT GTG ACT ATG
Klf4 Reverse	CAG TGG TAA GGT TTC TCG
Sox2 Forward	GCA GTA CAA CTC CAT GAC
Sox2 Reverse	CGA GTA GGA CAT GCT GTA
c-Myc Forward	CTA GTG CTG CAT GAA GAG
c-Myc Reverse	CAG ACA CCA CAT CAA TTTC

GAPDH was selected as a housekeeping gene. Oct4, Klf4, Sox2, and c-Myc were selected to measure mRNA levels of pluripotent genes.

Experiment 4. *Survival and Differentiation of Adenovirus-Generated Induced Pluripotent Stem Cells Transplanted into the Rat Striatum*

Transplantation

Thirty-two adult male Sprague-Dawley (Charles River, Rouen, France) rats weighing between 250-275 grams were used in this study. Twenty rats were unilaterally transplanted with 400,000 adenovirus-generated iPSCs, derived from TTFs (TTF-AD) and suspended in Hanks Balanced Salt Solution (Life Technologies). These iPSCs had been passaged 15-20 times. In addition, 12 rats were injected with 400,000 deactivated rat embryonic feeder cells (dREF). The iPSCs were used at passage 15-20, as previous studies have shown that epigenomic reprogramming is typically incomplete at early passages following derivation (Lister et al., 2011; Stadtfeld et al., 2010). Briefly, animals were anesthetized by i.p. injection of ketamine and

rompun, had their head shaved, and were placed into a stereotaxic device. A single burr-hole was drilled 0.7mm anterior and -2.8mm lateral to bregma. A Hamilton syringe was loaded with 400,000 iPSCs or dREFs at a concentration of 200,000 cells per µL. The Hamilton syringe was slowly lowered to -6.0 mm ventral compared to bregma and the cells and vehicle were injected at 0.8 µL per minute. Following injection, the syringe was left in place for 2 minutes, then raised to -5.6 mm from bregma and a second injection of 1 µL of cells was performed using the same procedure. At the conclusion of injections (a total of 400,000 cells), the Hamilton syringe was left in place for 3 minutes and then slowly retracted and the incision was sutured. The rats were monitored daily for weight gain, signs of infection, and atypical behaviors.

Perfusion, Sectioning, Immunohistochemistry, and Imaging

At 5-, 21-, 63-, and 90-days following transplantation, 5 rats transplanted with iPSCs and 3 rats transplanted with dREFs were randomly selected and overdosed with ketamine and rompun and intracardially perfused with ice cold PBS, followed by 4% paraformaldehyde. Their brains were then carefully removed and placed into 4% paraformaldehyde for 24 hours at 4° C, prior to being transferred into 30% sucrose for 48 hours at 4° C. The brains were then flash frozen using methylbutane and stored at -80°C prior to sectioning at 16 µm on a cryostat. The tissue sections were then mounted on pig-gel coated slides and processed using double fluorescent immunohistochemistry. Non-specific binding sites were blocked by incubating the tissue in 10% normal goat serum, 0.1% Triton X-100, and PBS for one hour at room temperature. The tissue was then incubated in primary antibody (1:500 dilution in PBS and 0.1% Triton X-100) overnight at 4° C.

Primary antibodies from Abcam included anti-rat CD11b (activated microglia) and anti-mouse IBA1 (macrophages); anti-rabbit Doublecortin (immature neurons) and anti-mouse Neural Cell Adhesion Marker (NCAM; mature neuron); anti-rabbit Glial Fibrillary Acidic Protein (GFAP; astrocytes); and anti-mouse Neuronal Nuclei (NeuN; mature neurons) and anti-rabbit Dopamine- and cyclic-AMP-Regulated Phosphoprotein of 32 kDa (DARPP-32; medium spiny neurons of the striatum). The tissue was then rinsed and incubated at room temperature for one hour with the appropriate secondary antibody. Secondary antibodies consisted of AlexaFluor488 and AlexaFluor594.

Fluorescent images were captured using a Zeiss Axiovert 200M at 20x magnification and confocal immunfluorescent images were captured using a Nikon Eclipse Ti A1R with a 40x oil objective. Images were analyzed using ImageJ (NIH). Images of the transplanted cells were captured from seven sections of each animal, starting at 0.7 mm anterior to bregma and 3 sections, approximately 200 µm apart, anterior and posterior to the transplant site. Average intensity of the label, counts of positively labeled cells, as well as percent of co-localization between the transplanted iPSCs and NeuN or DARPP-32 was analyzed between all groups using ImageJ (NIH, Maryland). Densitometric measures were taken from images taken in the striatum and the average intensities were normalized to the contralateral hemisphere. Cells were counted as positive cells if they showed: (1) antibody immunoreactivity within the cell body; (2) the nucleus of that cell was within the counting frame without touching the exclusion lines; and (3) the nucleus of that cell was in focus.

Experiment 5. *Intrastriatal Transplantation of Adenovirus-Generated Induced Pluripotent Stem Cells for Treating Neuropathological and Functional Deficits in a Rodent Model of Huntington's disease*

Animals

Fifty-six Sprague-Dawley rats (28 male and 28 female) at 7.5-8.5 weeks of age were used in this study. Rats were randomly assigned to one of six groups: Sham (5 males and 4 female; given injections of phosphate buffered saline; PBS); 3-NP iPSC 7d (5 male and 6 female rats injected with 3-NP and iPSC transplantation 7-days following the start of 3-NP administration); 3-NP iPSC 21d (6 male and 6 female rats injected with 3-NP and given iPSC transplantation 21-days following the start of 3-NP administration); 3-NP iPSC 42d (6 male and 6 female rats injected with 3-NP and given iPSC transplantation 42-days following the start of 3-NP administration); and 3-NP (6 male and 6 female) rats injected with 3-NP but not given transplants of iPSC to serve as controls.

3-NP Administration

3-NP administration was adapted from a previously established protocol (Rossignol et al., 2011). Briefly, rats were intraperitoneally injected with an increasing dose of 3-NP dissolved in PBS (pH 7.4) over 82 days. Rats received twice daily (at 0700 and 1900h) injections for nine consecutive days, twice daily injections every third day for five weeks, and a single injection (at 0700h) once a week for the duration of the study. Concentrations of 3-NP (for each injection) were 2.5 mg/kg (days 1-3), 3.75 mg/kg (days 4-6), 5 mg/kg (days 7-9), 6.25 mg/kg (days 12, 15, and 18), 7.5 mg/kg (days 21, 24, and 27), 8.75 mg/kg (days 30, 33, 36, 39, and 42), 10 mg/kg (days 47 and 54), 15 mg/kg (days 61 and 68) and 20 mg/kg (days 75 and 82).

Body Weight

Body weight was measured for four consecutive days prior to the administration of 3-NP to achieve a baseline weight for each animal. Baseline weight was recorded as the average weight of these four days. Body weight was monitored throughout the duration of the study, as metabolic alterations are common in animals receiving 3-NP (Beal, 1994; Brouillet et al., 1998). The recorded weights for each animal was averaged at the conclusion of each week and converted to a score representative of percent weight compared to baseline [(average weight/baseline weight)*100].

Accelerod Testing

All rats were tested for motor coordination on the accelerod two days prior to the administration of 3-NP (baseline), and for an additional ten weeks. The accelerod task (Acceler, Rota-Rod 7750; UGO Basile, Italy) was used to assess motor coordination. The rats were required to remain on a 6 cm diameter rod that increased from 4 RPM to 40 RPM over the course of 120 seconds. If the rat was not able to remain on the rotating rod for the full 120 seconds, they fell onto a foam pad located 75 cm below the apparatus.

iPSC Generation

The generation and characterization of the iPSCs followed a previously established/published protocol (Fink et al., in revision). Briefly, iPSCs were generated from tail-tip fibroblasts (TTF) from the tails of adult Sprague-Dawley rats and reprogrammed using our novel adenovirus pair (one adenovirus containing c-Myc, and the other adenovirus containing

Oct4, Sox2, and Klf4). Induced pluripotent stem cells were maintained on rat deactivated feeder cells and were transplanted between passage 25 and 30.

iPSC Transplantation

Thirty-five rats that had received 3-NP administration were giving bilateral transplantations of iPSCs at different time points to mimic the different stages of the progression of HD (i.e., 7-day transplantation, early intervention prior to the onset of motor disturbances; 21-day transplantation, intermediate intervention during the onset of motor disturbances, but prior to robust cell loss in the striatum; 42-day transplantation, late-stage intervention after robust motor deficits were observed and significant cell loss has occurred).

Rats were anesthetized for the duration of the surgery with a mixture of isoflurane and oxygen. The heads of the rats were shaved and disinfected using chlorehexiadin (Molnlycke Healthcare). Rats were placed into a stereotaxic, a midline incision was made on the scalp, and the skin was retracted, exposing bregma. Two burr holes were placed above the striatum (coordinates relative to bregma: anterior 0.5 mm; lateral +2.5 mm and -2.5 mm; tooth bar set at 0). The iPSCs were pre-labeled with Hoechst 33358 (5 µg/mL, Sigma) and re-suspended in Hanks Balanced Salt Solution (HBSS; Gibco) at a density of 200,000 cells per microliter. The cell suspension was loaded into a 10 µL Hamilton microsyringe, moved to the appropriate coordinates, slowly lowered into the striatum (6 mm ventral to dura), and injected at a constant rate over three minutes (0.33 µL/minute). Following the first injection, the microsyringe was left in place for three minutes to allow for the cells to diffuse, then moved dorsally 0.1 mm and a second injection at the same rate was performed. Following the second injection, the microsyringe remained in place for an additional three minutes before being slowly withdrawn

over a three-minute period. The microsyringe was then moved to the opposite hemisphere and the same procedure was followed. The scalp was then closed using sterile 9 mm wound clips and the rats were placed in a recovery cage until fully mobile, at which point, they were returned to their home cage. Rats were observed for 5 days post-transplantation for any signs of pain, discomfort, distress, or complications from surgery, none of which was observed in any of the rats.

Perfusion

At the conclusion of behavioral testing, half of the rats that were designated for immunohistochemical analysis were deeply anesthetized with an overdose of sodium pentobarbital, and transcardially perfused with ice cold 0.1 M PBS, followed by 4% paraformaldehyde (diluted in 0.1 M PBS, pH 7.4). The brains were rapidly removed, suspended in 4% paraformaldehyde for 24 hours at 4°C, and then transferred to 30% sucrose in 0.1 M PBS for 48 hours at 4°C. The brains were then flash frozen, using methylbutane, and stored at -80°C. Thirty micron thick, serial, coronal sections were cut at -20°C on a cryostat (Vibratome UltraPro 5000) and placed into 9 wells containing 0.1 M PBS.

Rapid Decapitation

Rats that were not used for immunohistochemical analysis were rapidly decapitated on the same day and had their brains removed, dissected (into the cortex, striatum, and remaining whole brain), and flash frozen using liquid nitrogen for mRNA analysis. Rapid decapitation was performed without the use of anaesthesia as to not compromise the results of the molecular analysis.

Histology

Brain tissue was labeled using cytochrome oxidase (CYO) and immunohistochemistry using either 3,3'-diaminobenzidine (DAB) or fluorescence for visualization (Rossignol et al., 2009). Briefly, tissue from a single well (containing striatal sections 270 microns apart) was used for each label.

CYO (metabolically active tissue) was used as previous studies have shown that injections of 3-NP cause significant striatal atrophy (Rossignol et al., 2011). Briefly, tissue designated for CYO analysis was submersed in solution of 800 µg of sucrose, 4 mg of cytochrome C, and 1 mg of DAB dissolved in 20 mL of phosphate-buffer for 4 hours at room temperature. The tissue was then transferred to deionised H_2O, mounted onto positively charged glass slides, and coverslipped using Depex (Electron Microscopy, Hatfield, PA).

Tissue designated for CD11b (activated microglia; Abcam, 1:500) and IBA1 (macrophages; Abcam, 1:500) DAB immunohistochemistry was used to determine the level of endogenous immune response to the 3-NP and the transplanted iPSCs. Tissue was placed into a solution of 0.3% hydrogen peroxide for ten minutes. The tissue was placed into the primary antibodies overnight at 4º C. The tissue was rinsed twice with PBS + 0.1% Triton X-100 (Sigma) and then incubated in the appropriately conjugated secondary antibodies (biotin; 1/300) for one hour at room temperature. The tissue was rinsed twice in PBS + 0.1% Triton X-100, and placed in an avidin-biotin peroxidase (ABC; Vector Laboratory, Bulingame, CA). Sections remained in the solution for 5 minutes, after which they were moved to the DAB solution (Vector Laboratory, Bulingame, CA). After remaining in the DAB solution for 5 minutes, the tissue was

transferred into deionised H_20. The tissue was mounted onto charged glass slides, were given a series of ascending alcohol rinses (70%, 95%, 100%), placed into xylene for 5 minutes, and coverslipped using Depex (Electron Microscopy, Hatfield, PA).

Tissue designated for fluorescent labeling had non-specific binding sites blocked by incubating the tissue in 10% normal goat serum, 0.1% Triton-X, and 0.1 M PBS for one hour at room temperature. The tissue was then transferred into a well containing the primary antibodies for 24 hours at 4°C. Primary antibody pairs used for doubling labeling included neuronal nuclei (NeuN, mature neurons; Chemicon; 1/500 dilution) and dopamine- and cAMP-regulated phosphoprotein of 32 kDa (DARPP32, D1 receptors located on the medium spiny neurons located in the striatum; Abcam; 1/500). Glial fibrillary acidic protein (GFAP, astrocytes; Abcam, 1:500) was used alone on separate sections. Following incubation in the primary antibodies, tissue was rinsed and transferred into a well containing the appropriately conjugated secondary antibodies for one hour at room temperature. Secondary antibodies included AlexaFluor488 and AlexaFluor594 (1/300, Invitrogen). Following incubation the tissue was rinsed, and mounted onto positively charged glass slides using Fluoromount (Sigma).

RNA Isolation

RNA isolation was performed from the non-perfused brain samples using a Qiagen All-prep system. All procedures followed the manufactures guidelines. Briefly, striatal tissue was homogenized using a lysis buffer and transferred to an AllPrep spin column and centrifuged at 8000 x g for 1 minute. The AllPrep spin column was then placed in a new collection tube, 300 µL of buffer RLT was added, and the sample was centrifuged at 8000 x g for 1 minute. Then, 350 µL of 70% ethanol was added to the flow-through and mixed thoroughly. All contents of the

flow-through were then added to an RNeasy spin column and centrifuged at 8000 x g for 1 minute. The flow-through was discarded, 700 μL of RW1 buffer was added to the RNeasy spin column, and the column was centrifuged at 8000 x g for 30 seconds. The flow-through was again discarded, and 500 μL of RPE buffer was added to the RNeasy spin column and the column was centrifuged at 8000 x g for 30 seconds. The RNeasy spin column was placed in a new collection tube, 30 μL of RNase-free water was added to the spin column, and the column was centrifuged at 8000g for 1 minute. Purified RNA, in the collection tube, was analyzed using a NanoDrop2000 spectrophotometer (ThermoScientific) and was stored at -20º C until used for cDNA synthesis. A QuantiTect Reverse Transcription Kit (Qiagen) was used for cDNA synthesis following the manufacturers' guidelines. Briefly, RNA was incubated at 42º C for 2 minutes in a genomic DNA elimination buffer. The solution was transferred to a reverse-transcription master mix and incubated at 42º C for 30 minutes and then 3 minutes at 95º C to inactivate the reverse transcriptase. The cDNA was stored at -20º C until used in quantitative PCR experiments.

Analyses of transcripts were performed by quantitative real-time polymerase chain reaction (RT-PCR) using 2x QuantiTect SYBR Green RT-PCR Master Mix (Qiagen). The glyceraldehyde 3-phosphate dehydrogenase gene (GAPDH) was used as an endogenous control gene. Primers consisted of brain-derived neurotrophic factor (BDNF) and tumor necrosis factor-alpha (TNF-α; Table 1). RT-PCR was performed on MyiQ (BioRad), using the following cycling conditions: 10 minutes at 95°C; then 40 cycles of 10 seconds at 95°C; 10 seconds at 50°C; and 30 seconds at 72°C. The fold change of each iPSC lineage was calculated using the delta-delta

CT normalizing the cycle threshold of each primer pair to GAPDH and then comparing this value to the normalized cycle threshold of a control sample.

Table 6. *Primer Sequences in Experiment Five*.

Primer	Sequence
GAPDH Forward	GTA TGT CGT GGA GTC TAC TG
GAPDH Reverse	GAG TTG TCA TAT TTC TCG TGG T
BDNF Forward	GAA GAG CTG CTG GAT GAG GAC
BDNF Reverse	TTC AGT TGG CCT TTT GAT ACC
TNF-α Forward	GTT CGG ATC CCA CTG TGA CT
TNF-α Reverse	GTC CCC AGA GCC AAT GAC TA

GAPDH was selected as a housekeeping gene. BDNF was selected to measure the mRNA levels of Brain-derived Neurotrophic Factor. TNF-α was selected to measure the mRNA levels of a protein associated with inflammation.

Imaging and Image Analysis

Fluorescent images were taken at 20x magnification with a Zeiss Axiovert 200M inverted fluorescent microscope with an apotome using Axiovision v4.8. The images were analyzed using ImageJ (National Institutes of Health, Bethesda, MD) for number of positively-labeled cells, number of transplanted cells, and density of the positively-labeled tissue. The brain tissue labeled with CYO, IBA1, and CD11b was scanned using a Nikon Coolscan IV and Nikon Scan v4 software. Cell counts, area and optical densitometry was measured for the cortex, striatum, lateral ventricle, and the whole brain, using ImageJ, at 1.0 mm anterior, 0.5 mm anterior, and 0 mm from bregma, (Paxinos and Watson, 1986).

Statistical Analysis

Experiment 1. *Reductions in Behavioral Deficits and Neuropathology in the R6/2 Mouse Model of Huntington's disease following Transplantation of Bone-Marrow-Derived Mesenchymal Stem Cells is Dependent on Passage Number*.

All statistical analyses were performed using SPSS v16 with an alpha level equal to 0.05. All behavioral data was analyzed using a repeated measures analysis of variance (ANOVA), to measure changes between genotypes and treatments across weeks. Histological data was analyzed using a one-way ANOVA. When appropriate, a Fisher's Protected Least Significant Difference (PLSD) *posthoc* test was performed.

Experiment 2. *Transplantation of Umbilical-Cord-Blood-derived Mesenchymal Stem Cells into the Striata of R6/2 Mice: Behavioral and Neuropathological Analysis*

All statistical analyses were performed using SPSS v16 with an alpha level equal to 0.05. All behavioral data was analyzed using a repeated measures analysis of variance (ANOVA), to measure changes between genotypes and treatments across weeks. Histological data was analyzed using a multivariate ANOVA. When appropriate, a Fisher's Protected Least Significant Difference (PLSD) *post hoc* tests were performed.

Experiment 3. *Adenovirus-Generated Induced Pluripotent Stem Cells*

All statistics were analyzed using SPSS v16.0. Multivariate analysis of variance (ANOVA) was used to analyze all data, except for the PCR measures comparing cell source and reprogramming methods, in which an univariate ANOVA was utilized. Protected least significant differences *posthoc* (PLSD) analyses were performed when appropriate. In all analyses, the significance was established at $p < 0.05$.

Experiment 4. *Survival and Differentiation of Adenovirus-Generated Induced Pluripotent Stem Cells Transplanted into the Rat Striatum*

All statistics were analyzed using SPSS v16.0. Multivariate analysis of variance (ANOVA) was used to analyze all data. Protected least significant differences *posthoc* (PLSD) analyses were performed when appropriate. In all analyses, the significance was established at $p < 0.05$.

Experiment 5. *Intrastriatal Transplantation of Adenovirus-generated Induced Pluripotent Stem Cells for Treating Neuropathological and Functional Deficits in a Rodent Model of Huntington's disease*

All statistical analyses were performed using SPSS v16 with an alpha level equal to 0.05. All behavioral data was analyzed using a repeated-measures analysis of variance (ANOVA), to measure changes between groups and treatments across weeks. Histological data was analyzed using a multivariate ANOVA. When appropriate, a Fisher's Protected Least Significant Difference (PLSD) *posthoc* test was performed.

CHAPTER V

PRESENTATION OF DATA

Experiment 1. *Reductions in Behavioral Deficits and Neuropathology in the R6/2 Mouse Model of Huntington's disease following Transplantation of Bone-Marrow-Derived Mesenchymal Stem Cells is Dependent on Passage Number.*

In Vitro Cell Characterization

Both low- and high-passage BM MSCs showed positive expression of SCA1, a marker of mouse MSCs and negative expression of CD45, a marker of hematopoietic stem cells (Figure 2). However, analysis of the flow cytometry data (Figure 3) revealed that low-passage BM MSCs displayed 15.3% positive expression of SCA1, while high-passage BM MSCs displayed 74.8% positive expression of SCA1, indicating that SCA1 changes over passages. Flow cytometry measures of CD45 revealed that 53.4% of low-passage BM MSCs expressed CD45, which decreased to 10.4% positive expression at high-passage. This data indicates that either a selection process is taking place over passages, with $SCA1^{+}/CD45^{-}$ cells proliferating at a higher rate, or that prolonged exposure to culture conditions causes expression levels to change. In either case, these data suggests that high-passage mouse BM MSCs may prove to more suitable for transplantation studies.

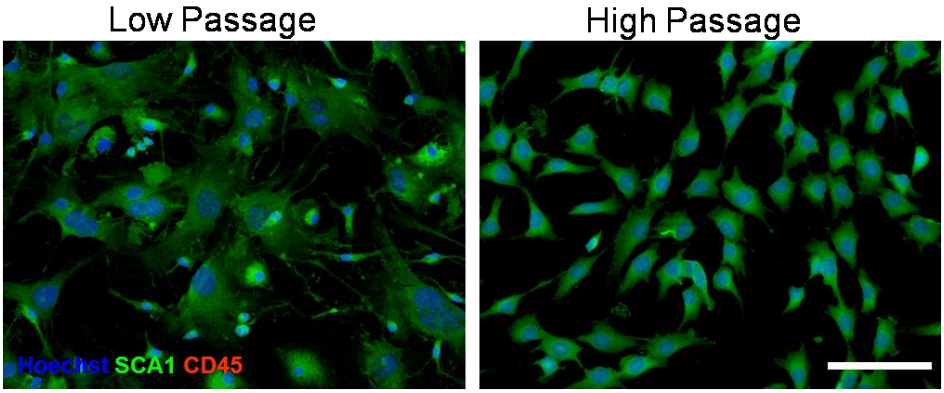

Figure 2. *Immunocytochemistry (ICC) of low- and high-passage bone-marrow mesenchymal stem cells (BM MSCs).*
Low- and high-passage BM MSCs displayed typical MSC morphology, expressed the mesenchymal stem cell marker SCA 1, and were negative for the hematopoietic stem cell marker CD45. Scale bar represents 100 µm.

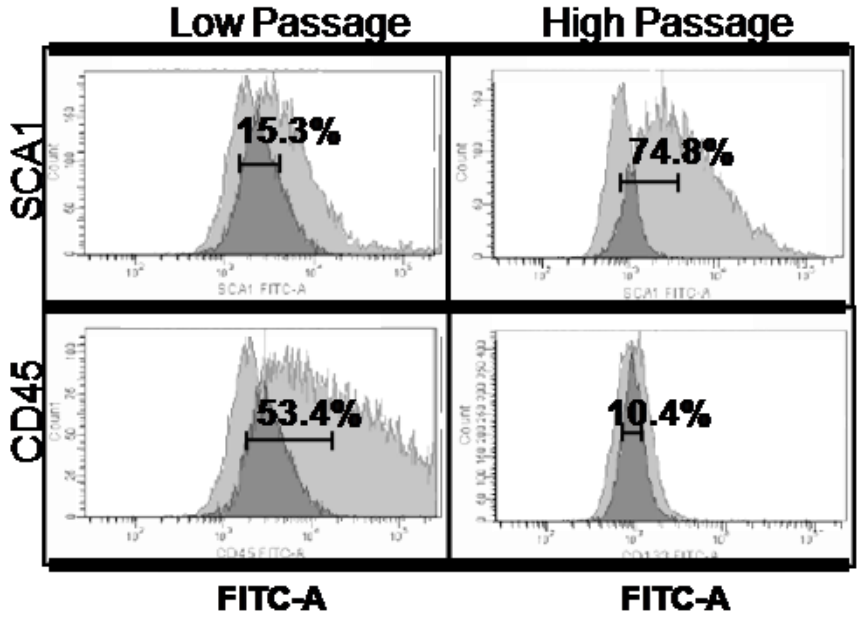

Figure 3. *Flow cytometry results of low- and high-passage bone-marrow mesenchymal stem cells (BM MSCs).*
An increase in the number of cells positively expressing SCA 1 was observed as passage number increased. Also, a decrease in the hematopoietic stem cell marker CD45 was observed as cell passage increased.

An independent *t-test* of BDNF gene expression revealed a significant difference between low- and high-passaged BM MSCs [$t_{(4)} = 9.120$, $p = 0.001$] with high-passage displaying a significantly higher expression of BDNF mRNA, suggesting that high-passage BM MSCs may prove to be more effective following intra-striatal transplantation due to pro-neuron survival trophic factor release (Figure 4).

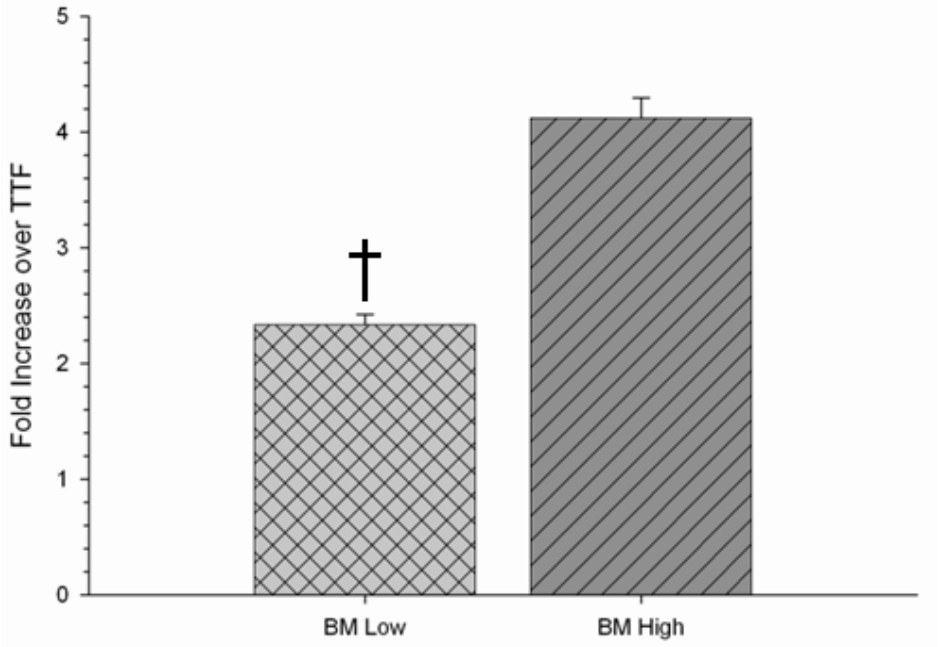

Figure 4. *In vitro quantitative RT-PCR of BDNF mRNA expression of bone-marrow mesenchymal stem cells (BM MSCs).*
A significant increase in mRNA levels of BDNF was observed in the high-passaged BM MSCs compared to low-passaged BM MSCs. (Note: † significant from high-passage BM MSCs; TTF are control cDNA isolated from mice tail-tip fibroblasts.) Bar graph represents mean value; error bars represents SEM.

Behavioral Results

In this aggressive model of HD, clear motoric deficits, tested on the rotarod, become apparent around 5 weeks-of-age. A repeated-measures ANOVA revealed a significant interaction between weeks and group [$F_{(18,174)} = 2.247$, $p = 0.004$] as well as a significant between-group

difference for the latency to fall during the rotarod task [$F_{(3,29)} = 12.092$, $p = 0.001$; Figure 5]. A PLSD *post hoc* analysis revealed significant motoric deficits between R6/2 and WT mice at all time-points during the study. Mice transplanted with low-passage BM MSCs displayed only modest benefits in their performance the rotarod task, with deficits delayed by one week, relative to non-transplanted R6/2 controls.

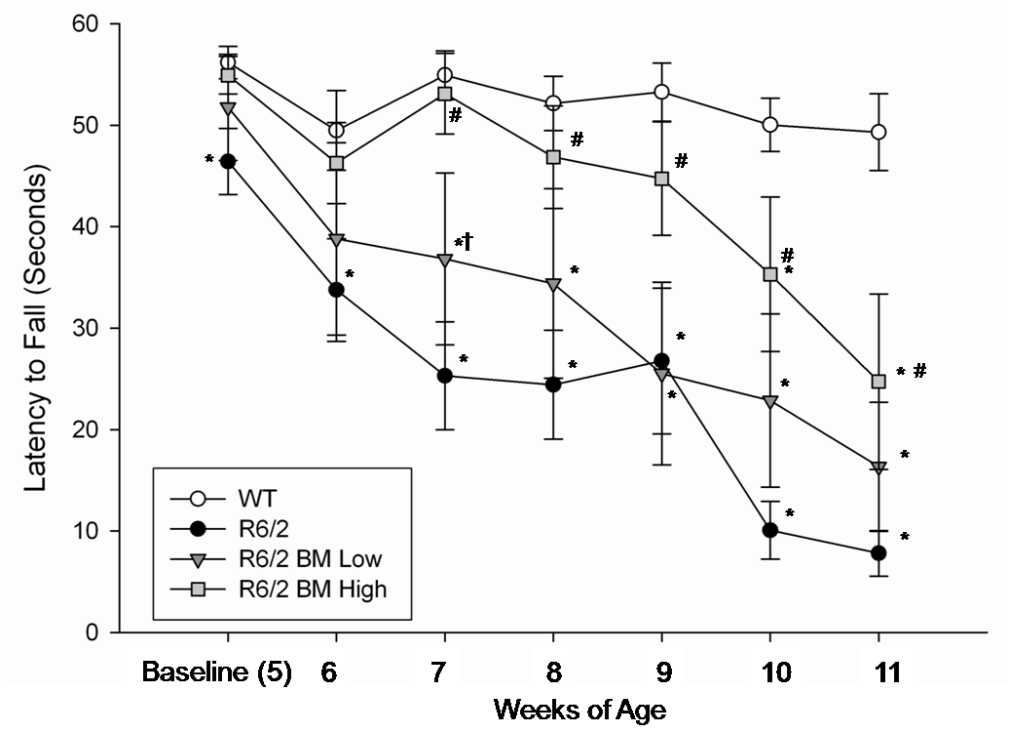

Figure 5. *Motor coordination assessment of R6/2 mice following bone-marrow mesenchymal stem cell (BM MSC) transplantation.*
A significant decline in motor coordination was observed in untreated R6/2 mice when compared to WT mice. The R6/2 mice that received transplantation of high-passage BM MSCs displayed significantly longer latencies to fall compared to untreated R6/2 mice starting at 7-weeks of age and continuing throughout the study. (Note: * significant from WT; # significant from R6/2; † significant from high-passage BM MSCs) Line graph represents mean value; error bars represents SEM.

However, in the R6/2 group that was transplanted with high-passage BM MSCs, the latency to fall from the rotarod was comparable to WT mice starting at baseline (when the mice were 5 weeks old) and continuing until the animals were 10 weeks old. Rotarod performance of mice with high-passage BM MSC transplants were statistically different than non-transplanted R6/2 mice, beginning at 7-weeks of age, with this trend continuing throughout the duration of the study. A significant difference on the rotarod task was also observed between high-passage BM MSC and low-passage BM MSC when the mice were 7 weeks old. Although high-passage BM MSC transplanted mice eventually showed a decline in motor coordination on the rotarod, they still had significantly longer latencies to fall off the rotarod than untreated R6/2 mice, suggesting behavioral sparing occurred, even at the late-stages of the progressive HD-like deficits.

Analysis of cognition through MWM testing reveal significant spatial learning deficits in the R6/2 mice, appearing between 5-7 weeks-of-age. A repeated-measures ANOVA revealed significant differences between groups for the probability of correctly finding the hidden platform [$F_{(3, 33)} = 13.143$, $p = 0.001$] and a significant interaction between week and group [$F_{(15,165)} = 3.014$, $p = 0.001$; Figure 6]. A PLSD *post-hoc* analysis revealed significant differences between R6/2 and WT mice during the baseline testing period as well as significant differences when the mice were 8-, 9-, 10-, and 11-weeks old.

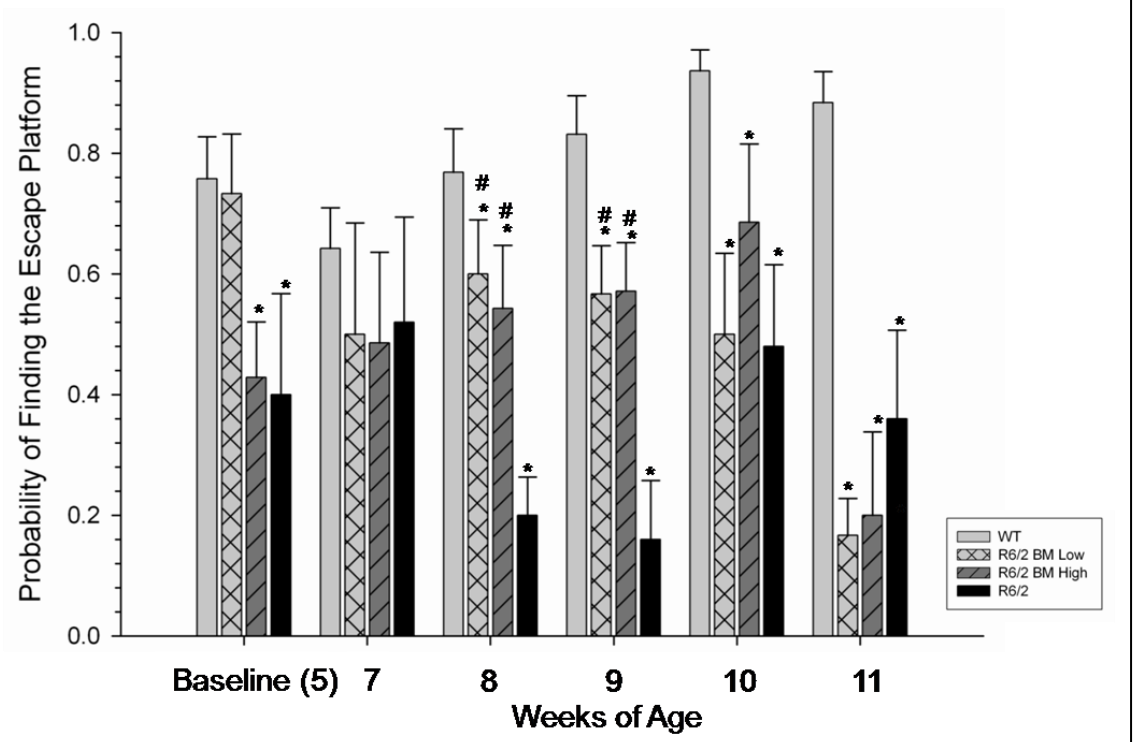

Figure 6. *Spatial memory assessment of R6/2 mice following bone-marrow mesenchymal stem cell (BM MSC) transplantation*.
Untreated R6/2 mice displayed significant impairment in spatial memory at 5-, 8-, 9-, 10-, 11-weeks of age when compared to WT mice. Mice receiving either low- or high-passage BM MSCs displayed an intermediate sparing of spatial memory at 8- and 9-weeks of age. (Note: * significant from WT; # significant from R6/2; † significant from high-passage BM MSCs.) Bar graph represents mean value; error bars represents SEM.

For mice that received transplantation of BM MSCs, an intermediate effect in cognitive performance was observed when the mice were 8- and 9-weeks old, where they had a significantly higher probability to find the hidden platform than untreated R6/2 mice, but still a significantly lower probability to find the hidden platform than WT mice. However, at 9- and 10-weeks of age, both transplant groups declined in cognitive performance to the untreated R6/2 level.

These data indicate that, while a preservation of cognitive function is possible following transplantation of either low- or high-passage BM MSCs, these mice display similar cognitive dysfunction in the late-stage of the HD-like progressive of cognitive deficits.

The limb-clasping response is a reliable behavioral phenotype observed in many transgenic animals, and may be related to cortical dysfunction in this mouse model of HD (Dey et al., 2010; Lalonde & Strazielle, 2011; Samadi et al., 2013). A repeated-measures ANOVA revealed main effect of group in the limb-clasping response task [$F_{(3,37)} = 20.204$, $p = 0.001$], and a significant interaction between week and group [$F_{(18,222)} = 9.740$, $p = 0.001$; Figure 7]. Confirming this phenotypic behavior, PLSD *post hoc* analysis revealed significant differences between R6/2 and WT mice beginning at 8-weeks of age and continuing for the duration of the study. A PLSD *post hoc* analysis also revealed R6/2 mice transplanted with high-passage BM MSCs showed a delay in onset of limb clasping until 10 weeks of age, at which point these animals also showed significantly fewer limbs clasped compared to R6/2 mice transplanted with low-passage BM MSCs. Significant differences were also observed between high-passage BM MSC group and untreated R6/2 mice starting at 9-weeks of age. Interestingly, R6/2 mice receiving transplants of low-passage BM MSC displayed significantly more limbs clasped, compared to WT mice, during all testing weeks, whereas untreated R6/2 mice did not start showing significantly more clasping behavior than WT mice until the mice were 8 weeks old.

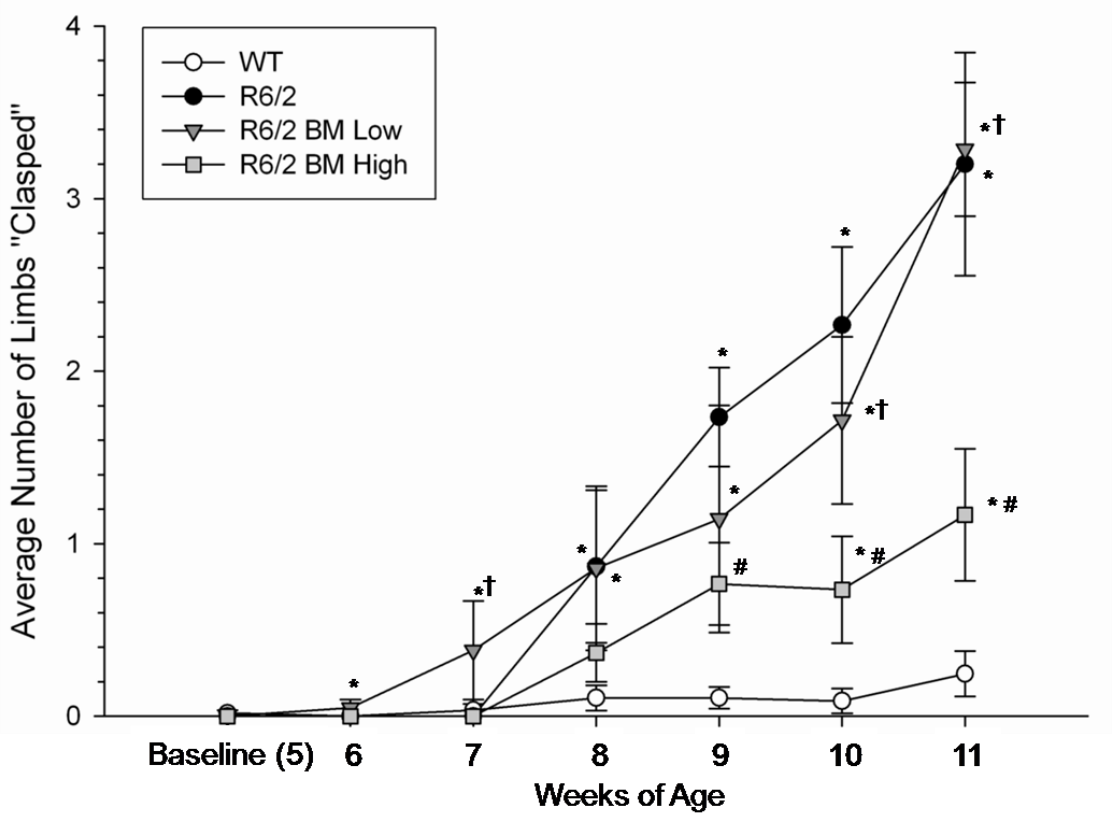

Figure 7. *Limb-clasping response of R6/2 mice following bone-marrow mesenchymal stem cell (BM MSC) transplantation.*
Untreated R6/2 mice had significantly more limb-clasping responses than WT mice starting at 8-weeks of age, with this impairment continuing for the duration of the study. R6/2 mice that received transplantations of high-passage BM MSCs had significantly fewer limb-clasping responses than untreated R6/2 mice for the duration of the study, starting at 9-weeks of age. (Note: * significant from WT; # significant from R6/2; † significant from high-passage BM MSCs) Line graph represents mean value; error bars represents SEM.

Histological Results

Six weeks following transplantation, when mice were 11.5 weeks old, brains were preserved and analyzed for gross morphology and mitochondrial integrity, as well as transplanted cell survival and immune reaction. Scans from five levels (approximately 100-, 300-

, 500-, 700-, and 900 µm anterior to bregma) of CYO stained tissue were outlined, and total area of the brain was analyzed for each animal (Figure 8A) each section was normalized to the corpus callosum. A one-way ANOVA revealed significant between group differences in the area of the whole brain from the sections analyzed [$F_{(3,105)} = 3.209$, $p = 0.026$]. A PLSD *post hoc* analysis revealed that total brain area in untreated R6/2 mice was significantly smaller than WT animals, suggesting general brain atrophy. This brain atrophy was not observed in R6/2 mice transplanted with low- or high-passage BM MSCs, as both groups were not significantly different from the WT group (Figure 8B).

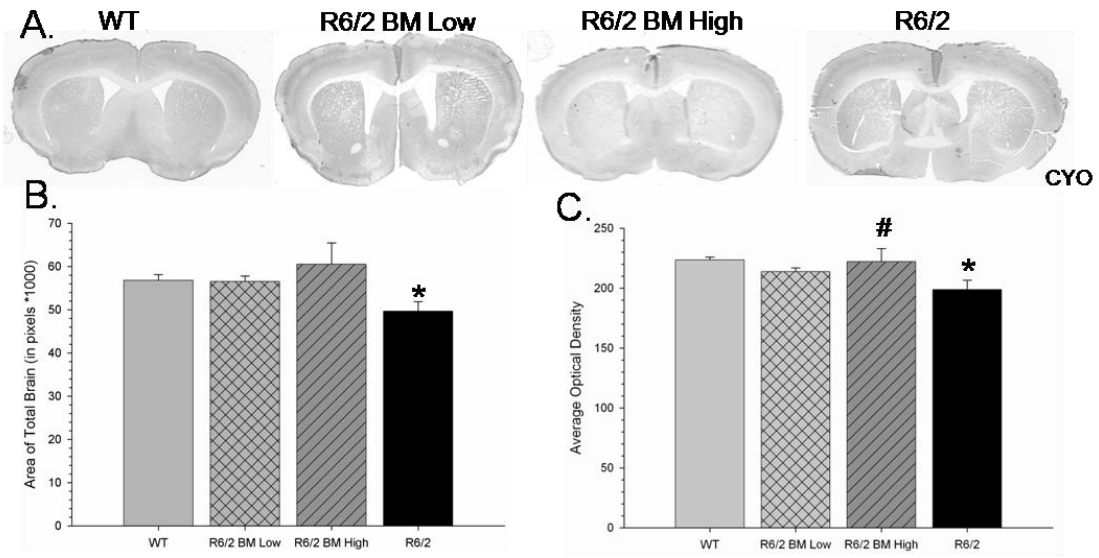

Figure 8. *Measures of brain area and evidence of metabolic integrity in the striata of mice receiving bone-marrow mesenchymal stem cell transplantations*.
Gross morphology of the brain near the area of transplantation can be visualized with cytochrome oxidase labeling (A). Untreated R6/2 mice had a significant decrease in total brain area when compared to WT mice (B). Optical densitometric measures of cytochrome oxidase in the striata labeled tissue revealed significantly less metabolic activity in the striata of untreated R6/2 mice when compared to WT mice at the time of necropsy. R6/2 mice that received transplantation of high-passage BM MSCs had significantly higher levels of metabolically active tissue than untreated R6/2 mice (C). (Note: * significant from WT; # significant from R6/2) Line graph represents mean value; error bars represents SEM.

Optical densitometric analysis of CYO labeling in the striatum revealed a between-group difference [$F_{(3,105)} = 5.896$, $p = 0.002$], with untreated R6/2 mice having less density of CYO labeling in the striatum, when compared to WT mice. Mice transplanted with low-passage MSCs displayed in intermediary effect, which was not significantly different from either WT or untreated R6/2 mice. Importantly, amount of CYO-labeled tissue in R6/2 mice transplanted with high-passage BM MSCs was indistinguishable from those levels observed in WT mice (Figure

8C). This data suggests that transplantation of either low- or high-passage BM MSCs can prevent the loss of metabolically active tissue, but transplantation of high-passage significantly reduces the level of metabolic loss when compared to untreated R6/2 mice.

Analysis of the number of Hoechst-labeled BM MSCs in the striatum at six weeks following transplantation, revealed no significant differences between low- and high-passage groups [$t_{(43)} = 1.372$, $p = 0.233$], demonstrating that both low- and high-passage BM MSCs were capable of surviving in the brain (Figure 9B). Analysis of images taken from fluorescent microscopy revealed that transplanted cells did not co-localize with IHC-labeled tissue for mature neurons (NeuN) and astrocytes (GFAP; Figure 9A), suggesting that BM MSCs did not differentiate into tissue of a neuronal lineage. Optical densitometry analysis of GFAP labeled tissue from the areas around the transplant site revealed no significant differences between groups [$F_{(3,88)} = 0.440$, $p = 0.725$; Figure 9C].

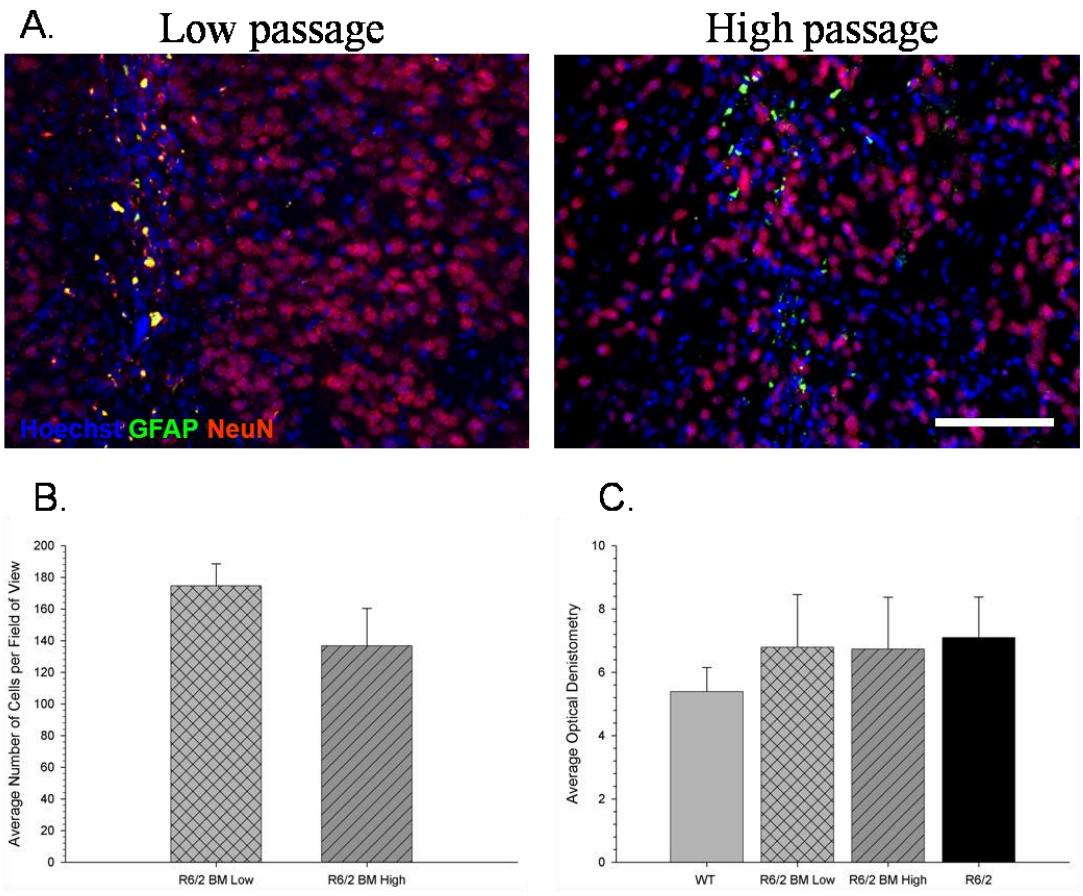

Figure 9. *Immunohistochemical analysis of the transplanted bone-marrow mesenchymal stem cells (BM MSCs).*
No neuronal or glial differentiation was observed from the transplanted BM MSCs as seen by the lack of co-localization between the BM MSCs (blue) with NeuN (red) or GFAP (green), respectively (A). No significant differences were observed in the amount of surviving BM MSCs between low- and high-passage BM MSCs (B). Also, no significant differences were observed between all groups in densitometric measures of GFAP around the transplant site (C).

mRNA Expression

As neurotrophic factors play an important role in the pathology of HD, mRNA was isolated from the striatum of mice 6 weeks following transplantation. RT-PCR analysis of BDNF

expression revealed a significant main effect of group [$F_{(3,15)} = 4.134$, $p = 0.032$; Figure 10A]. A PLSD *post hoc* analysis revealed that untreated R6/2 mice had a significant reduction in BDNF expression compared to WT mice. Both BM MSC transplant groups had significantly higher expression of BDNF compared to untreated R6/2 mice. Analysis of expression levels of the BDNF receptor TrkB revealed no significant differences between groups [$F_{(3,15)} = 1.895$, $p = 0.184$; Figure 10B], although a strong trend was observed between WT and R6/2 mice. Similar to TrkB, a one-way ANOVA revealed no significant between-group differences in gene expression of NGF in the tissue dissected from the striata [$F_{(3,13)} = 2.232$, $p = 0.147$] although a strong trend was observed between WT and R6/2 mice (Figure 10C). Analysis of pro-inflammatory gene TNF α revealed no significant between group differences in gene expression [$F_{(3,15)} = 2.664$, $p = 0.095$; Figure 10D].

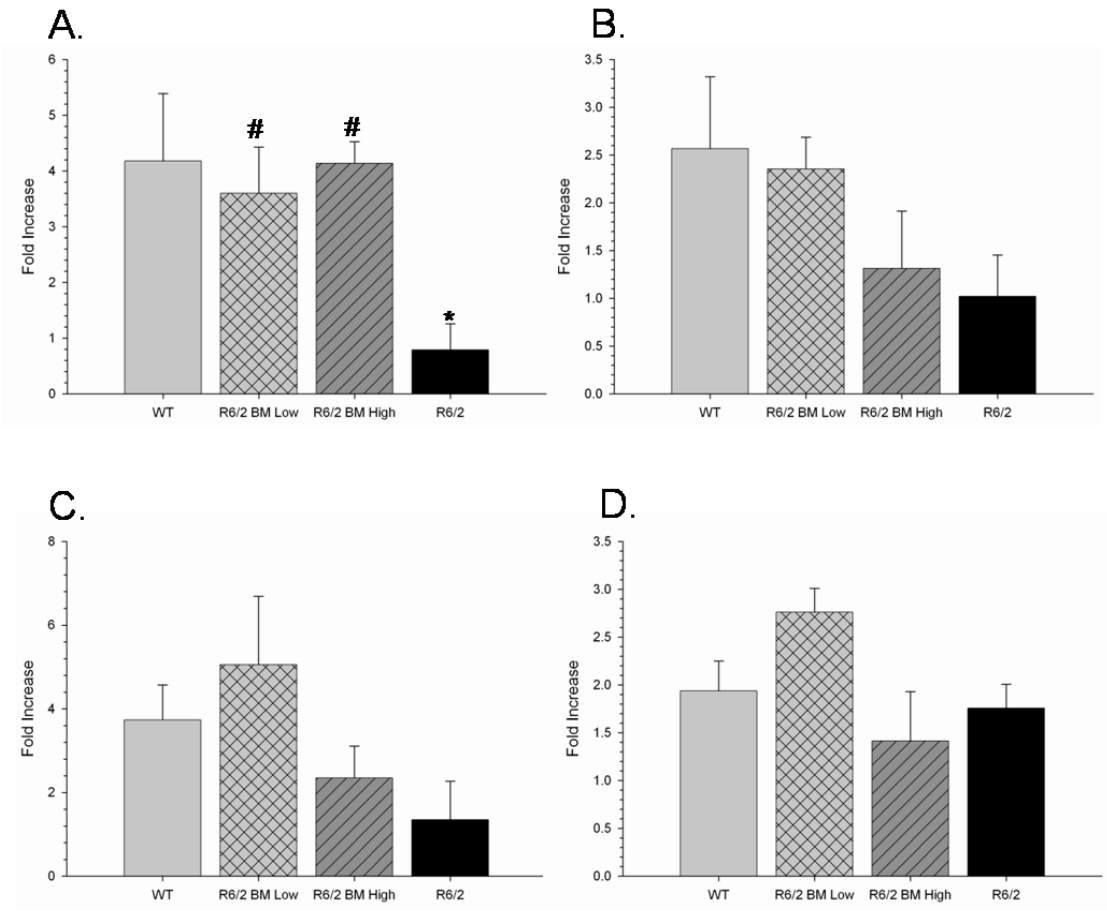

Figure 10. In vivo quantitative RT-PCR of BDNF, TrkB, NGF, and TNF α mRNA expression following transplantation of bone-marrow mesenchymal stem cells (BM MSCs).

Untreated R6/2 mice had significantly lower expression of BDNF than WT, R6/2 mice receiving low-passage BM MSCs, and R6/2 mice receiving high-passage BM MSCs (A). No significant differences were observed in the expression levels of TrkB (B), NGF (C), or TNF α (D) between groups. (Note: * significant from WT; # significant from R6/2) Bar graph represents mean value; error bars represents SEM.

Experiment 2. *Transplantation of Umbilical-Cord-Blood-derived Mesenchymal Stem Cells into the Striata of R6/2 Mice: Behavioral and Neuropathological Analysis*

In Vitro Cell Characterization

Measures of ICC for both low- and high-passage UCB MSCs showed positive expression of SCA1, a marker of mouse MSCs (Figure 11). Flow cytometry revealed that low-passage UCB MSCs displayed 31.2% positive expression of SCA-1 and high-passage UCB MSCs displayed 30.3% positive expression of SCA-1 (Figure 12), contrasting what was observed previously, where expression of SCA1 increased over passages in bone-marrow derived MSCs. Flow cytometry confirmed ICC analysis revealing that 58.0% of the low-passaged UCB MSCs were positive for CD45, a marker of hematopoietic stem cells, while 1.7% of the high-passaged UCB MSCs were positive for CD45. The high expression of CD45 at low-passage is most likely due to the fact that the UCB MSCs are isolated from umbilical cord blood, which contains a high proportion of hematopoietic stem cells. However, this data indicates that CD45 expression is decreasing over passages, either due to prolonged exposure to culture conditions or a selection process occurring during the expansion of cells.

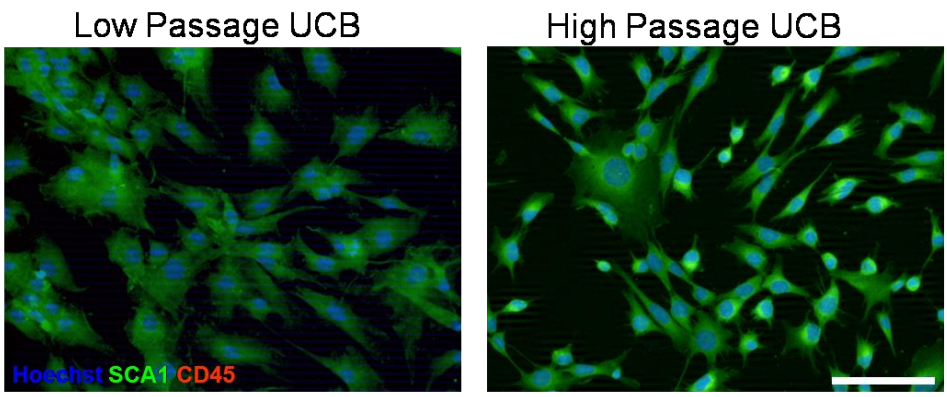

Figure 11. *Immunocytochemistry (ICC) of low- and high-passaged umbilical cord blood mesenchymal stem cells (UCB MSCs).*
Low- and high-passaged UCB MSCs expressed the MSC marker SCA1, were negative for the hematopoietic stem cell marker CD45, and displayed typical MSC morphology. Scale bar represents 100 µm.

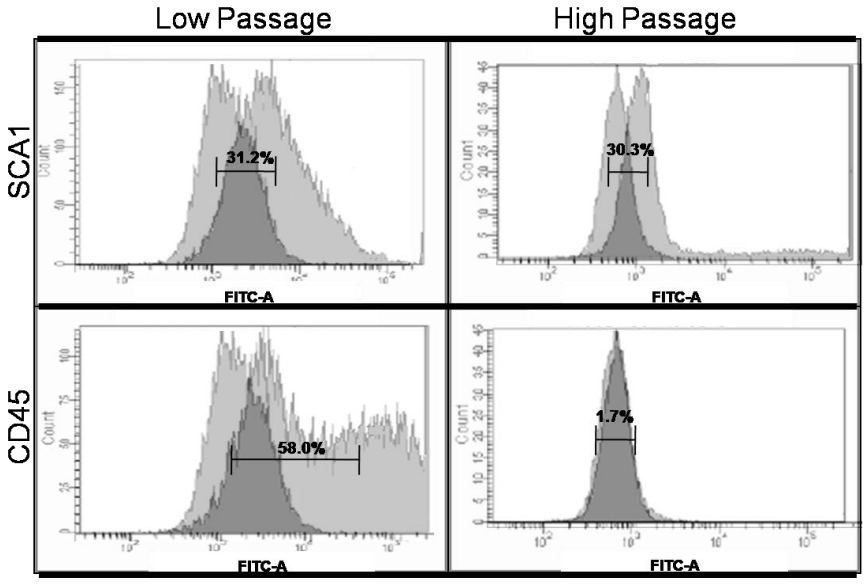

Figure 12. *Flow cytometry results of low- and high-passaged umbilical cord blood mesenchymal stem cells (UCB MSCs).*
The number of cells positively expressing SCA1 remained relatively stable as passage number increased. A decrease in the hematopoietic stem cell marker CD45 was observed as cell passage increased.

Characterization of UCB MSCs through mRNA isolation and RT-PCR revealed a significant differences in gene expression of BDNF between low- and high-passaged UCB MSCs [$t(4) = 21.488$, $p < 0.001$], with low-passaged cells displaying a significantly higher expression of the mRNA for BDNF (Figure 13). As BDNF is related to the pathology of HD (Zuccato et al., 2011), these results suggest that the low-passage UCB MSCs may be a more suitable cell for transplantation because they expressed the highest amount of BDNF, surprisingly, these results are in contrast to what was previously observed in our study with bone-marrow MSCs, whereby murine MSCs that have been maintained in culture for more than 40 passages had higher expression of BDNF mRNA than those that had been maintained in culture for less than 8 passages.

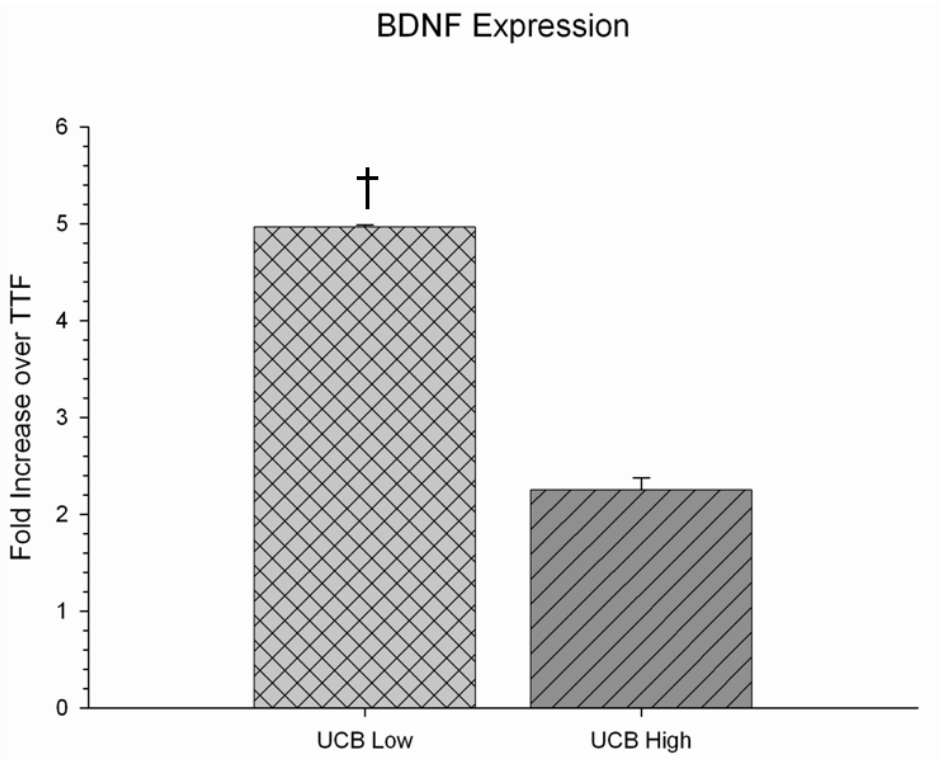

Figure 13. *In vitro quantitative RT-PCR of BDNF mRNA expression of umbilical cord blood mesenchymal stem cells (UCB MSCs).*
A significant decrease in mRNA levels of BDNF was observed in the high-passaged UCB MSCs compared to low-passaged UCB MSCs. (Note: † significant from high-passage UCB MSCs; TTF are control cDNA isolated from mice tail-tip fibroblasts.) Bar graph represents mean value; error bars represents SEM.

Behavioral Results

In the rotarod task, a repeated-measures ANOVA revealed significant between-group differences for the latency to fall [$F_{(3,36)} = 13.575$, $p < 0.01$] (Figure 14). A significant interaction was observed between weeks and group [$F_{(18,216)} = 5.286$, $p < 0.001$]. PLSD analysis revealed significant differences between R6/2 and WT mice during the baseline testing period as well as significant differences during all testing weeks. Transplantation of low-passage UCB MSCs did not infer significant motor benefits, as these animals were similar to R6/2 control mice at all

time-points. However, significant differences were observed between R6/2 and high-passage UCB MSC mice at 10 weeks of age.

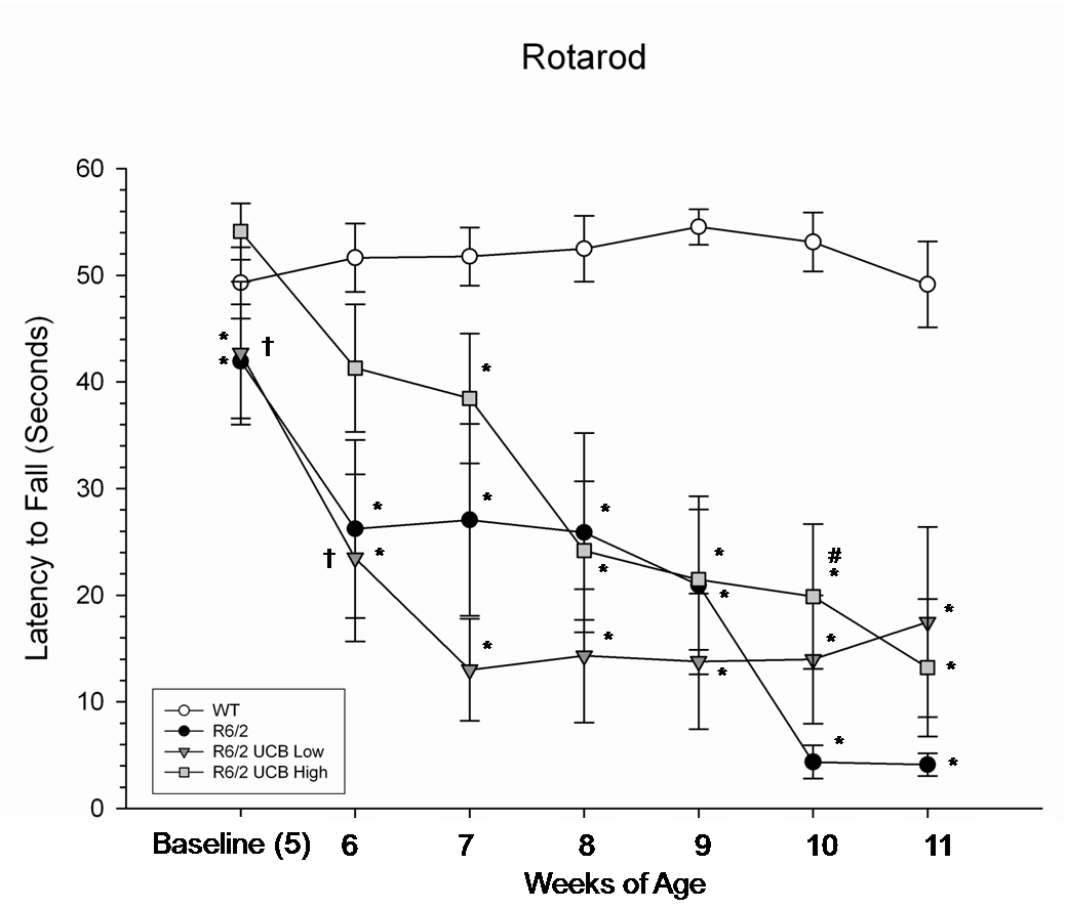

Figure 14. *Motor coordination assessment of R6/2 mice following umbilical cord blood mesenchymal stem cell (UCB MSC) transplantation.*
A significant decline in motor coordination was observed in untreated R6/2 mice when compared to WT mice. The R6/2 mice that received transplantation of high-passage UCB MSCs displayed significantly longer latencies to fall, compared to untreated R6/2 mice at ten weeks of age. (Note: * significant from WT; # significant from R6/2; † significant from high-passage UCB MSCs) Line graph represents mean value; error bars represents SEM.

In the MWM task, a repeated-measures ANOVA revealed significant differences between groups for the probability of correctly finding the hidden platform [$F_{(3,37)} = 4.806$, $p < 0.01$](Figure 15). Each trial was scored as "correct" if the mouse was capable of finding the hidden platform in less than sixty seconds and the probability of a "correct" trial was calculated at the end of each testing session (number of correct trials/number of total trials). In this task, untreated R6/2 mice begin to display impairment in spatial memory beginning at 9-weeks-of-age and continuing for the duration of the study. Significant differences were also observed between WT and low-passage UCB MSC at 7-, 9-, and 10- weeks of age. Significant differences were also observed between WT and high-passage UCB MSC at 8-, 9-, and 10-weeks of age. Although no significant differences were observed between the UCB MSC transplant groups and the untreated R6/2 group, trends were observed at 11-weeks of age, with the transplanted groups (low-passage $p = 0.13$; high-passage $p = 0.10$) having a higher probability of finding the hidden platform.

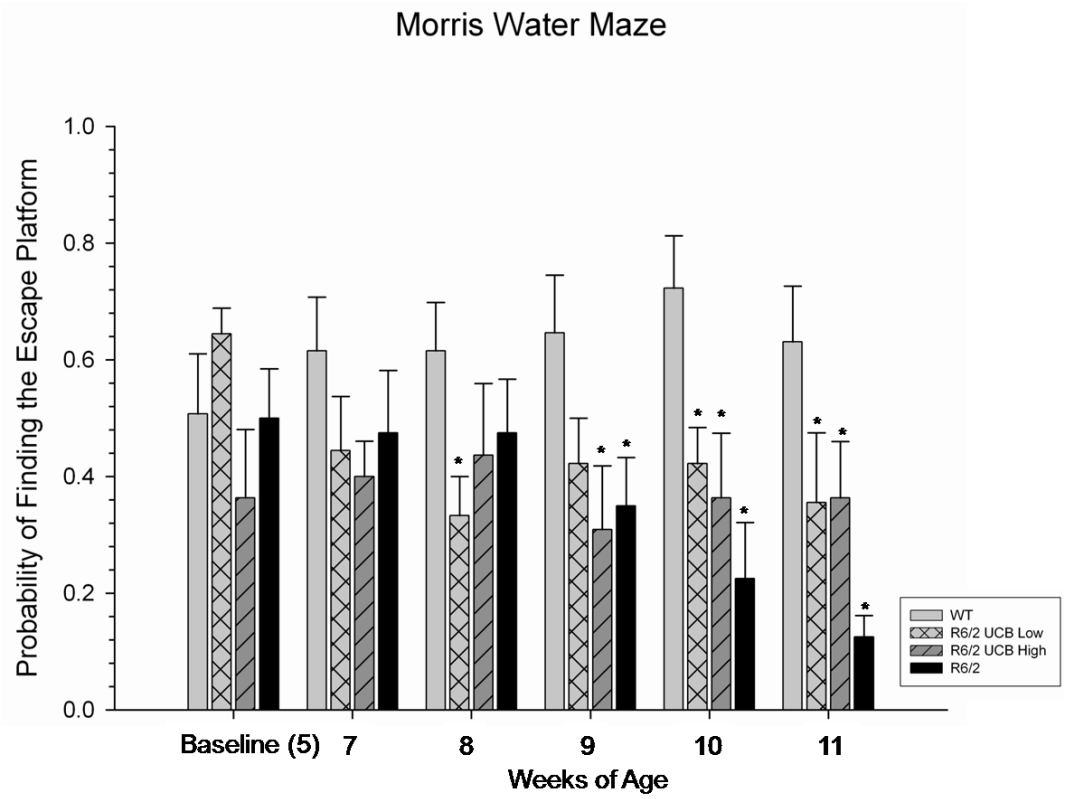

Figure 15. *Spatial memory assessment of R6/2 mice following umbilical cord blood mesenchymal stem cell (UCB MSC) transplantation*.
Untreated R6/2 mice displayed significant impairment in spatial memory at 9-, 10-, 11-weeks of age when compared to WT mice. Mice receiving either low- or high-passaged UCB MSCs did not display sparing of this spatial memory task. (Note: * significant from WT) Bar graph represents mean value; error bars represents SEM.

A repeated-measures ANOVA revealed significant differences between groups for limb-clasping [$F_{(3,42)} = 8.259$, $p < 0.001$], as well as a significant interaction was observed between weeks and group [$F_{(18,252)} = 4.845$, $p < 0.001$](Figure 16). This phenotypic difference observed in R6/2 mice began at 8 weeks of age. No effect of UCB MSC transplantation was observed, as all transplanted animals had similar scores, relative to untreated R6/2 mice. However, a significant

difference was observed between transplant groups, as the low-passage transplanted mice clasped more limbs than the high-passaged transplanted mice at 7-weeks of age. Contrary to what has been previously observed in our lab using bone-marrow MSCs, a reduction of the limb-clasping was not observed in the animals that received transplantation of UCB MSCs.

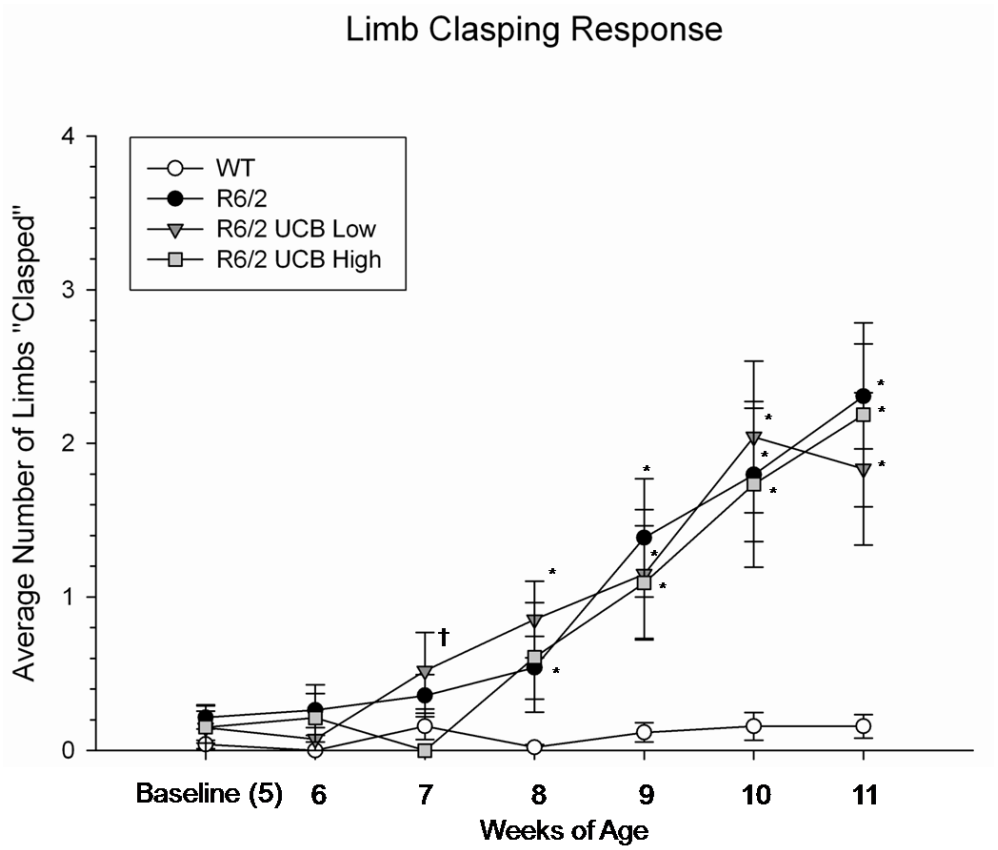

Figure 16. *Limb-clasping of R6/2 mice following umbilical cord blood mesenchymal stem cell (UCB MSC) transplantation*.
Untreated R6/2 mice had significantly more limb-clasps than did WT mice, starting at 8-weeks of age, with this impairment continuing for the duration of the study. Mice receiving either low- or high-passaged UCB MSCs were similar to untreated R6/2 mice. (Note: * significant from WT; # significant from R6/2; † significant from high-passage BM MSCs) Line graph represents mean value; error bars represents SEM.

Histological Results

Following perfusion and histochemical analysis of CYO labeled tissue, a one-way ANOVA revealed significant between group differences in the area of the whole brain from the sections analyzed [$F_{(3,109)} = 4.414$, $p < 0.01$](Figure 17A & B). PLSD analysis revealed that the untreated R6/2 mice had significantly smaller brain areas than did WT mice, suggesting generalized brain atrophy. The mice that received transplantation of high-passaged UCB MSCs did not significantly differ from WT mice on measures of brain area, an observation that was not detected in the low-passaged UCB MSC transplanted mice. Optical densitometric measures of metabolic activity of striatal tissue revealed a significant between-group difference [$F_{(3,109)} = 7.846$, $p < 0.001$](Figure 17C). PLSD tests revealed that R6/2 mice had significantly less CYO labeling than WT and R6/2 mice transplanted with low- or high-passage UCB MSCs. While transplantation of low-passage UCB MSCs did not protect against the loss of overall brain area, the low-passaged UCB MSCs were able to reduce the loss of metabolic activity in striatal tissue, compared to untreated R6/2 mice as determined by optical densitometric measures. Transplantation of high-passaged UCB MSCs preserved significantly more metabolic activity in striatal tissue than what was observed in either untreated R6/2 mice and, interestingly, WT mice.

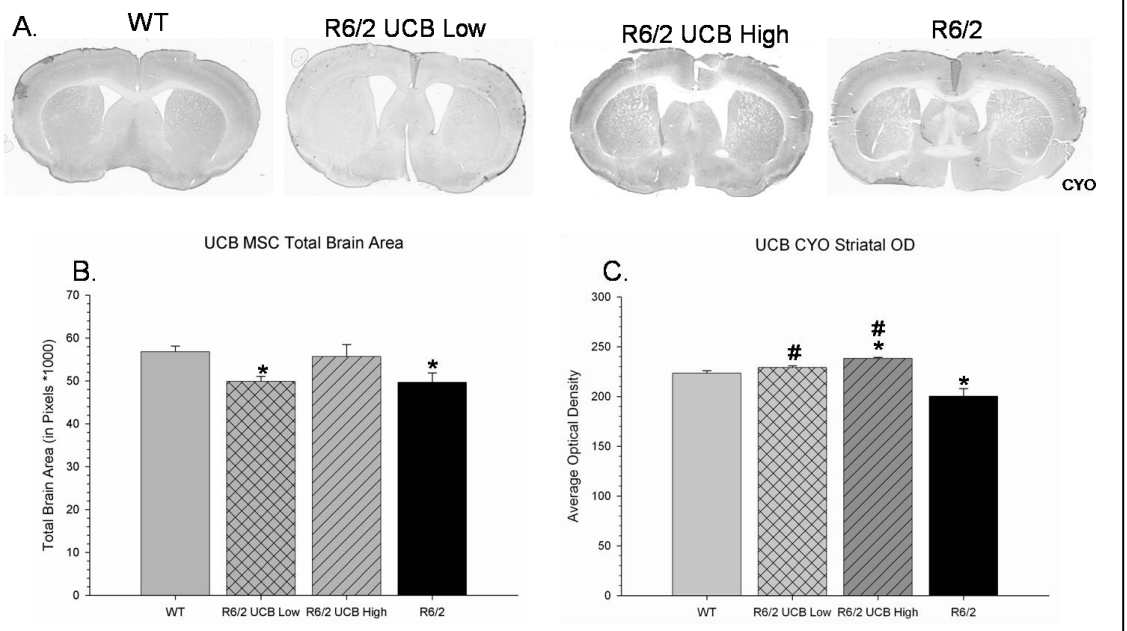

Figure 17. *Measures of brain area and evidence of integrity of the metabolic tissue in the striata of mice receiving umbilical cord blood mesenchymal stem cell transplantations.*
Gross morphology of the brain near the area of transplantation can be visualized with cytochrome oxidase labeling (A). Untreated R6/2 mice and mice that received transplantation of low-passaged UCB MSCs had a significant decrease in total brain area when compared to WT mice (B). Optical densitometric measures of cytochrome oxidase in the striata revealed significantly less metabolic activity of striatal tissue in untreated R6/2 mice, when compared to WT mice at the time of necropsy (C). R6/2 mice that received transplantation of low- or high-passaged UCB MSCs had significantly higher levels of metabolic activity in striatal tissue than did untreated R6/2 mice. (Note: * significant from WT; # significant from R6/2) Line graph represents mean value; error bars represents SEM.

Student's *t*-test revealed a significant difference in the number of surviving UCB MSCs between the low- and high-passaged groups at 6 weeks following transplantation [$t(55) = 3.104$, $p < 0.05$](Figure 18B). It was observed that mice receiving transplantation of high-passage UCB MSCs had significantly more surviving cells at 6 weeks post-transplantation than mice receiving low-passaged UCB MSCs. This may explain why mice receiving high-passage UCB MSCs

tended to show slightly more behavioral sparing, less brain area loss, and significantly higher CYO measures of metabolic activity in the striatum than mice receiving low-passage UCB MSCs, in spite of the fact that low-passaged UCB MSCs had a higher expression of BDNF *in vitro.* A one-way ANOVA revealed no significant between-group differences in measures of optical densitometry of GFAP from the area around the transplant site [$F_{(3,71)} = 2.265$, $p > 0.05$](Figure 18C). This data suggests that the deficits observed in the R6/2 mice are probably not due to astrocyte activation, and any behavioral or histological sparing that was observed, is unlikely to be due to either the up- or down-regulation of astrocytes in the brain. It also demonstrates that the number of passages a cell undergoes does not significantly modulate astrocyte activation following intra-striatal transplantation.

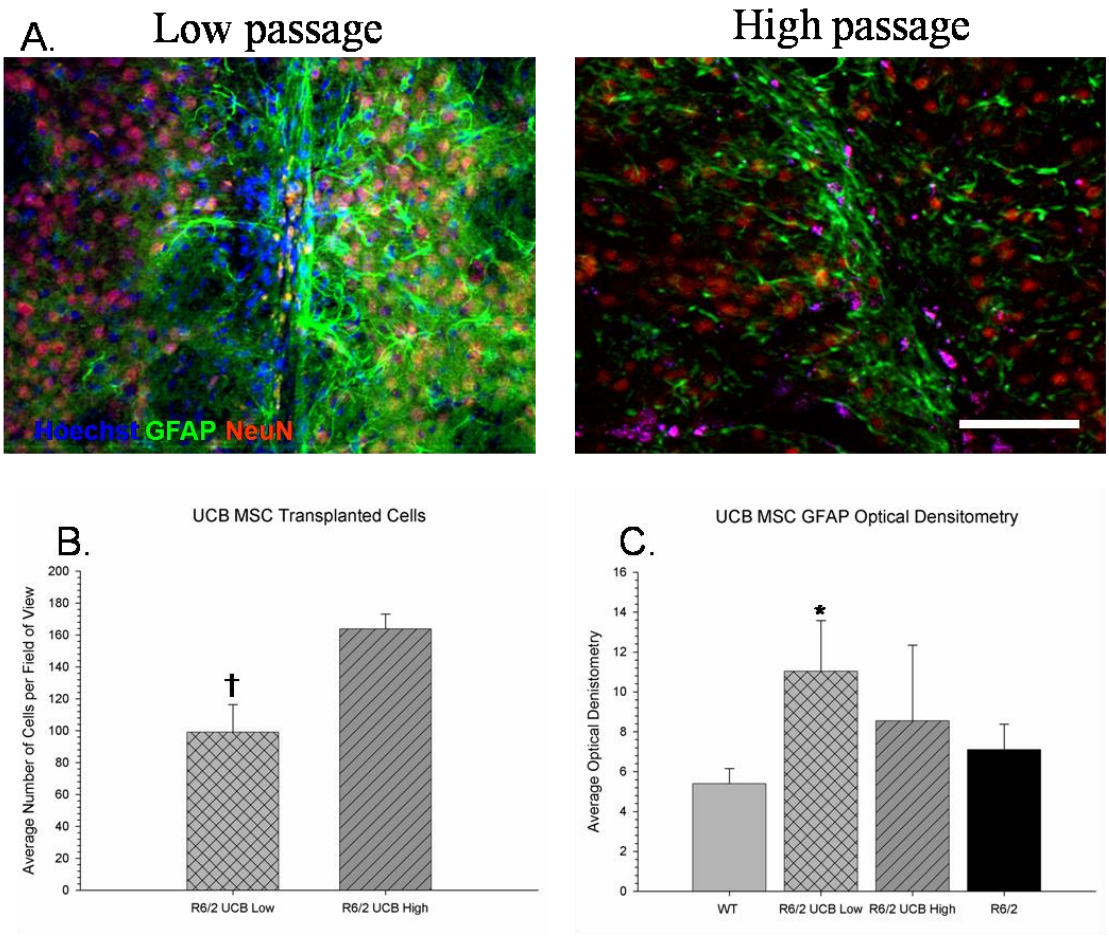

Figure 18. *Immunohistochemical analysis of the transplanted umbilical cord blood mesenchymal stem cells (UCB MSCs).*
No neuronal or glial differentiation was observed from the transplanted UCB MSCs as seen by the lack of co-localization between the UCB MSCs (blue) with NeuN (red) or GFAP (green), respectively (A). A decrease significant difference in the amount of surviving transplanted cells was observed in low-passage UCB MSCs, when compared to high-passage UCB MSCs (B). A significant increase in GFAP optical densitometry around the transplant site was observed in the R6/2 mice that received transplantation of low-passage UCB MSCs (C).

In contrast to what was hypothesized, little to no co-localization of the transplanted UCB MSCs with the mature neuronal marker NeuN was revealed, suggesting that these cells did not

differentiate into mature neurons *in vivo* following transplantation. This is in contrast to what has been previously reported following transplantation of UCB MSCs in the brain (Ding et al., 2007; Koh et al., 2008; Medicetty et al., 2004; Zhang et al., 2011), but similar to what has been observed following bone-marrow MSC transplantation (Dey et al., 2010; Lescaudron et al., 2003; Rossignol et al., 2009, 2011).

Experiment 3. *Adenovirus-Generated Induced Pluripotent Stem Cells*

iPSC Generation

It was observed that iPSC colonies could be generated with tail-tip fibroblasts (TTF) and mesenchymal stem cells (MSC) with either the single-cassette lentivirus (LN) or the combination of adenoviruses (AD). All transfection conditions displayed typical iPSC colony morphology and were readily expanded once placed onto deactivated feeder cells (Figure 19). Transfection efficiency was similar between reprogramming method. However, it was observed that MSCs more readily formed typical iPSC colonies than TTFs (Table 7). An average of 0.011% of MSCs was reprogrammed into iPSC-like colonies after exposure to either the adenovirus pair or the single-cassette lentivirus. An average of 0.006% of TTFs was reprogrammed into iPSC-like colonies after exposure to either the adenovirus pair or the single-cassette lentivirus. It is not surprising that MSCs displayed a higher reprogramming efficiency, as it has been previously found that adult stem cells are more readily converted to iPSCs than are cells that are further differentiated in the same specimen (Tan, Eminli, Hettmer, Hochedlinger, & Wagers, 2011). These present findings indicate that both the adenoviruses and the lentivirus are capable of inducing iPSC-like colonies at a similar efficiency. While, it should be noted that reported

efficiencies can vary between studies due to the various criteria used for delineating iPSC colonies and whether the initial number of starting cells or the amount of proliferated cells are used in the calculation (Ho et al., 2011). Despite this variability, the efficiencies observed in this study are similar to those previously published [for review: (Y. Zhang et al., 2012)].

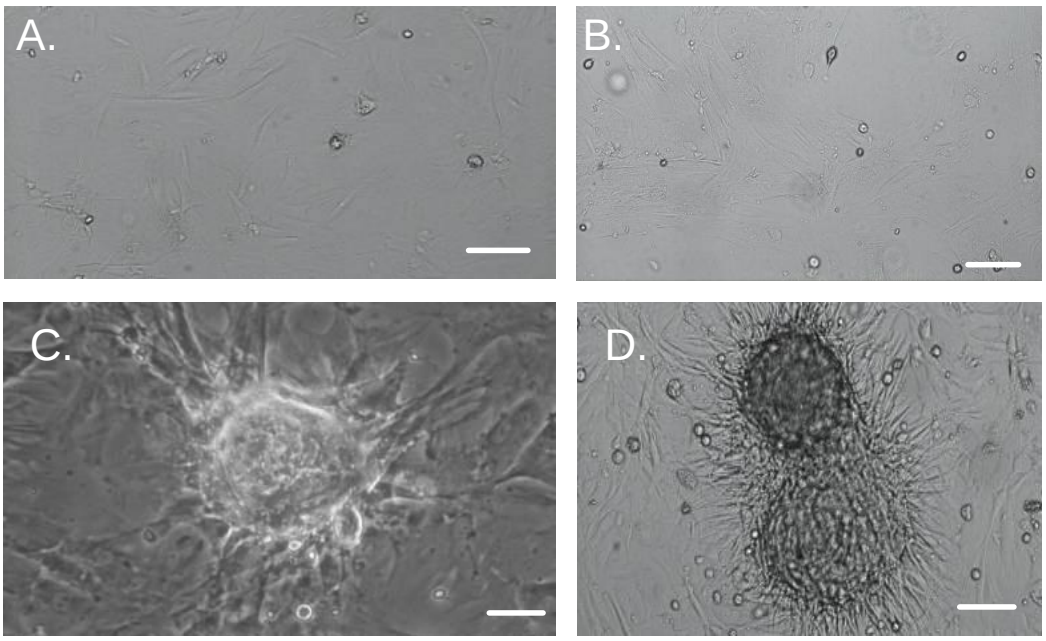

Figure 19. *iPSC induction.*
Both MSCs (A) and TTFs (B) were reprogrammed using either a single cassette lentivirus or a combination of adenoviruses. All conditions reliably created iPSC colonies (C) that were expanded on deactivated feeder cells (D). A, B, and D are imaged at 10x, scale bar equal to 100 μm. C imaged at 20x with a scale bar equal to 50 μm.

Table 7. *Reprogramming efficiencies of iPSCs.*

Cell Type	Reprogramming efficiency
MSC-AD	0.0107%
MSC-LN	0.012%
TTF-LN	0.00625%
TTF-AD	0.00637%

The efficiency of reprogramming methods were determined by dividing the total number of iPSC colonies observed per well at 20 days post-transfection to the total number of starting cells.

iPSC Characterization

All iPSCs generated for this study displayed an up-regulation of pluripotent markers as assessed by immunocytochemistry, flow cytometry, and quantitative RT-PCR. Immunocytochemistry revealed that all lineages of iPSCs (TTF-AD, TTF-LN, MSC-AD, and MSC-LN) displayed typical morphology of pluripotent cells and were positive for markers SSEA3, SSEA4, TRA-1-60, Nanog, and Oct4 (Figure 20). No observable differences were noted between the four lineages of iPSCs that were analyzed. Also, TTFs, MSCs, or deactivate rat embryonic fibroblasts (dREF) did not show positive expression of the pluripotent markers (data not shown).

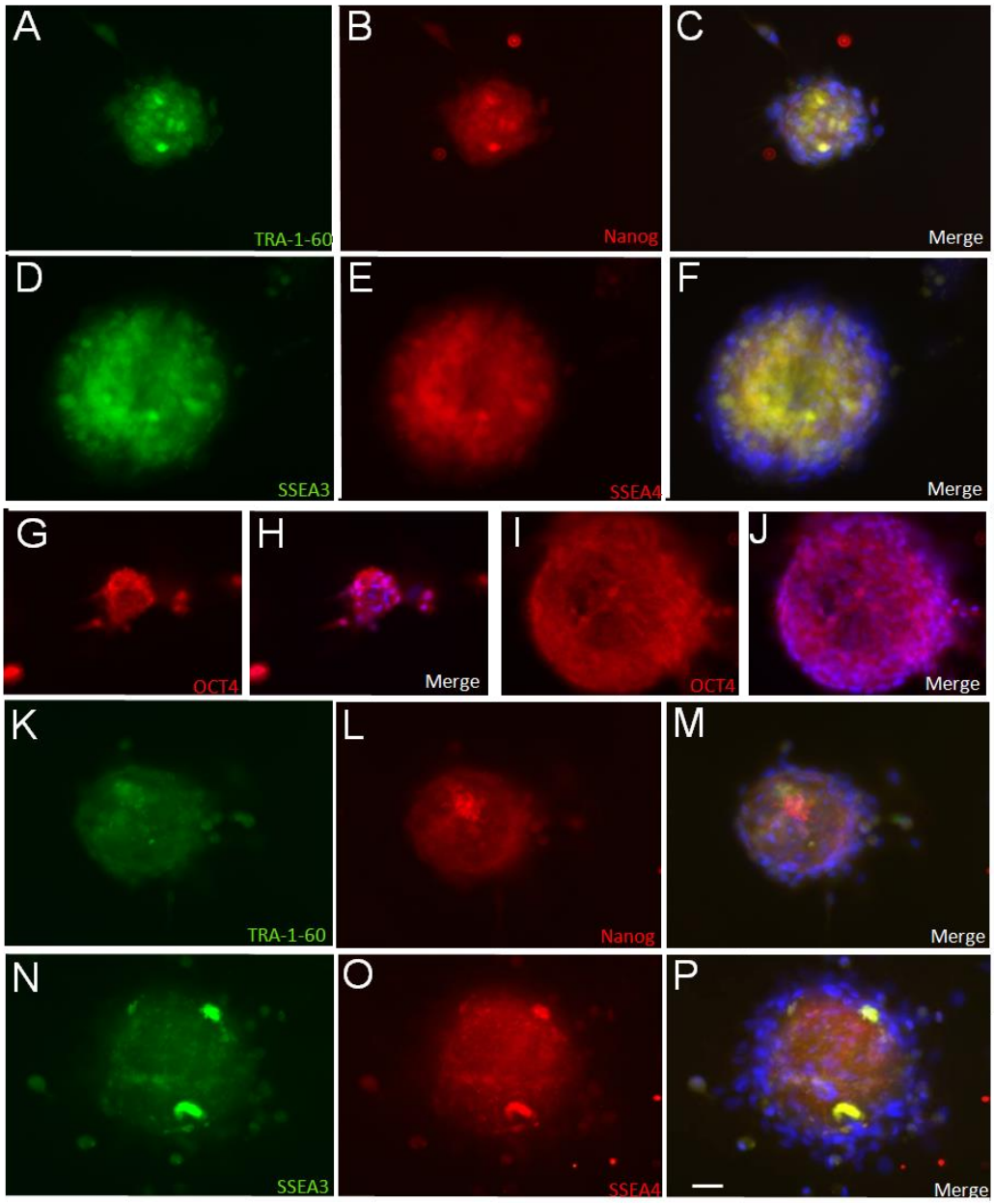

Figure 20. *Immunocytochemistry of iPSC.*
ICC revealed that tail-tip fibroblasts reprogrammed with adenoviruses expressed pluripotent makers TRA-1-60 (A), Nanog (B), SSEA3 (D), SSEA4 (E), and Oct4 (G). Tail-tip fibroblasts reprogrammed with a lentivirus also expressed pluripotent markers TRA-1-60 (K), Nanog (L), SSEA3 (N), SSEA4 (O), and Oct4 (I). Merged images are displayed in C, F, H, J, M, and P. MSC-AD and MSC-LN displayed similar expression of pluripotent markers (data not shown), while TTF, MSC, or dREF did not express pluripotent markers. All images were taken at 20x; scale bar equal to 50μm.

Flow cytometry revealed that both TTFs and MSCs had an up-regulation of pluripotent markers following reprogramming, irrespective of whether they were generated via lentiviral or adenoviral approaches (Figure 21). All lineages displayed up-regulation of SSEA4, Tra-1-60, Nanog and Oct4 when compared to the source cells (TTF or MSC) and to the feeder cells (dREF). There was no observable difference between lentiviral or adenoviral reprogramming methods. However, TTFs, regardless of reprogramming method, displayed a higher expression of pluripotent markers when compared to MSCs. While MSCs appeared to form iPSCs colonies at a higher rate, the colonies generated from TTFs appear to be more efficiently reprogrammed.

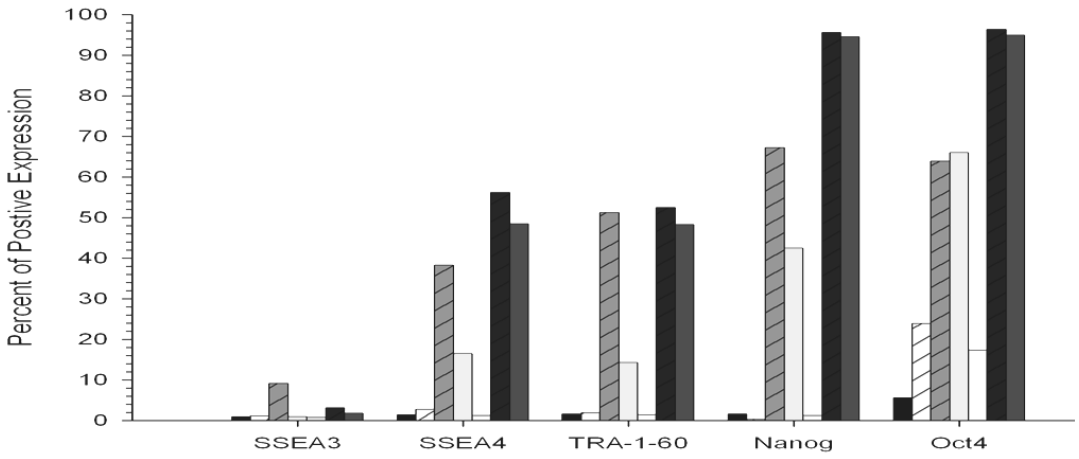

Figure 21. *Flow cytometry data revealed that all iPSC lineages displayed an upregulation of pluripotent markers SSEA4, TRA-1-60, Nanog, and Oct4 compared to both starting cell types (MSC and TTF) as well as deactivated rat embryonic fibroblasts (dREF).*

Quantitative RT PCR revealed that all of the generated lineages of iPSCs expressed an up-regulation of pluripotent genes. However, changes of expression were apparent between cell source and reprogramming method (Figure 22). It was observed that the up-regulation of the reprogramming genes was consistent between MSCs and TTFs, when the lentivirus was used.

This may be due to the integrative nature of the lentivirus and the forced expression of the reprogramming genes. It was observed in the adenoviral-reprogramming condition that expression levels were higher for Oct4, Klf4, and c-Myc in the reprogrammed TTFs as compared to MSCs, indicating that the cell source is important when reprogramming with adenoviruses. A significant effect of the reprogramming method was observed for the pluripotent gene Oct4 [$F_{(3, 11)} = 132.99$, $p < 0.001$] (Figure 22A), Klf4 [$F_{(3, 11)} = 1199.322$, $p < 0.001$] (Figure 22B), and c-Myc [$F_{(3, 11)} = 582.45$, $p < 0.001$] (Figure 22D), with adenovirus-generated iPSCs displaying greater fold increases than lentiviral-generated iPSCs.

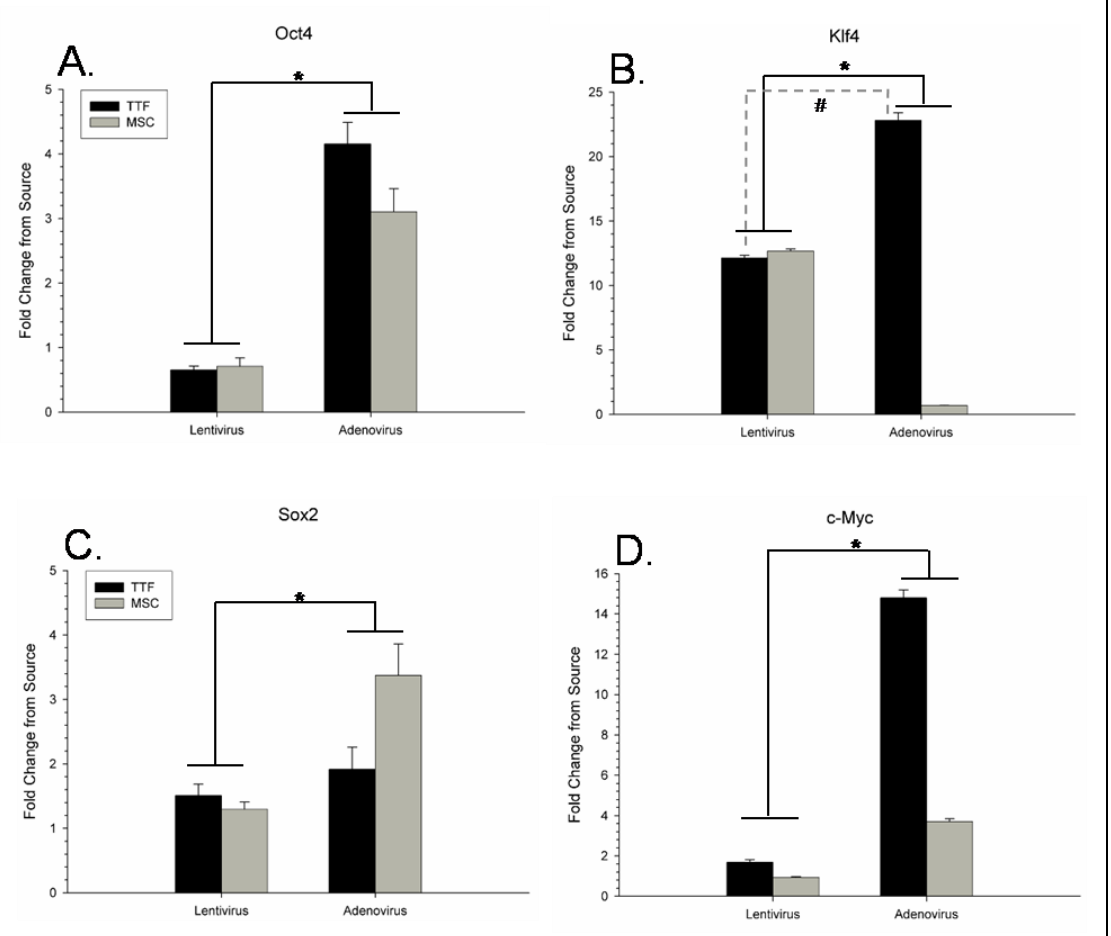

Figure 22. *Quantitative RT PCR of iPSCs*.
Quantitative RT PCR revealed that all iPSCs generated had an upregulation of genes responsible for regulating pluripotency. It appears that Oct4 (A), Klf4 (B) and c-Myc (D) expression is dependent on the reprogramming method employed and that adenoviral reprogramming produced greater increases, regardless of cell source. It should be noted that Klf4 (B) and Sox2 (C) were dependent on the starting cell source with TTF producing greater increases for Klf4 and MSCs produced greater increases for Sox2. (*Significant difference between lentivirus and adenovirus; # Significant source difference; bar graph represents mean value; error bars represents SEM).

However, it should be noted that starting cell source also had a significant effect on Klf4 expression, with TTFs displaying the highest expression of Klf4 [$F_{(3, 11)} = 1087.26$, $p< 0.001$]. A

significant interaction was observed for the pluripotent gene Sox2 [$F_{(3, 11)} = 6.959$, $p < 0.05$], with MSC-generated iPSCs producing a greater increase of Sox2 when compared to TTF-generated iPSCs (Figure 22C). Also, a significant effect on the reprogramming method was observed for Sox2 [$F_{(3, 11)} = 15.35$, $p < 0.01$], with adenovirus-generated iPSCs producing a larger increase (Figure 22C). Lastly, a significant interaction of cell source and reprogramming method was observed for the expression of c-Myc [$F_{(3, 11)} = 582.45$, $p < 0.001$], with TTFs and adenovirus-generated iPSCs yielding greater increases than MSC or lentiviral-generated iPSCs (Figure 22D). These findings demonstrate the importance of the cell source, as well as the type of reprogramming method that is employed for producing highly pluripotent cells.

Adenoviral transfection was capable of activating pluripotent genes in both MSCs and TTFs in a manner similar to lentiviral reprogramming for the genes Klf4 and Sox2. This approach yielded greater increases for the genes Oct4 and c-Myc, suggesting that endogenous activation of pluripotent genes is dependent on reprogramming methods. It was observed that the expression of pluripotent genes were more consistent between lines of lentivirus-generated iPSCs, regardless of the cell source, suggesting their expression was forced. Given that with TTFs being more readily converted to iPSCs, it is apparent that the cell source has an impact on reprogramming when the adenovirus pair is used. Taken together, quantitative RT PCR suggests that TTFs are a more desirable cell source for reprogramming into iPSCs and adenoviral transfection is comparable, if not more effective, than lentiviral transfection for the generation of iPSCs.

In Vitro Differentiation of iPSCs

Immunocytochemistry revealed that all lineages of iPSCs (TTF-AD, TTF-LN, MSC-AD, and MSC-LN) differentiated into neuronal-like cells. During differentiation, iPSCs changed from a colony formation into cells that displayed a neuronal-like morphology. These neuronal-like cells were positive for neuronal (NCAM) and neural progenitor (Nestin) cell markers (Figure 23). No between-group differences were observed in the percentage of differentiated iPSCs that were positive for NCAM [$F_{(3,33)} = 1.578$, $p > 0.05$]. However, a significant between-group difference was observed in the percentage of differentiated iPSCs that were positive for Nestin [$F_{(3,33)} = 3.321$, $p < 0.05$]. Protected least significant difference (PLSD) analyses revealed that the TTF-AD lineage displayed significantly less co-localization with Nestin than both the MSC-LN and TTF-LN lineages (Figure 23Q). The lower expression of Nestin in the TTF-AD group may be indicative of these cells shifting from a progenitor state to a more fully differentiated state than the other differentiated iPSCs. These data show that all of the generated iPSC colonies were capable of differentiating into neuronal-like cells, regardless of starting cell source or reprogramming method.

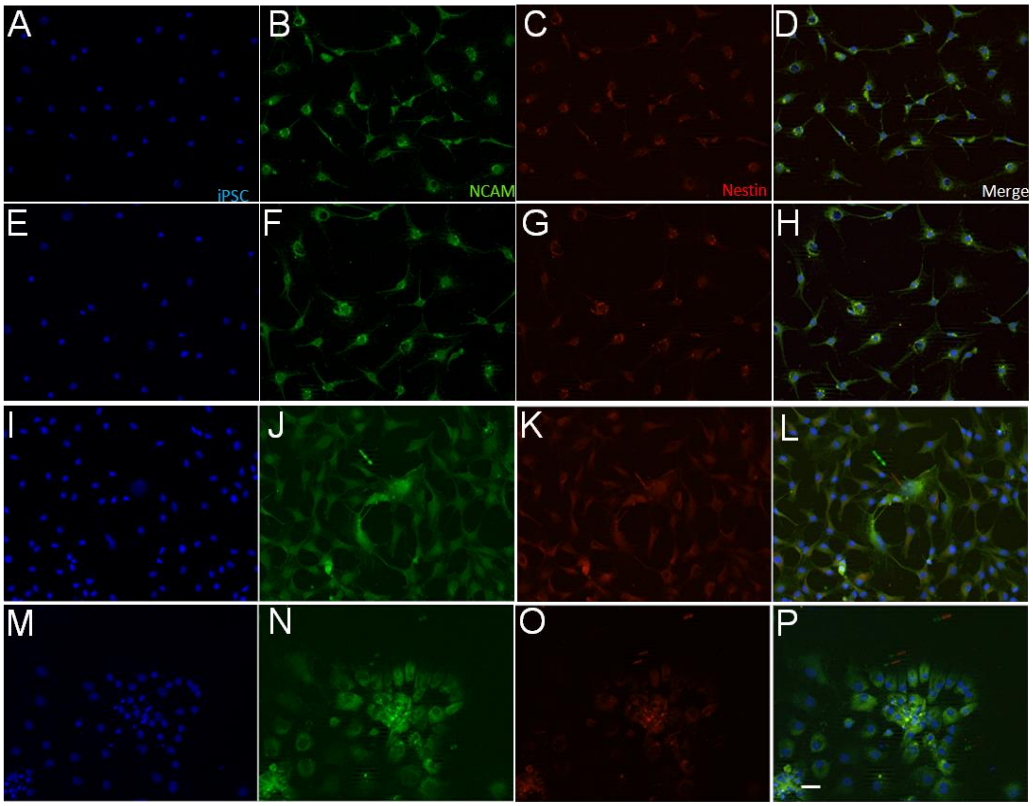

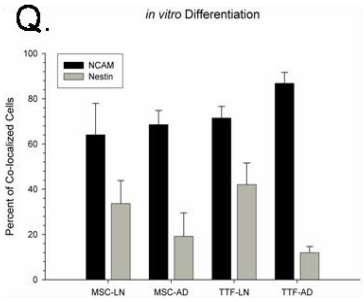

Figure 23. *Immunocytochemistry of in vitro differentiation of mesenchymal stem cells (MSC) or tail-tip fibroblasts (TTF) iPSCs from adenovirus (AD) or lentivirus (LN) transfection into neural rosettes*.
All lineages of iPSCs were capable of differentiating into neuronal precursor cells. Co-localization between iPSCs (blue) and NCAM (green) was observed for all lineages of iPSCs, indicating differentiation into neuronal phenotypes (Q). Some iPSC lineages also displayed co-localization with Nestin (red) a marker of immature neural development. (A-D) MSC-LN; (E-H) MSC-AD; (I-L) TTF-LN; (M-P) TTF-AD. All images were taken at 20x, scale bar equal to 50μm. Bar graph represents mean value; error bars represents SEM.

Experiment 4. *Survival and Differentiation of Adenovirus-Generated Induced Pluripotent Stem Cells Transplanted into the Rat Striatum*

Transplantation of iPSCs: Survival and Differentiation

Based on the *in vitro* analysis, it was determined that TTF-AD iPSCs would be the best choice for our transplantation work. The TTF-AD iPSCs were chosen because of their non-integrative nature, their consistently high levels of pluripotency (as measured by ICC, flow cytometry, and quantitative RT PCR), and their ability to readily differentiate into neuronal lineages *in vitro.* Following intrastriatal transplantation, in the rat, the TTF-AD iPSCs were capable of surviving up to 90-days (Figure 24M). A significant difference between iPSC- and dREF-transplanted rats was observed in the optical densitometric measures for macrophages, detected by IBA1 [$F_{(7,141)} = 6.500$, $p < 0.01$], with the highest expression in the 21-day iPSC transplant group (Figure 24Q). A significant between-group difference was also observed in the optical densitometry for the activated microglia marker, CD11b [$F_{(7,141)} = 3.435$, $p < 0.01$] with the iPSC group showing the highest densities at 7- and 21-days post-transplantation (Figure 24R). These data suggest that iPSCs derived from tail-tip fibroblasts and reprogrammed with adenoviruses, are capable of surviving in the brain of a healthy, adult rat for up to 90-days and that the up-regulation of both IBA1 and CD11b at 21 days post-transplantation suggests an immune response from the host that dissipates over time.

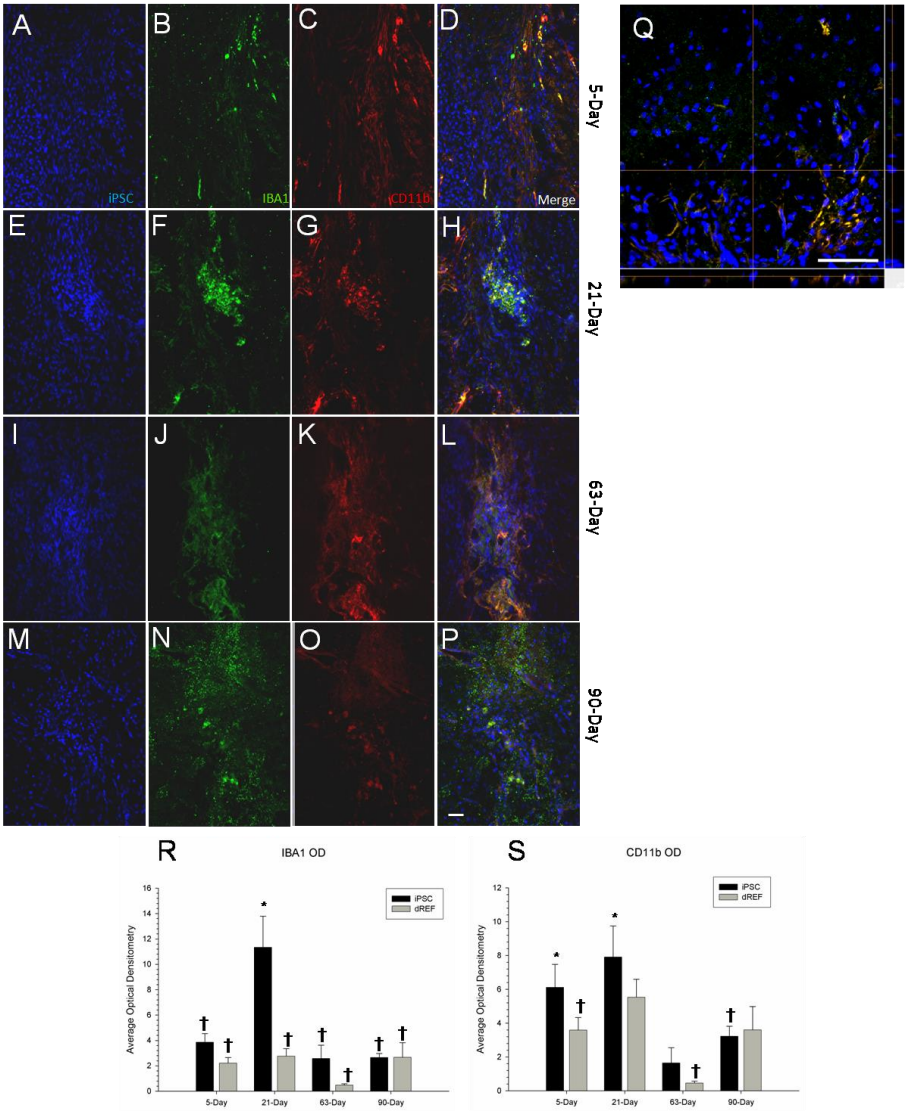

Figure 24. *Immune response to transplanted iPSCs*.
Activated microglia (IBA1; red) and macrophages (CD11b; green) were present at the site of iPSC (blue) transplantation. IBA1 expression was significantly unregulated 21-days following iPSC transplantation, but significantly decreased over time suggesting a tolerance to the cell transplantation (R). CD11b expression was downregulated between 21- and 63-days in the iPSC transplanted rats (S). (A-D) 5-day survival; (E-H) 21-day survival; (I-L) 63-day survival; (M-P) 90-day survival. (A-P) taken at 20x; (Q) 40x confocal image from 21-day survival group (the time point in which the greatest immune response was observed); scale bar equal to 50µm. (* Significant 63 day dREF; † Significant from 21 day iPSC group) Bar graph represents mean value; error bars represents SEM)

Albeit not in neural transplantations, other groups have shown that terminally differentiated cells, developed from iPSCs, elicit a limited immune response when subcutaneous injections, skin grafts, or bone marrow transplantation were performed (Araki et al., 2013). The early inflammatory response observed in this study may have been caused by the innate cell immunity and that this response may be adaptive in nature, thus leading to tolerance induction of the graft (Boyd, Rodrigues, Lui, Fu, & Xu, 2012).

A significant between-group difference was observed in the optical densitometric measures for GFAP [$F_{(7,175)} = 7.096$, $p < 0.01$], with the 5-day and, especially the 21-day iPSC groups having the highest measures of GFAP (Figure 25M). The GFAP response was localized to the needle tract in both the iPSC and dREF transplant groups and this decreased after 21-days suggesting that the astrocyte activation may be due to the surgical procedure, rather than a specific reaction to the transplanted cells. Very little GFAP was observed within the transplant of either cell type, suggesting that there was no astrocyte infiltration within the transplanted cells. Co-localization was also analyzed for GFAP and the transplanted iPSCs or dREF with less than 1% of the cells showing any co-localization (data not shown), suggesting that the transplanted cells did not differentiate into glial-phenotypes.

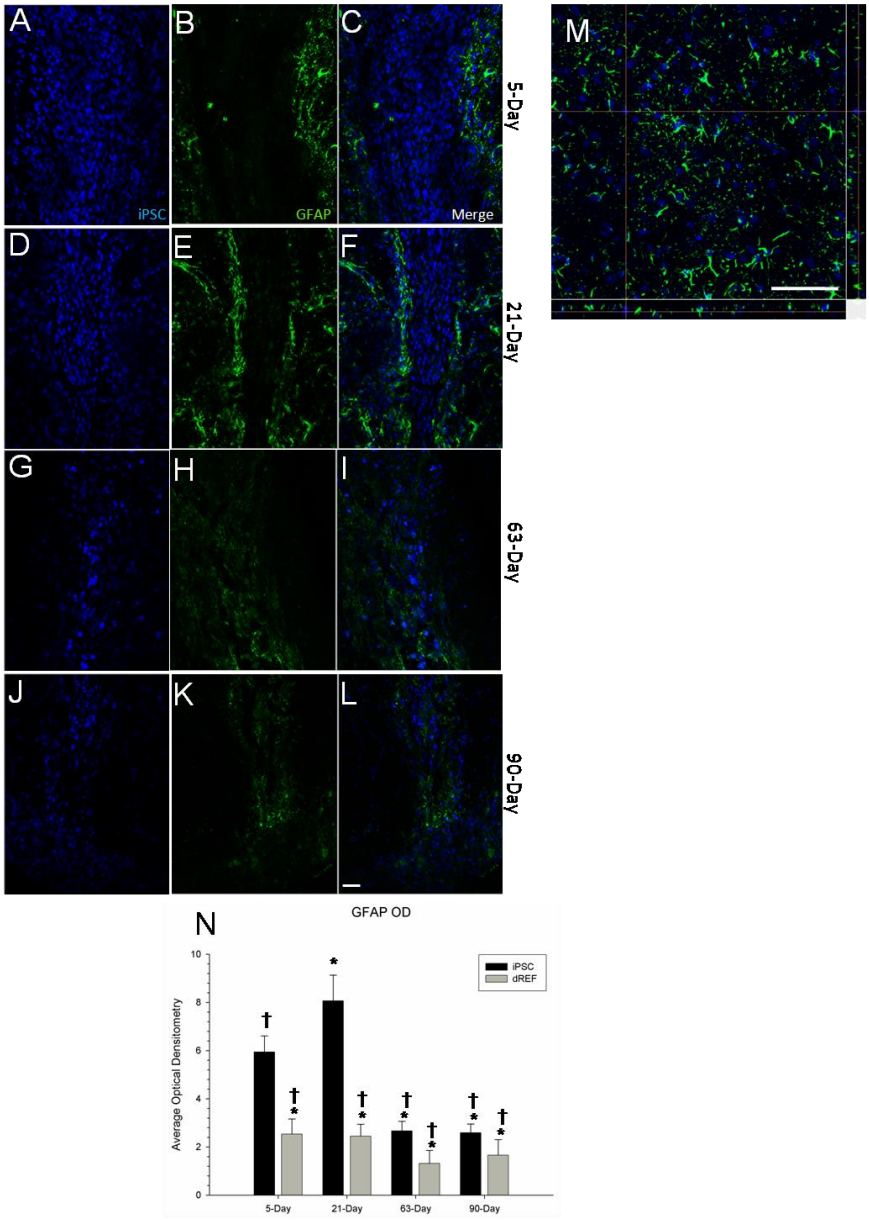

Figure 25. *Astrocyte activation to the transplanted iPSCs*.
Astrocytes (GFAP; green) were present around the needle track following transplantation of iPSCs (blue). An upregulation of GFAP was observed at 21-days (N), but decreased at 63- and 90-days. (A-C) 5-day survival; (D-F) 21-day survival; (F-I) 63-day survival; (J-L) 90-day survival. (A-L) taken at 20x; (M) 40x confocal image from 21-day survival group (the time point in which the greatest astrocytic density was observed); scale bar equal to 50μm. (* Significant from 5 day iPSC; + Significant from 21 day iPSC group) Bar graph represents mean value; error bars represents SEM)

No significant differences were observed between groups for the number of cells at each transplant site [$F_{(7,111)} = 1.845$, $p = 0.086$] (Figure 26Q). Although an immune response of activated microglia (CD11b), macrophages (IBA1), and astrocytes (GFAP) were present around the transplantation site, the transplanted cells (both iPSC and dREF) survived for the entire 90-day study in the brains of healthy, adult rats. It should be noted that pluripotent cells can survive, in the absence of immunosuppressants, following transplantation into the heart of mice (Nussbaum et al., 2007) or into the bone marrow of rats (Fändrich et al., 2002). Although both iPSCs and dREFs had similar survival rates in the present study, there were significant between-group differences in the percentage of transplanted cells that co-localized with the mature neuron marker, NeuN [$F_{(7,111)} = 16.321$, $p < 0.001$] (Figure 26R) and the medium spiny marker, DARPP-32 [$F_{(7,111)} = 9.342$, $p < 0.001$] (Figure 26S). The iPSCs co-localized with NeuN significantly more than did the dREFs at all-time points, except for in the 63 days transplantation group. Similarly, more iPSCs co-localized with DARPP-32 than did dREFs at all-time points, suggesting that the transplanted iPSCs can differentiate into region-specific.

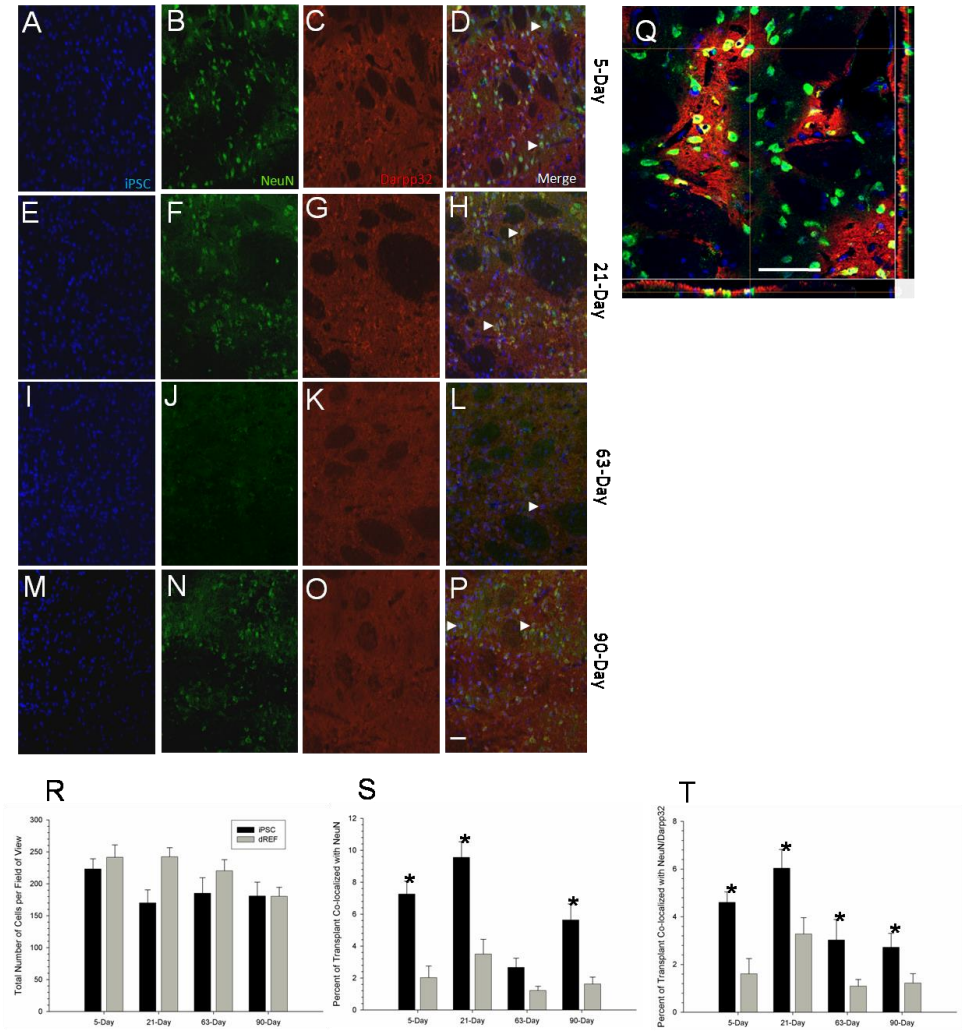

Figure 26. *Neuronal differentiation of transplanted iPSCs*.
Transplanted iPSCs (blue) displayed co-localization (white arrowheads) with a mature neuronal marker (NeuN; green) and a specific medium spiny neuron marker (Darpp32; red) within the striatum of healthy rats. No significant differences were observed in the number of surviving cells at any time point between iPSC- or dREF-transplants (R). Transplanted iPSCs displayed significantly more co-localization with NeuN than their dREF counterparts at all time points, except for at 63-days (S). However, transplanted iPSCs had significantly more co-localization with Darpp32 than did their dREF counterparts at all time points (T). (A-D) 5-day survival; (E-H) 21-day survival; (I-L) 63-day survival; (M-P) 90-day survival (S). (A-P) taken at 20x; (Q) 40x confocal image from 21-day survival group (the time point in which the greatest amount of iPSC co-localization was observed) ; scale bar equal to 50µm. (* Significant from corresponding dREF) Bar graph represents mean value; error bars represents SEM)

Experiment 5. *Intrastriatal Transplantation of Adenovirus-generated Induced Pluripotent Stem Cells for Treating Neuropathological and Functional Deficits in a Rodent Model of Huntington's disease*

Weight Analysis

A repeated-measures analysis of variance (ANOVA) revealed a significant interaction between groups over time for the percentage change in weight [$F_{(13,494)} = 6.686$, $p < 0.001$](Figure 27). A significant between-group difference was also observed [$F_{(4,38)} = 15.203$, $p < 0.001$]. PLSD analysis revealed significant differences between Sham rats and all other groups across all weeks of testing. Significant differences in body weight across all weeks of testing were also observed between 3-NP rats that received iPSC transplants at either 7-or 21-days and those that did not receive transplants.

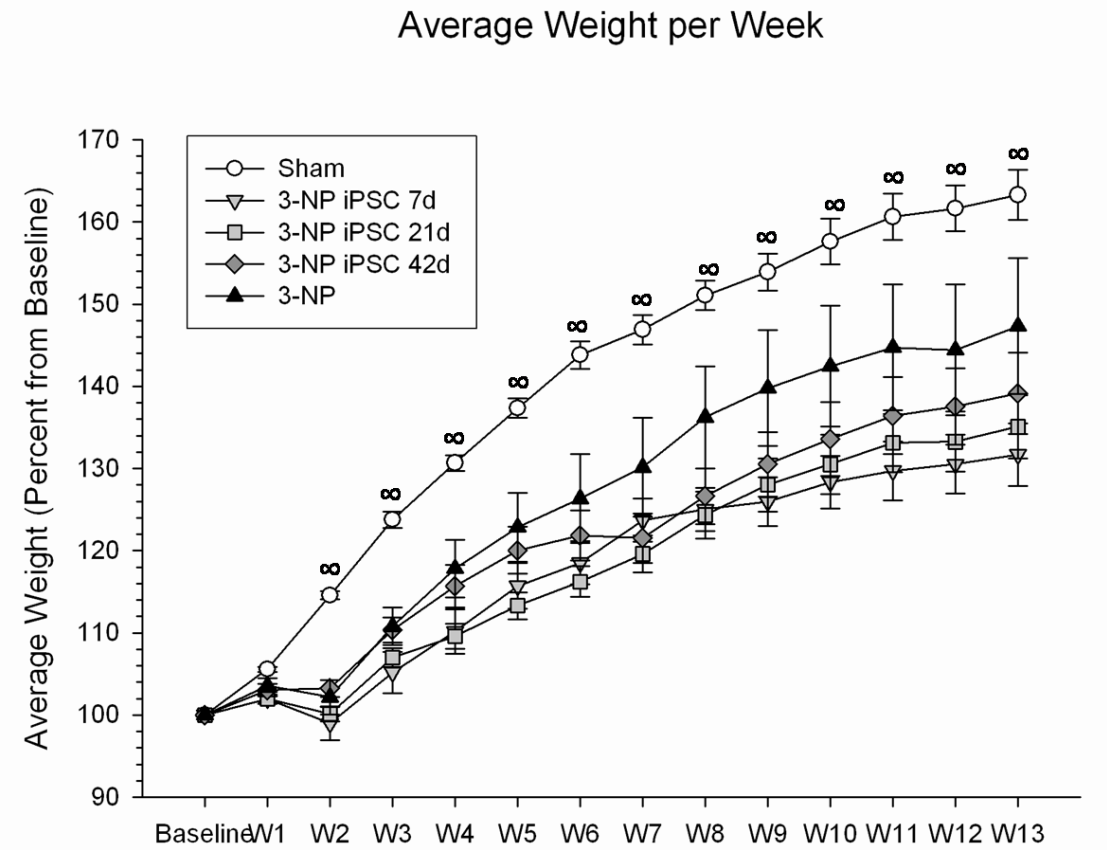

Figure 27. *Body weight*.
A repeated-measures ANOVA revealed a significant interaction of group and time for the percentage change in baseline weight. Starting at week 2 all rats that received 3-NP, regardless of iPSC transplantation, had significantly reduced weight when compared to sham injected rats. (Line graph represent mean value; error bars represent SEM; arrows indicate the time of iPSC transplantation for each group; ∞ significantly different from all groups, $p < 0.05$)

Behavioral Results

A repeated-measures ANOVA revealed significant between-group differences for the latency to fall in the accelerod task [$F_{(4,31)} = 6.021$, $p = 0.001$](Figure 28). A PLSD analysis revealed significant differences between Sham and 3-NP rats starting at week 2 and continuing for the duration of the study. 3-NP-treated rats transplanted with iPSCs after 7-days were

significantly different from Sham rats at weeks 2, 4, 5, and 6. 3-NP rats transplanted with iPSCs after 21-days were significantly different from Sham animals at weeks 4, 5, and 6. The 3-NP-treated rats in the 7-day and 21-day transplant groups displayed motor dysfunction when compared to Sham rats at one week post-surgery, but then displayed a significant preservation of motor abilities, as indicated by a significantly longer latency to fall when compared to rats receiving only 3-NP.

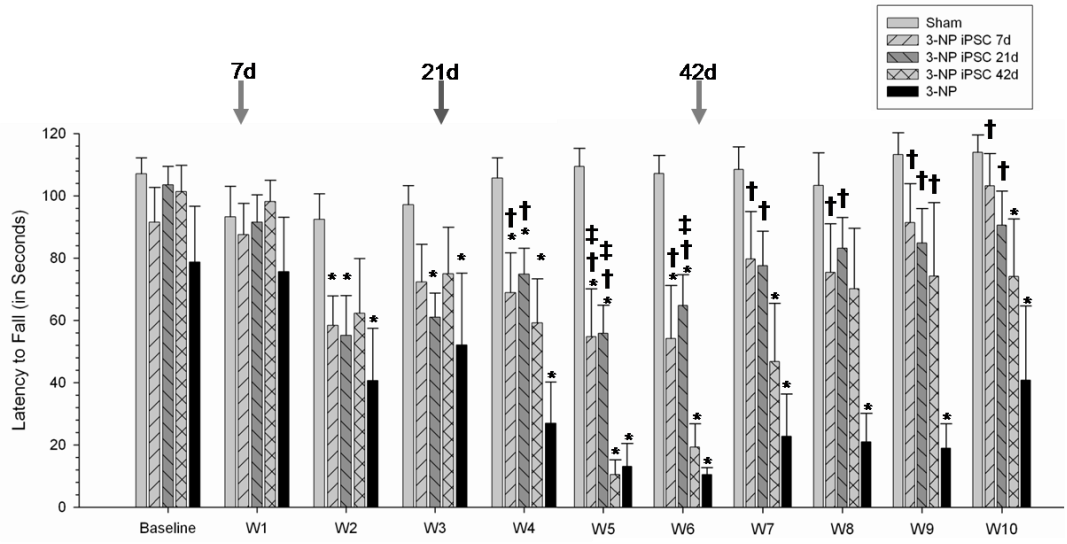

Figure 28. *Accelerod data from iPSC transplanted 3-NP rats*.
Analysis of motor coordination revealed significant between-group differences for the latency to fall in the accelerod task. Starting at week 4, and continuing throughout the study, 3-NP rats that received iPSC transplantation at either 7- or 21-days had significantly higher latencies to fall than 3-NP rats that did not receive transplants. Also, 3-NP rats that received transplantation of iPSCs at 42 days showed significantly higher latencies to fall at week 9 than 3-NP rats that did not receive transplants. (Bar graph represent mean value; error bars represent SEM; arrows indicate the time of iPSC transplantation for each group; * significantly different from Sham rats, $p < 0.05$; † significantly different from 3-NP rats, $p < 0.05$; # significantly different from 3-NP iPSC 7d rats, $p < 0.05$; ‡ significantly different from 3-NP iPSC 42d rats, $p < 0.05$).

3-NP rats transplanted with iPSCs after 42-days were significantly different from Sham rats at weeks 4, 5, 6, 7, and 10. However, starting at week 4, and continuing throughout the study, 3-NP animals that received iPSC transplantation at either 7- or 21-days had significantly higher latencies to fall than untreated 3-NP rats. Also, 3-NP rats that received transplantation of iPSCs at 42-days showed significantly higher latencies to fall at week 9 than untreated 3-NP rats. Interestingly, rats in the 42-day group displayed significant motor impairments, similar to rats receiving 3-NP without transplants prior to receiving transplantation, but then displayed significant motor recovery three weeks following transplantation.

Histological Results

A one-way ANOVA of the brain scans labeled with CYO (Figure 29A) revealed significant between-group differences in optical densitometry of striatal tissue [$F_{(4,64)} = 14.770$, $p < 0.001$](Figure 29B), striosome area [$F_{(4,119)} = 3.783$, $p < 0.01$](Figure 29C), and in the area of the lateral ventricles [$F_{(4,32)} = 13.377$, $p < 0.001$](Figure 29D). A PLSD revealed that the striatal optical densitometry for 3-NP controls and 3-NP receiving iPSC transplantation at 42-days were significantly lower than Sham rats, indicating decreased metabolic activity in the striatum. A PLSD also revealed that animals receiving iPSC transplantation at 7- or 21-days had significantly higher measures of optical densitometry in the striatum than untreated 3-NP rats or 3-NP rats that received iPSC transplantation at 42-days, suggesting a preservation of the metabolic activity in the striatum.

This finding corresponds to other studies that have shown transplantation of human embryonic neuronal stem cells reduce striatal atrophy in animals with surviving grafts (Lee et al., 2005; Pineda et al., 2007; Roberts et al., 2006).

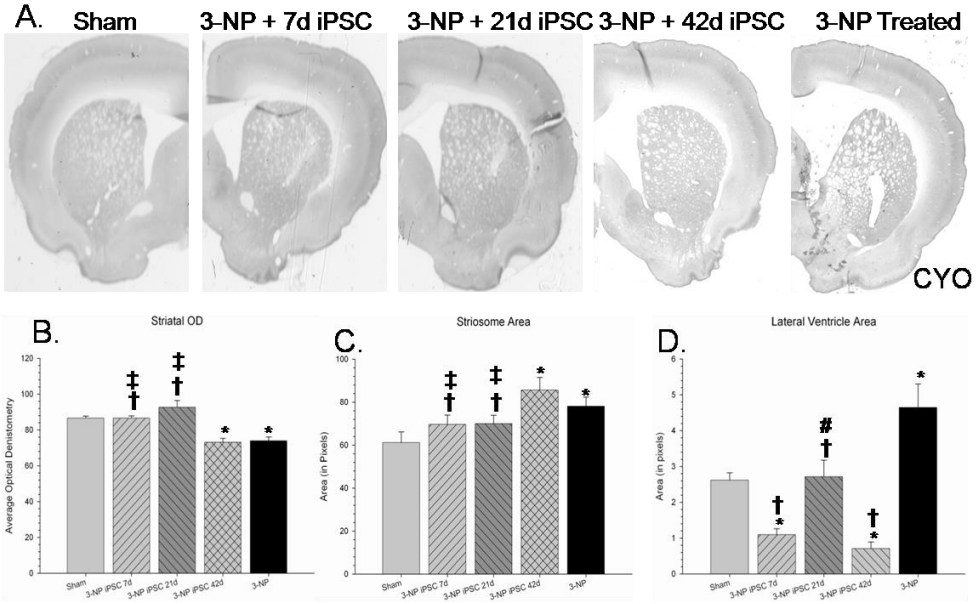

Figure 29. *Analysis of cytochrome oxidase (CYO) labeling (A).*
Analysis of the brain scans labeled with CYO revealed significant between-group differences in optical densitometry measures in the striatum (B). It was also revealed that rats receiving iPSC transplantation at 7- or 21-days had significantly higher optical densitometry measures in the striatum than 3-NP rats that did not receive transplants or 3-NP rats that received iPSC transplantation at 42 days. In addition, analysis of the striosome area revealed significant between-group differences (C). Rats receiving iPSC transplantation at 7- or 21-days had significantly smaller striosome area when compared to 3-NP rats that did not receive transplants or 3-NP rats that received iPSC transplantation at 42 days. Scans from the same sections also revealed significant between-group differences in the area of the lateral ventricles (D). All groups receiving iPSC transplantation had significantly smaller lateral ventricles when compared to 3-NP rats that did not receive transplants. (Bar graph represent mean value; error bars represent SEM; * significantly different from Sham rats, $p < 0.05$; † significantly different from 3-NP rats without transplants, $p < 0.05$; # significantly different from 3-NP iPSC 7d rats, $p < 0.05$; ‡ significantly different from 3-NP iPSC 42d rats, $p < 0.05$).

A PLSD revealed that the area of the striosomes were significantly larger for 3-NP and 3-NP receiving iPSC transplantation at 42-days groups when compared to Sham rats. A PLSD

revealed that rats receiving iPSC transplantation at 7- or 21-days had significantly smaller striosome area when compared to 3-NP control or 3-NP receiving iPSC transplantation at 42-days. A significant increase in striosome size was observed in 3-NP rats without transplants, when compared to Sham rats, indicating a reorganization of striatal tissue. This striosome enlargement was prevented by the transplants in the 7-day and 21-day transplant groups, suggesting that following transplantation of iPSCs at these time points prevents this reorganization of striatal tissue.

Lastly, PLSD analysis revealed that 3-NP controls had significantly larger lateral ventricles when compared to Sham rats. All groups receiving iPSC transplantation had significantly smaller lateral ventricles when compared to untreated 3-NP rats. Interestingly, rats receiving iPSC transplantations at either 7- or 42-days had significantly smaller lateral ventricles than Sham rats.

A one-way ANOVA revealed significant between-group differences in the average optical densitometry of CD11b [$F_{(4,103)} = 9.758$, $p < 0.001$](Figure 30A), IBA1 [$F(_{4,213}) = 7.252$, $p < 0.001$](Figure 30B), and GFAP [$F_{(4,100)} = 5.807$, $p < 0.001$](Figure 31A). A PLSD revealed that groups receiving 3-NP, regardless of iPSC transplant had a higher optical densitometry of CD11b than Sham rats. It was also shown that 3-NP rats receiving iPSC transplantation at either 7- or 42-days had significantly higher optical densitometry for CD11b labeling in the striatum than did 3-NP control rats.

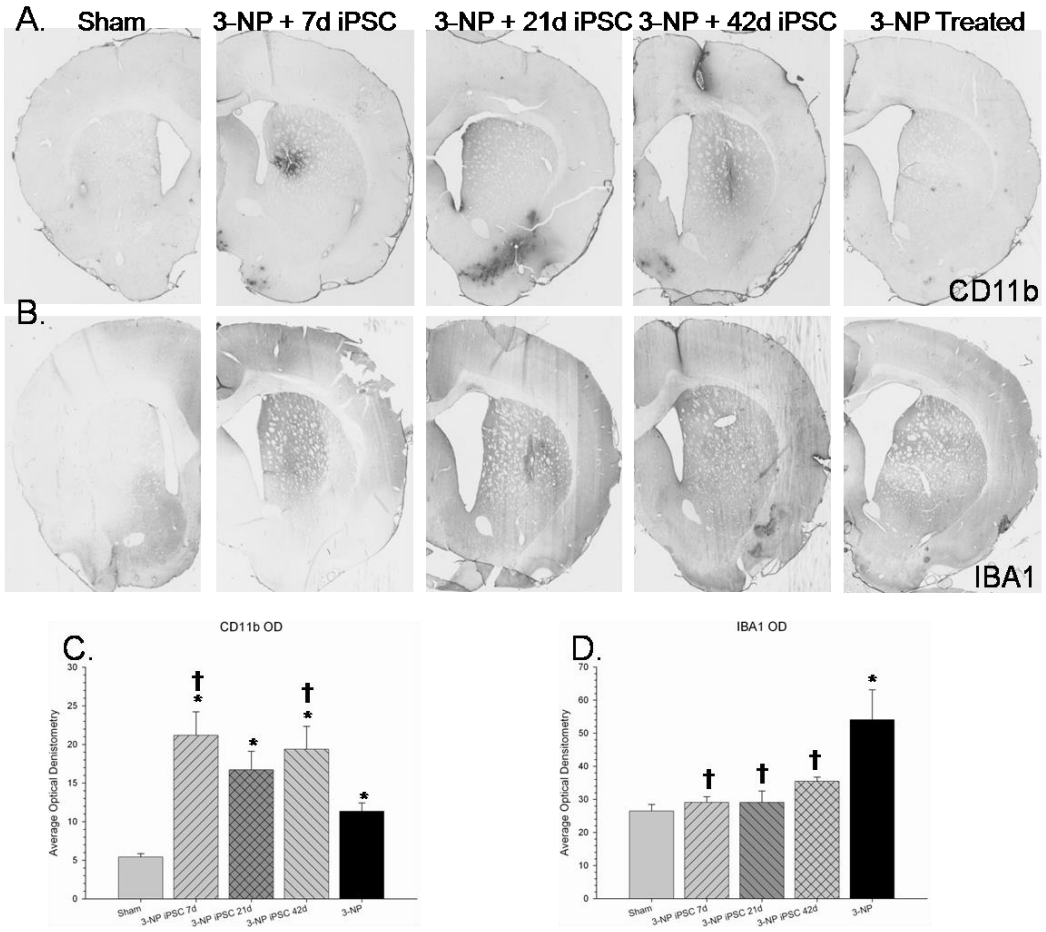

Figure 30. *Analysis of the immune response as measured by optical densitometry of CD11b (A) and IBA1 (B) to 3-NP and transplanted iPSCs.*
Analysis of expression levels revealed significant between-group differences in the average optical densitometry of CD11b, with all groups receiving 3-NP having a higher optical densitometry measures for CD11b than Sham rats (C). Significant between-group differences in the average optical densitometry of IBA1 (D) was also observed revealing that 3-NP rats without transplants had significantly more macrophage infiltration than Sham rats and all rats receiving iPSC transplantation. (Bar graph represent mean value; error bars represent SEM; * significantly different from Sham rats, $p < 0.05$; † significantly different from 3-NP rats, $p < 0.05$).

A PLSD analysis revealed that 3-NP rats receiving iPSC transplant at either 21- or 42-days displayed significantly higher GFAP labeling than Sham rats and 3-NP rats that received transplantation of iPSCs at 7-days. The 3-NP rats receiving iPSC transplantation at 7-days displayed significantly more astrocyte activation than 3-NP control rats. A PLSD analysis revealed that 3-NP control rats had significantly more macrophage infiltration, as determined by IBA1 labeling, relative to Sham rats and all rats receiving iPSC transplantation. Immunohistochemical analysis of astrocyte activation around the transplant site revealed that astrocyte activation was dependent on iPSC transplantation. Rats in the 21-day or 42-day transplant groups displayed more astrocyte activation than the Sham rats or rats in the 7-day transplant group.

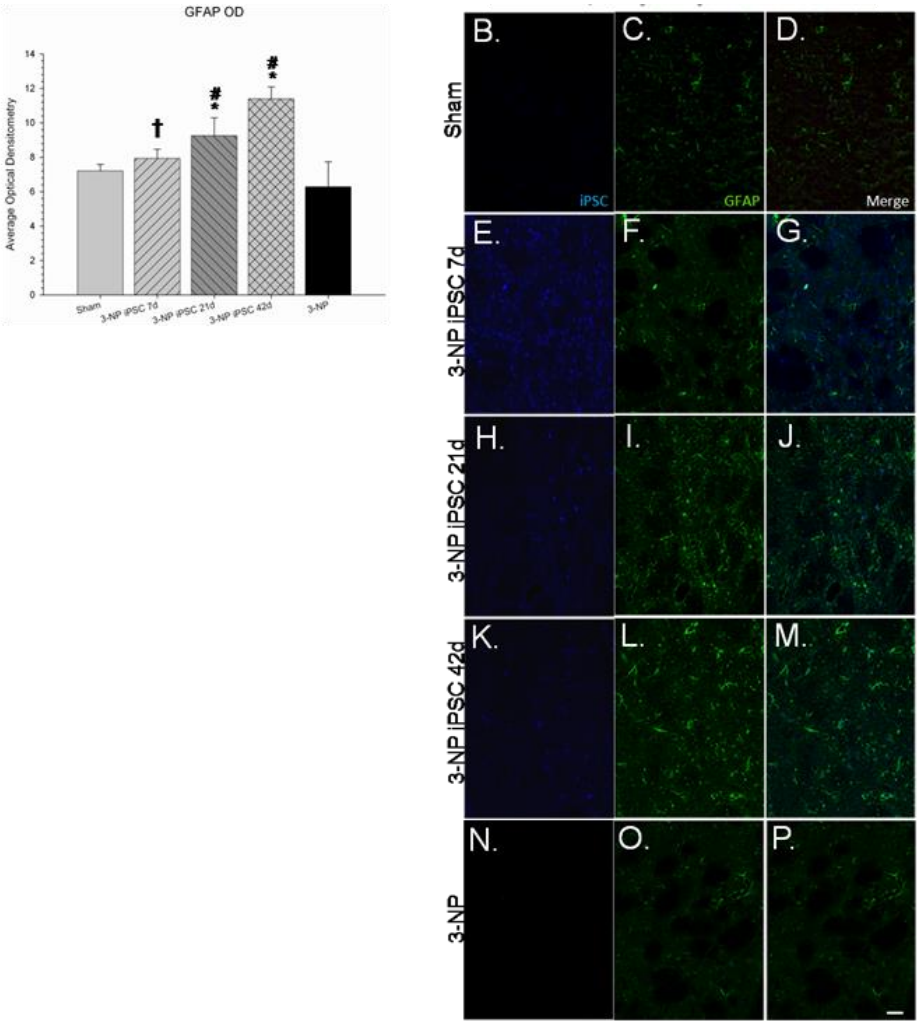

Figure 31. *Optical densitometry of GFAP from the transplant site.*
Astrocytes (GFAP: green) were observed around the transplanted iPSCs (blue), but no co-localization was observed between the two labels. A significant between-group difference in the average optical densitometry of GFAP (A) was observed. It was revealed that 3-NP rats receiving iPSC transplant at either 21- or 42-days displayed significantly higher GFAP labeling than Sham rats and 3-NP rats that received transplantation of iPSCs at 7-days. The 3-NP rats receiving iPSC transplantation at 7-days displayed significantly more astrocyte activation than 3-NP rats that did not receive transplants. Sham rats are shown in B-D; 7d iPSC rats are shown in E-G; 21d iPSC rats are shown in H-J; 42d rats are shown in K-M; 3-NP rats that did not receive transplants are shown in N-P. (Scale bar equal to 50μm; bar graph represent mean value; error bars represent SEM; * significantly different from Sham rats, $p < 0.05$; † significantly different from 3-NP rats, $p < 0.05$; # significantly different from 3-NP iPSC 7d rats, $p < 0.05$).

All rats receiving transplants displayed surviving iPSCs around the injection site at the conclusion of the study. However, using rare-event stereology, a significant between-group effect was observed for the average number of surviving iPSCs [$F_{(2,39)} = 8.709$, $p = 0.001$](Figure 32A). A PLSD revealed that the 7-day transplantation time-point had significantly more surviving iPSCs than the 21- or 42-day transplantation group. The increased transplant survival observed in the 7-day group is likely due to the timing of the transplant. Perhaps early intervention, prior to widespread cell loss in the striatum, would allow for these cells to integrate more efficiently.

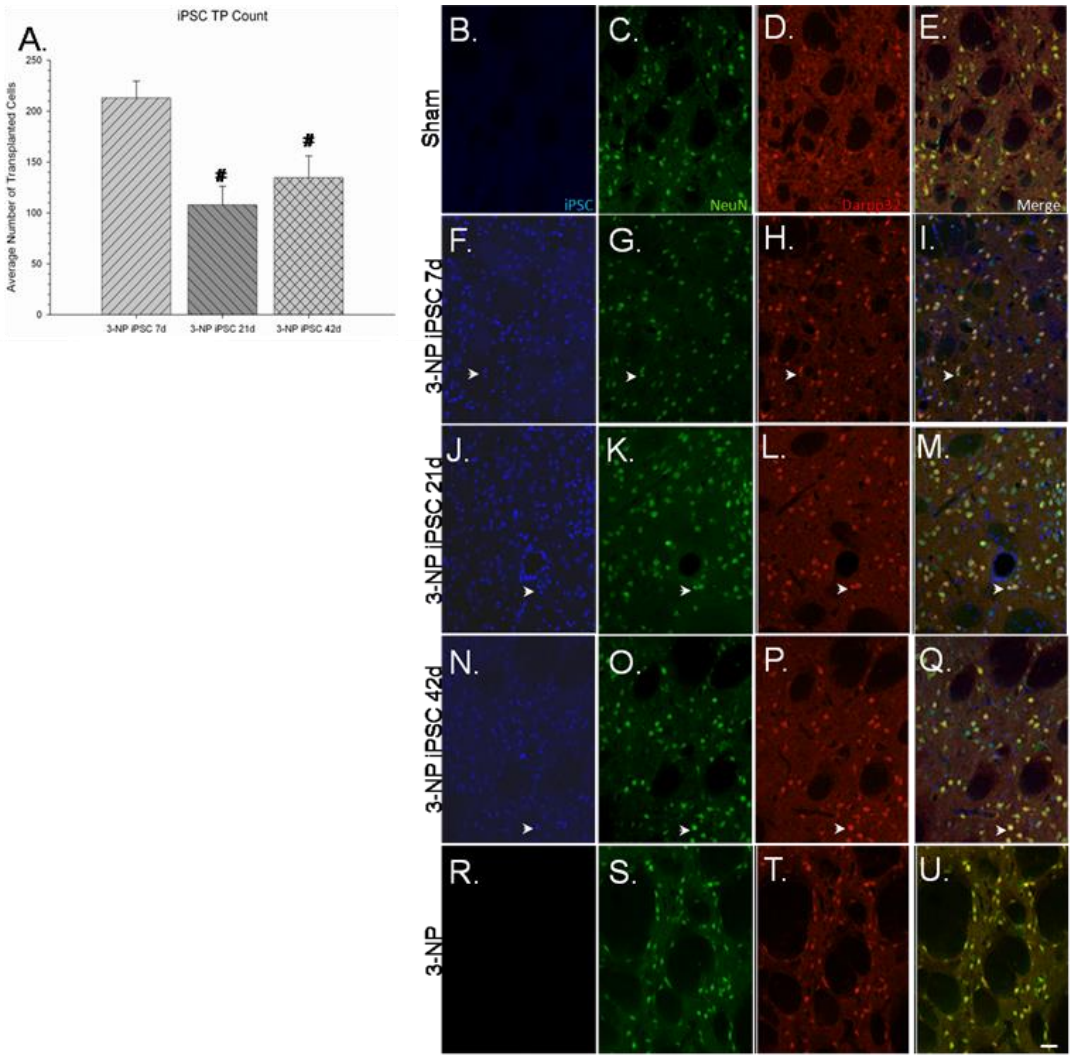

Figure 32. *Immunohistochemical analysis of transplanted iPSCs (blue), mature neurons (NeuN; green), and medium spiny neurons (Darpp32; red).*
All transplanted rats displayed surviving iPSCs (blue) around the injection site at the conclusion of the study. However, a significant between-group effect was observed for the average number of surviving iPSCs (A). It was revealed that the 7-day transplantation time point had significantly more surviving iPSCs than the 21- or 42-day transplantation group. Sham rats are shown in B-E; 7d iPSC rats are shown in F-I; 21d iPSC rats are shown in J-M; 42d rats are shown in N-Q; 3-NP rats that did not receive transplants are shown in R-U. (Scale bar equal to 50μm; co-localization is shown by white arrowheads; bar graph represent mean value; error bars represent SEM; # significantly different from 3-NP iPSC 7d rats, $p < 0.05$).

One-way ANOVA revealed a significant between-group difference in the number of NeuN positive cells in the area around the transplant site [$F_{(4,95)} = 4.374$, $p < 0.05$](Figure 33A). A PLSD revealed that 3-NP control rats and 3-NP rats receiving iPSC transplants at 42-days had significantly fewer NeuN-positive cells than Sham rats. A PLSD revealed that 3-NP rats that received iPSC transplantation at 7-days had a significantly greater amount of NeuN-positive cells than the 3-NP control rats or the 3-NP rats receiving transplantation at either 21- or 42-days. A significant between-group difference was found in the number of transplanted iPSC cells co-localizing with NeuN [$F_{(2,39)} = 7.896$, $p = 0.001$](Figure 33B). PLSD revealed that the 7-day transplantation group had more iPSCs co-localized with NeuN than either the 21- or 42-day group. This difference is likely due to the extra survival time and signalling factors that these cells were exposed to in the brain of the rats.

Similarly, a significant between-group difference was observed in the number of DARPP32-positive cells in the area around the transplant site [$F_{(4,114)} = 2.814$, $p < 0.05$](Figure 33C). A PLSD revealed that 3-NP control rats had significantly fewer DARPP32-positive cells in the area around the transplant site compared to Sham rats. It was also found that 3-NP rats receiving iPSC transplantation at 21-days had significantly more DARPP32-positive cells than 3-NP control rats. However, no between-group differences were observed in the number of iPSCs co-localizing with DARPP32 [$F_{(2,39)} = 0.083$, $p > 0.05$](Figure 33D).

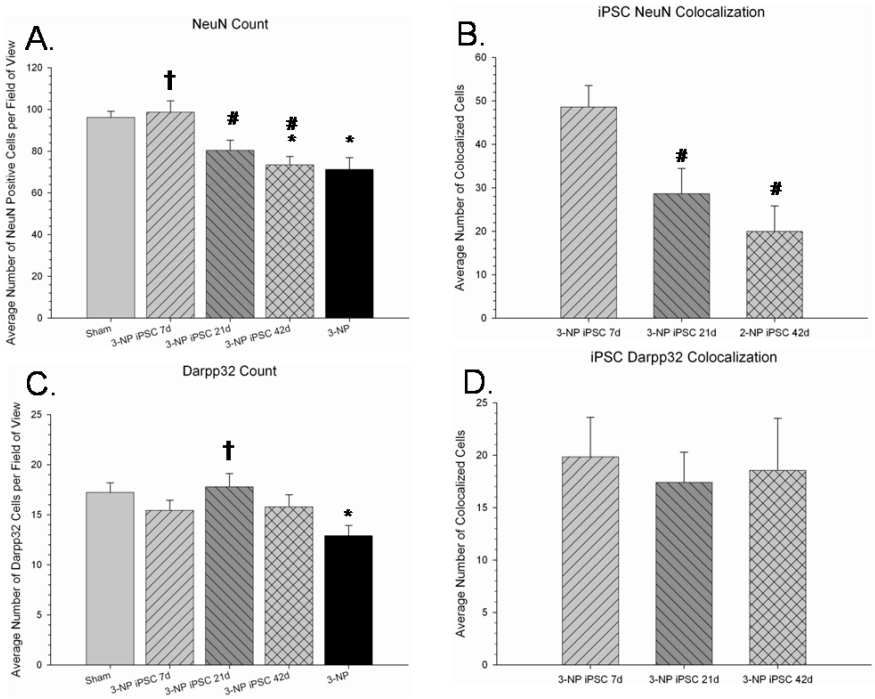

Figure 33. *Cell counts of mature neurons, medium spiny neurons, and co-localization with transplanted iPSCs.*
A significant between-group difference in the number of NeuN positive cells in the area around the transplant site (A) was observed. It was revealed that 3-NP rats that received iPSC transplantation at 7-days had a significantly greater amount of NeuN-positive cells than the 3-NP rats that did receive transplants or the 3-NP rats receiving transplantation at either 21- or 42-days. A significant between-group difference was found in the number of transplanted iPSC cells co-localizing with NeuN (B). It was found that the 7-day transplantation group had more iPSCs co-localized with NeuN than either the 21- or 42-day group. A significant between-group difference was observed in the number of DARPP32-positive cells in the area around the transplant site (C). It was found that 3-NP rats receiving iPSC transplantation at 21-days had significantly more DARPP32-positive cells than 3-NP control rats. However, no between-group differences were observed in the number of iPSCs co-localizing with DARPP32 (D). (* significantly different from Sham rats, $p < 0.05$; † significantly different from 3-NP rats, $p < 0.05$; # significantly different from 3-NP iPSC 7d rats, $p < 0.05$; ‡ significantly different from 3-NP iPSC 42d rats, $p < 0.05$)

mRNA Expression

Quantitative RT PCR of striatal tissue revealed no significant differences in the mRNA expression of BDNF between all groups [$F_{(4, 18)} = 0.443$, $p > 0.05$](Figure 34A). Quantitative RT PCR of striatal tissue did, however, did reveal a significant difference in the mRNA expression of TNF-α [$F_{(4, 18)} = 4.776$, $p < 0.05$](Figure 34B), with the 3-NP 21d and 42d group having significantly lower levels than Sham and the 3-NP 7-day iPSC transplant groups.

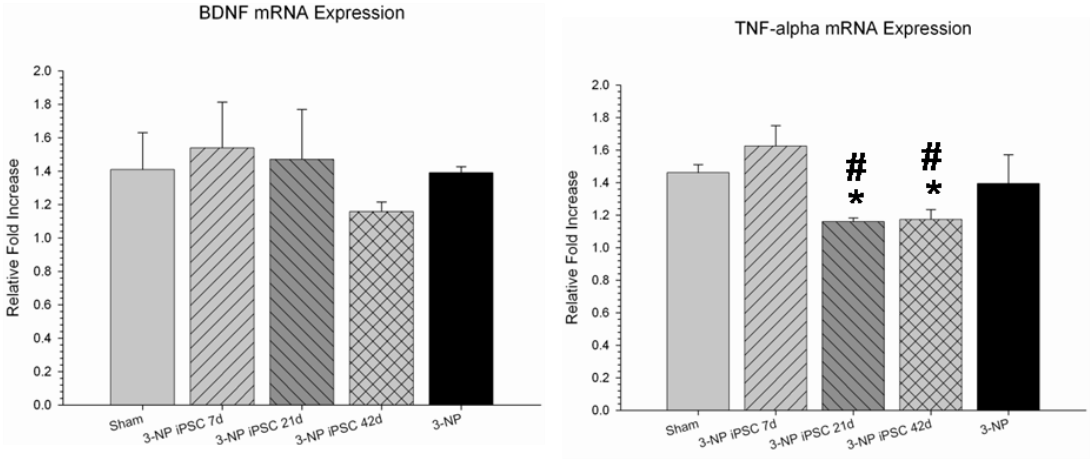

Figure 34. *Quantitative RT PCR of striatal tissue for mRNA expression of BDNF and TNF-α.*
Quantitative RT PCR of striatal tissue revealed no significant differences in the mRNA expression of BDNF between all groups (A), but did reveal a significant between-group difference in the mRNA expression of TNF-α (B). No reduction in BDNF expression was observed in the 3-NP rats without transplantation, indicating that behavioral deficits are not due to the depletion of this trophic factor. The downregulation of TNF-α in the rats that received transplantation of iPSCs at 21- and 42-days is indicative of a general deactivation of the immune response to the transplanted cells. (Bar graph represent mean value; error bars represent SEM; * significantly different from Sham rat, $p < 0.05$; # significantly different from 3-NP iPSC 7d rats, $p < 0.05$).

CHAPTER VI

DISCUSSION

Experiment 1. *Reductions in Behavioral Deficits and Neuropathology in the R6/2 Mouse Model of Huntington's disease following Transplantation of Bone-Marrow-Derived Mesenchymal Stem Cells is Dependent on Passage Number*

This study demonstrates four main findings: (1) transplantation of BM MSCs into the striata of R6/2 mice significantly delay the progressive motor and cognitive dysfunction associated with this model; (2) the beneficial effects of these cells is dependent on the number of times they have been passaged; (3) transplantation of these cells can preserve anatomical features in the R6/2 brain, even in the absence of evidence for neuronal differentiation; (4) transplantation of BM MSCs can prevent/restore the decreased expression of BDNF in the striata of R6/2 mice.

The data from this study corroborates earlier findings from our lab demonstrating a reduction in behavioral deficits and neuropathology in an HD model following transplantation of BM MSCs (Dey et al., 2010; Lescaudron et al., 2003; Rossignol et al., 2011). This study shows that BM MSCs were capable of slowing the progressive decline in motor and cognitive performance in a R6/2 mouse model of HD. The efficacy of MSCs in treating HD-like deficits have also been observed in the quinolinic acid (QA) rat model of HD, using BM MSCs (Edalatmanesh et al., 2010). Other sources of MSCs, such as adipose-derived MSCs reduced the motor deficits in the R6/2 mouse model (Im et al., 2013). While the suggested mechanisms of action of transplanted MSCs being reported in these studies are different, the overall results of these studies provide converging evidence for the potential use of MSCs as a therapy for HD.

Contrary to what was observed in our previous study using rat BM MSCs, it is apparent that, in this model, mouse BM MSCs are more therapeutically beneficial after extended periods

in culture. The high-passage mouse BM MSCs displayed higher mRNA expression of BDNF *in vitro* and these high-passaged cells were capable of significantly delaying the onset of both motor and cognitive deficits in an aggressive mouse model of HD. As no changes in the expression of GFAP was observed, the deficits observed in the R6/2 mice are likely not due to astrocyte activation and any behavioral or histological sparing that was observed is not due to either the up- or down-regulation of astrocytes in the brain. The differences in behavioral outcomes between transplantation of low- and high-passage BM MSCs was not due to differences in the immunomodulatory effects of these cells, as the cells did not significantly modulate astrocyte activation following intrastriatal transplantation. While our study suggests that high-passage mouse BM MSCs are more suitable for transplantation in the R6/2 model, it is important to note, that this is likely to be different for transplantation of rat or human MSCs (Bertolo et al., 2013; Chang et al., 2012; Lennon, Schluchter, & Caplan, 2012; Li et al., 2012; Rossignol et al., 2009).

Contrary to late-stage human HD, late-stage R6/2 mice do not have massive loss of striatal neurons. However, significant decreases are observed in the levels of metabolic activity within the striatum, which is suggestive of striatal dysfunction (Morton et al., 2005).This study was able to demonstrate a neuroprotective effect of transplanted BM MSCs. These results are similar to what has been observed following MSC transplantation into the N171-82Q mouse model of HD (Snyder et al., 2010), although few surviving transplanted cells were reported in this study. In QA lesion-models, a reduction of striatal atrophy has been observed following MSC transplantation, with a small number of surviving cells 16 weeks after transplantation (Amin et al., 2008; Lin et al., 2011).

The ability for MSCs to survive following transplantation into the brain is currently being studied at several labs, with widely varying results being reported. In the current study, no significant difference in the number of surviving MSCs was found at six weeks following transplantation. This is similar to other studies that have observed robust MSC survival following transplantation in a QA rat (Bantubungi et al., 2008; Sadan et al., 2008). We have recently reported that transplantation of rat BM MSCs into the rat striatum decreases the general activity of the hypoimmunogenic dendritic cells, macrophages, and T lymphocytes, which translated into reducing the probability of MSC rejection (Rossignol et al., 2009).

As the numbers of surviving BM MSCs in the present study was not different between the two different passage groups after transplantation, the differences observed in behavioral and histological sparing between mice receiving low- or high-passaged MSCs were not due solely to the number of MSCs in the brain. Further, as BM MSCs were not seen to differentiate into neuronal-lineage cells, replacement of lost- or damaged-cells is not responsible for the behavioral and histological results. Therefore, other mechanisms such as secretion of trophic factors, like BDNF, need to be identified to account for the therapeutic effects of the transplanted MSCs.

It has been found that patients with symptomatic HD, with lower serum concentrations levels of BDNF have significantly impaired motor and cognitive performances, relative to individuals with normal BDNF levels (Ciammola et al., 2007; Conforti et al., 2008). It is also shown that BDNF is very important for survival and differentiation of striatal neurons, and that lower BDNF may be a causative factor in the deterioration of specific neuronal populations that is observed in HD (Zuccato et al., 2001).

In the current study, transplantation of BM MSCs in the striata of R6/2 mice significantly restored BDNF expression levels. As the loss of BNDF mRNA expression has been shown to be significantly reduced in 6-week old R6/2 mice (Samadi et al., 2013), we postulate that the secretion of BDNF from transplanted BM MSCs when R6/2 mice were 5-weeks of age prevented this age-dependent loss of BDNF mRNA expression in these R6/2 mice.

Our findings confirm those of Jiang and colleges (2011) who observed an upregulation of BDNF following MSC transplantation in a toxic lesion model of HD. The capacity of MSCs to secret growth factors and other neuroprotective factors *in vitro* and *in vivo* following transplantation has been well documented (Dey et al., 2010; Rehman et al., 2004; Wang, Crisostomo, Herring, Meldrum, & Meldrum, 2006). However, based on the current evidence, we are unable to determine if the BDNF is secreted from the transplanted cells, or if it is upregulated in brain tissue as a result of BM MSC transplantation. Testing these hypotheses has become a focus of future studies in our lab.

Experiment 2. *Transplantation of Umbilical-Cord-Blood-derived Mesenchymal Stem Cells into the Striata of R6/2 Mice: Behavioral and Neuropathological Analysis*

The four major findings of this study were: (1) transplantation of UCB MSCs into the striata of R6/2 mice provided transient behavioral sparing compared to mice that did not receive stem cell transplants; (2) while transplants of UCB MSCs did not significantly reduce behavioral deficits, transplantation of high-passage UCB MSCs resulted in significant reduction in neuropathology, albeit providing only transient behavioral sparing; and (3) the number of times the cells were passaged significantly altered the number of surviving cells and the astrocyte activation to the transplant 6.5 weeks following the transplant, while the UCB MSCs did express

the mRNA for BDNF *in vitro*, this alone was not able to provide significant behavioral sparing, suggesting that transient reduction in behavioral deficits following transplantation of UCB MSCs is not solely due to BDNF expression but likely due to a release of several trophic factors and immunomodulating cytokines (Rossignol et al., 2009).

Data from this study demonstrates that transplantation of UCB MSCs, while providing transient behavioral sparing, did not provide robust reductions of deficits to the extent of those previously observed in our lab following transplantations of bone-marrow-derived MSCs (Dey et al., 2010; Lescaudron et al., 2003; Rossignol et al., 2011). Transplantation of high-passaged UCB MSCs were capable of delaying the motor deficits compared to untreated R6/2 mice when the mice were 6- and 10-weeks of age and these mice also had significantly lower limbs-clasping scores, relative to R6/2 mice that received transplants of low-passaged UCB MSCs at 7-weeks-of-age.

While long-term behavioral sparing was not observed following intrastriatal UCB MSC transplantation in these mice, significant reductions in neuropathology, in terms of preserved optical densitometric measures of CYO labeling in the striatum of R6/2 mice that received either low- or high-passaged UCB MSCs. Mice that received high-passaged UCB MSCs had lower measures of brain atrophy when compared to untreated R6/2 mice. The trend for reduced neuropathological deficits observed in the high-passaged groups, relative to the low-passaged group may be in part due to the number of surviving cells and a lower immune response to those cells. It was observed that there were significantly more surviving cells in the high-passaged group and that there was a significant increase in the optical densitometric measures of GFAP in

the low-passaged group, suggesting that the low-passaged group may be subjected to a greater immune response, resulting in fewer surviving cells.

The fact that this study demonstrates that high-passaged UCB MSCs provided greater behavioral and neuropathological sparing than low-passaged UCB MSCs, even though the low-passaged UCB MSCs displayed a higher expression of mRNA for BDNF *in vitro*, is an interesting finding and suggests that the mechanism behind MSC-mediated recovery is not solely dependent on BDNF, but probably involves a host of other trophic and immunomodulatory factors. While it has been suggested that deficits in BDNF production play a causal role in the progression of HD (Zuccato et al., 2011) and the increasing levels of BDNF may underscore behavioral sparing following MSC transplantation into rodent models of HD, the immune response to these cells also needs to be closely examined.

A main goal of utilizing MSCs isolated from the UCB was that these cells may possess greater levels of pluripotency than other adult MSCs, due to their intermediate developmental status between the fetus and the adult. However, in our lab, MSCs isolated from the UCB, while displaying typical MSC morphology and protein expression, did not express markers of pluripotency and were unable to differentiate into neuronal phenotypes, *in vivo*, following intrastriatal transplantation.

Contrary to what was observed in previous work with bone-marrow derived MSCs, R6/2 mice that received transplantation of either low- or high-passaged UCB MSCs did not display the same level of behavioral sparing on measures of rotarod, Morris Water Maze, or limb-clasping performance.

Experiment 3. *Adenovirus-Generated Induced Pluripotent Stem Cells*

This experiment compared iPSCs derived from bone marrow MSCs and TTFs that were generated using either a single cassette lentivirus or a combination of adenoviruses. All reprogrammed cells showed expression of pluripotent markers SSEA3, SSEA4, Tra-1-60, Nanog, and Oct4 by flow cytometry and immunocytochemistry. Quantitative PCR revealed that TTFs reprogrammed with the novel adenoviral combination created for this study, expressed the highest overall expression of pluripotent genes, relative to the other iPSC lineages tested in this study, suggesting that these cells may possess more pluripotency. The findings from this experiment also suggest that adenoviral transfection of somatic cells may hold more clinical relevance for therapeutic interventions, due to the fact that the viral constructs are not integrated into the genome and the cells showed similar levels of pluripotency.

Experiment 4. *Survival and Differentiation of Adenovirus-Generated Induced Pluripotent Stem Cells Transplanted into the Rat Striatum*

The observed survival, absence of tumors, and neuronal differentiation into highly region-specific cells, suggest that adenovirus-generated tail-tip fibroblast iPSCs may provide a safe and viable alternative to ESCs and MSCs for therapeutic treatment of CNS disorders.

While it has been suggested that iPSCs may be hypoimmunogenic when transplanted into other organs of the body (Araki et al., 2013; Boyd et al., 2012; Pearl, Kean, Davis, & Wu, 2012), the degree of immunogenicity of iPSCs when transplanted into the brain is still unknown. The present findings provide new evidence concerning the degree of immunogenicity of transplanted iPSCs in the brain. While an inflammatory response, in the form of activated microglia, macrophages, and astrocytes, was observed around the transplantation site, long-term survival of

the transplanted iPSCs was also observed, suggesting that the host immune system developed some tolerance to at least a large subset of the transplanted iPSCs. However, the degree to which iPSCs are immunologically privileged may be highly dependent on a continuum of factors, including the timing, location, and health of the host brain (Pearl et al., 2012). Nonetheless, the ability of the transplanted iPSCs to differentiate into region-specific neurons, in the presence of the immune response, suggests that these cells also may be sufficiently robust to survive and differentiate when transplanted into a host brain that is compromised by damage or disease.

While the intact striatum may not provide the ideal environment for studying the efficacy of the transplanted cells (Labandeira-Garcia, Wictorin, Cunningham, & Björklund, 1991), this study provides proof-of-principle that iPSCs derived in this manner can survive and differentiate into mature neuronal phenotypes *in vivo*. Preliminary findings from our lab suggest that these iPSCs are at least as therapeutically efficacious in a rat model of HD than in the healthy rat striatum (Fink et al., in revision). In addition to this study, our lab has transplanted the tail-tip fibroblast adenovirus-generated iPSCs into the brain of over 100 rats. Although only gross morphological changes (i.e., cresyl violet and cytochrome oxidase) have thus far been examined, no aberrant cell growth or cell masses have been observed, suggesting that these cells do not form teratomas following transplantation into the brains of either healthy wild-type or rodents with the HD transgene.

Experiment 5. *Intrastriatal Transplantation of Adenovirus-Generated Induced Pluripotent Stem Cells for Treating Neuropathological and Functional Deficits in a Rodent Model of Huntington's disease*

The results of this experiment indicate that transplantation of iPSCs are an effective means for treating behavioral and morphological deficits in the 3-NP rat model of HD. At nine

weeks following the administration of 3-NP, all rats that received transplantation of iPSCs performed at levels that were not significantly different from Sham controls, but had significantly longer latencies to fall off the accelerod task, relative to rats that received 3-NP without transplants. Data from the early- and middle-stage intervention indicated that iPSCs may be able to prevent the progressive loss of motor coordination, as measured on the accelerod, and that late-stage transplantation of iPSCs can promote behavioral recovery. Transplantation of pluripotent cells, isolated from fetal tissue, have produced evidence of similar preservation of motor function in animal models of HD (Armstrong et al., 2000; Bernreuther et al., 2006; Dunnett et al., 1998; McBride et al., 2004; Ryu et al., 2004; Song et al., 2007), but this is the first study, to our knowledge, that demonstrates functional recovery in an HD rodent model using iPSCs.

Histological analysis revealed that rats receiving 3-NP without transplants displayed a significant decrease in metabolically active tissue in the striatum and had significant larger lateral ventricles, when compared to Sham rats. Rats in the 7-day or 21-day transplant groups had neither the decrease in metabolic activity, as measured by reduced optical density of CYO-labeled striatal tissue at the end-points of the study nor did they have the significant lateral ventricle enlargements that were observed in the 3-NP rats that did not receive the transplants. Interestingly, rats in the 42-day group had lower metabolic activity in the striatum, but no significant enlargement of the lateral ventricles.

An analysis of activated microglia (CD11b) revealed that all rats that received 3-NP had significantly more activated microglia than Sham rats, and that rats in the 7-day and 42-day groups had more activated microglia than rats receiving 3-NP without transplantation, indicating

possible immune responses to the transplanted cells. An analysis of macrophage infiltration (IBA1) revealed that the 3-NP rats that did not receive transplants had significantly more macrophage infiltration than all other groups, indicating that the transplants protected against 3-NP-induced macrophage infiltration and did not activate a host macrophage response. The immune response, in terms of the iPSC-transplant-induced activated microglia and macrophage response observed in this study has also been reported previously in a study (Experiment 4; Johann et al., 2007). Although an obvious immune response was observed, transplanted cells were still visualized, indicating a long-term tolerance of the graft by the host tissue.

Less than 1% of iPSCs displayed co-localization with the astrocyte marker GFAP, suggesting that they did not differentiate into glial lineages. It has been previously reported that following transplantation of embryonic neural stem cells that the majority of the transplanted cells differentiated into glial lineage (Johann et al., 2007). This discrepancy in the amount of GFAP labeling between our study and the previous work may be due in part to the specific location the neural stem cells were harvested and/or the type of culture media used prior to transplantation.

Similar to transplantation of these iPSCs into a healthy rat striatum (Experiment 4), transplantation into the striata of a 3-NP brain revealed survival and differentiation of into mature, region-specific neurons in the brain of the rats at all time points. Significant neuronal loss was also observed in the 3-NP rats without transplants, when compared to Sham rats, but this loss of neurons was prevented by transplants in rats in the 7-day group. Counts of iPSCs that differentiated into neuronal lineages (as measured by co-localization with NeuN; white

arrowheads in Figure 32F-Q) revealed that the 7-d group had significantly more iPSCs that differentiated into neuronal lineages than iPSCs that were transplanted at 21- or 42-days.

The lack of differences between transplantation time points and DARPP32 differentiation may explain why the 7-day iPSC transplant group demonstrated such robust survival, even with longer exposure to the 3-NP toxin. While it was clearly demonstrated that the transplanted iPSCs can express neuronal phenotypes following transplantation, it may be that more time was needed, *in vivo*, for the majority of the transplanted cells to differentiate into mature, medium spiny neurons.

Quantitative RT PCR for mRNA expression of BDNF revealed no significant differences between all groups, suggesting that the motor and histological deficits associated with 3-NP administration were not due to a depletion of BDNF and that the motor recovery and anatomical preservation observed in the iPSC transplant group were not due to trophic support alone, as was observed in previous work with mesenchymal stem cell transplantation in our lab (Dey et al., 2010; Dunbar et al., 2006; Lescaudron et al., 2003; Rossignol et al., 2011).

Quantitative RT PCR revealed significant between-group differences in the mRNA expression for TNF-α, with the 21-day and 42-day transplant groups showing reduced levels of TNF-α, relative to those in the Sham and 7-day transplant groups. TNF-α is implicated to play a central role in initiating the cascade of cytokines that are responsible for an immune response in the brain (Nadeau & Rivest, 1999) and can be a general indicator of the immune response following cell transplantation. None of the 3-NP iPSC transplanted groups showed an upregulation of mRNA expression of TNF-α, suggesting that there was not a secondary immune

response to these cells. These data, along with immunohistochemistry of IBA1 and CD11b, suggests that the transplanted cells are tolerated by the host immune system.

CHAPTER VII

CONCLUSION

The results from this dissertation further validate the potential use of adult stem cells for therapeutic transplantation for HD. Taken together, these studies demonstrate that the severity of motor dysfunction and neuropathological loss of neurons in the striatum is reduced following transplantation of adult stem cells in animal models of HD (Figure 35). Two of the main goals following stem cell transplantation are to either provide cell-protection or neuro-regeneration/neural replacement (Karussis, Petrou, & Kassis, 2013; Ronaghi, Erceg, Moreno-Manzano, & Stojkovic, 2010). While the results from this dissertation indicate the therapeutic potential of stem cell transplantation, there are still major hurdles that need to be addressed prior to their use in the clinic. For example, the standardization of isolating, propagating, and storing the cells without compromising their stability, as well as testing the differentiation capacity and paracrine release of the cells *in vitro* need to be performed in a rigorous manner prior to their use in clinical trials (Andressen, 2013). Cells that are being considered for transplantation therapies also need to be rigorously examined for their ability to survive, differentiate, and functionally integrate into the targeted brain region in the absence of tumor formation or a large immune response from the host tissue (Andressen, 2013). The results from this dissertation suggest that two sources of adult stem cells, BM MSCs and adenovirally-produced iPSCs, significantly reduce functional and neuropathological deficits following intrastriatal transplantation, likely through release of trophic factors and immunomodulating cytokines or neuronal differentiation.

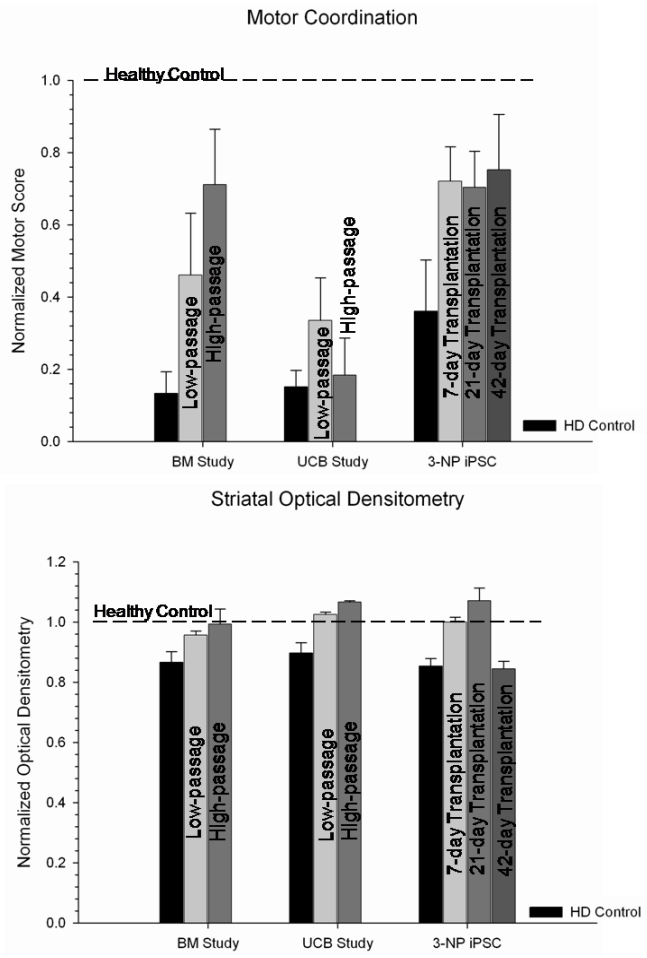

Figure 35. *Normalized motor coordination score and optical densitometry in the striatum of HD animals receiving stem cell transplantations.*
HD animals that received either high passage BM MSCs or early intervention of iPSCs (i.e., 7- or 21-day transplant groups) had both preservation of motor coordination and levels of metabolic activity in the striatum.

This dissertation delineates several possible mechanisms that MSCs may provide in lieu of neuronal differentiation such as trophic support and immunomodulation. These hypotheses are supported from studies of other neurological disorders (Huang et al, 2013; Lin et al, 2013; Han et al, 2013; Uccelli et al, 2011). Transplantation of BM MSCs can delay the progression of HD-like

symptoms and neuropathology through trophic support thru release of BDNF and immunomodulation in the R6/2 mouse. The results from these five experiments suggest that BM MSCs and iPSCs provide the greatest efficacy following transplantation into animal models of HD when compared to MSCs isolated from extra-embryonic tissue such as the umbilical cord.

Results from Experiment 1 suggest that preservation of BDNF levels plays a critical role in the progression of HD symptoms and may be the main mechanism behind the behavior sparing and reductions in neuropathological deficits, but other neurotrophic factors are critical for reducing the disease progression as well. It has been shown that viral delivery of glial-derived neurotrophic factor (GDNF) can ameliorate accelerod deficits and reduce hind-limb clasping in the N171-Q82 mouse model of HD, similar to our findings in the R6/2 model (McBride et al., 2006). Clearly, more work is needed to delineate the relative contribution of the sundry putative factors that may underlie the functional benefits exerted by the transplanted MSCs. Experiment 1 provided additional evidence that transplantation of BM MSCs hold significant promise for delaying the onset of motor, cognitive, and neuropathological deficits in HD, most likely through the release of neurotrophic factors, specifically BDNF. This study also underscored the need to consider passage number when evaluating the efficacy of MSCs transplantation therapies.

The results from Experiment 2 demonstrate that UCB MSCs may also hold significant therapeutic value for reducing the neuropathological changes observed in the R6/2 rodent model of HD, albeit to a lesser degree than bone-marrow-derived MSCs. While the cells cultured in our standard MSC medium did not express markers of pluripotency, changing the protocols for cell extraction from the umbilical cord (Fong et al., 2007; Mitchell et al., 2003) or exposing the UCB

MSCs to different culture conditions (Fu et al., 2004) may increase the therapeutic efficacy of these cells.

The results from Experiment 3 and Experiment 4 demonstrate that the use of iPSCs mitigates many of the issues that arise with the use of ESCs. The four lineages of iPSCs that were generated in study three all displayed characteristics of pluripotent cells, were easily isolated from non-embryonic tissue, and were easily expandable *in vitro*. In addition, no tumors were observed after the iPSC transplantation into immune competent brain in Experiment 4, suggesting that adenoviral-generated iPSCs could be safe for transplantation. Finally, the finding that iPSCs differentiated into region-specific neurons helps to validate their use as a potential cell-replacement strategy for damage or disease to the central nervous system.

Results from Experiment 5 represent an initial finding of behavioral recovery and neuronal/morphological sparing in an animal model of HD model following transplantation of iPSCs. It has been previously demonstrated that transplantation of human ESC-derived neurons can promote restoration of motor function in a quinolinic-acid lesion mouse model of HD (Ma et al., 2012). In their study, the lateral-ganglionic-eminence-like cells were able to survive for at least four months and express both markers of GABAergic neurons and βIII-tubulin. However, their transplant was performed in immune deficient SCID mice (Ma et al., 2012). Our data is the first to date to demonstrate that cells, reprogrammed to a pluripotent state, can reduce HD-like deficits in a non-immune suppressed, progressive model of HD. These data also suggest that transplantation of iPSCs, derived from tail-tip fibroblasts and reprogrammed with our adenovirus pair, are safe (i.e., no evidence of tumor formation or observable side effects), can survive in a neurodegenerating brain, and can differentiate into region-specific neuronal phenotypes. Further,

this study suggests that when transplantation of iPSCs is done early in the progression of the disease, it not only prevents a decline in motor function, but also preserves the anatomical features in the brain. Overall, rats that received iPSC transplantation at 7-days following the administration of 3-NP did not display motor dysfunction, did not exhibit a decrease in metabolic activity or enlargement of the lateral ventricles, did not display significant neuronal loss, and had the highest number of surviving iPSCs at the end point of this study. As such, this study supports the hypothesis that our newly-described method of producing iPSCs may prove to therapeutically efficacious and clinically relevant for the treatment of HD.

This dissertation also presents novel findings supporting the use of iPSCs for cell replacement strategies. The novel method, in which the iPSCs were generated, without viral integration, presents a more clinically relevant cell type for transplantation studies. This is also the first study, to the knowledge of this author, that transplanted iPSCs have shown both behavioral recovery and reductions in neuropathology in an animal model of HD. Transplantation of adenovirus generated iPSCs can promote behavioral recovery and reduce neuropathology through neuronal differentiation, opening the possibility of neuronal replacement.

Results from the MSC transplantation studies suggest that neuroprotection occurred due to paracrine effects of the transplanted cells. However, the first two experiments in this dissertation suggest that the number of times the cells are passaged is also a critical variable to examine. The results from Experiment 5 suggest that the behavioral sparing and reductions of neuropathology are not due solely to the release of trophic factors or immunomodulating cytokines, but that the recovery observed was linked to the differentiation of transplanted iPSCs

into region-specific neurons. This is supported by showing a positive correlation for the number of BM MSCs found in the striatum and motor performance scores ($r = 0.871$, $n = 23$, $p < 0.001$; Figure 36A). However, the number of surviving UCB MSCs and motor performance score were not as strongly correlated ($r = 0.546$, $n = 29$, $p = 0.002$; Figure 36B), suggesting that the source from which the MSCs are isolated plays a large role in the behavioral outcome following transplantation. When performing the same analysis for the number of iPSCs found in the striatum and motor performance score, no correlation is found ($r = 0.326$, $n = 28$, $p = 0.09$; Figure 36C), however, a positive correlation was found between the number of iPSCs that were co-localized with NeuN and the motor performance score ($r = 0.662$, $n = 28$, $p < 0.001$; Figure 36D). These findings suggest that the source of MSCs greatly affect the ability of these cells to provide behavioral sparing and that, in BM MSC transplantation, the greater the number of cells, the more behavioral sparing occurs, likely through an increased level of physiologically relevant trophic support and immunomodulation. Also, the behavioral sparing or recovery observed following transplantation of iPSCs is not solely dependent on the number of surviving cells, but is more strongly correlated to the number of these transplanted cells that differentiate into neuronal lineages.

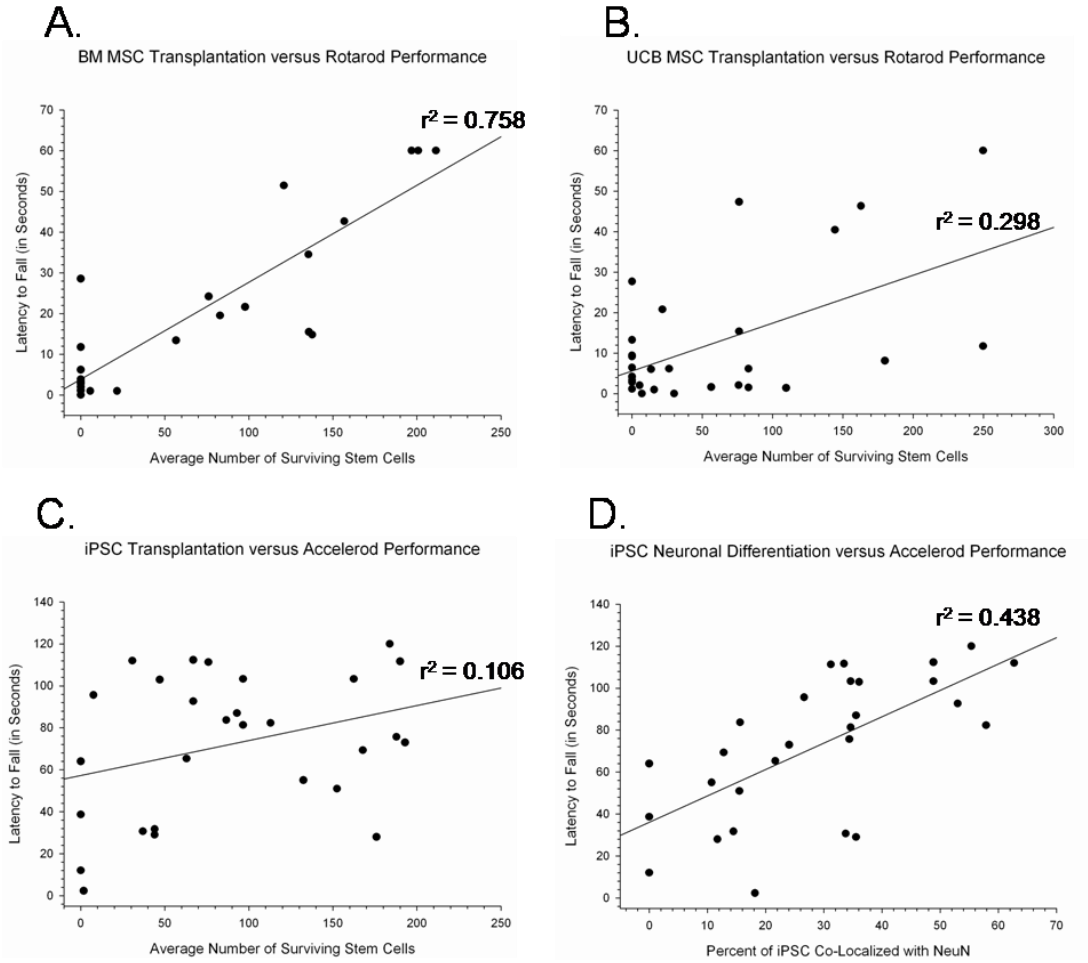

Figure 36. *Correlation between number of surviving stem cells and motor coordination.*
A positive correlation was observed between the number of BM MSCs in the striatum and the latency to fall (A). A modest positive correlation was observed between the number of UCB MSCs in the striatum and the latency to fall (B). No correlation was observed between the number of iPSCs in the striatum and the latency to fall (C), however, a positive correlation was observed between the amount of iPSCs that were co-localized with NeuN, a mature neuronal marker, and the latency to fall (D).

Similar to what was observed for motor performance, a positive correlation for the number of BM MSCs found in the striatum and striatal optical densitometry (r = 0.556, n = 14, *p*

< 0.039; Figure 37A), albeit a weaker correlation than was observed for motor performance. A similar positive correlation was observed in the number of surviving UCB MSCs and striatal optical densitometry (r = 0.504, n = 16, *p* = 0.047; Figure 37B). When performing the same analysis for the number of iPSCs found in the striatum and striatal optical densitometry, no correlation was found (r = 0.563, n = 12, *p* = 0.057; Figure 37C), however, a positive correlation was found between the number of iPSCs that were co-localized with NeuN and optical densitometry measures of CYO labeling in the striatum (r = 0.806, n = 12, *p* = 0.002; Figure 37D). These findings suggest that as the number of surviving MSCs increase, either UCB or BM, the optical density of striatal tissue also increases. The optical density levels of cytochrome oxidase labeling indicate the relative amount of metabolic activity in the striatum at the end-points of the experiments. However, as observed in the rats that received transplantation of iPSCs, no correlation was observed between the number of surviving cells and optical density of CYO-labeled striatal tissue, but a positive correlation was observed between the number of iPSCs that co-localized with NeuN and these optical density measures suggesting that the increase in metabolic activity of striatal tissue observed in the 3-NP rats may be linked to the number of iPSCs that differentiate into neuronal lineages.

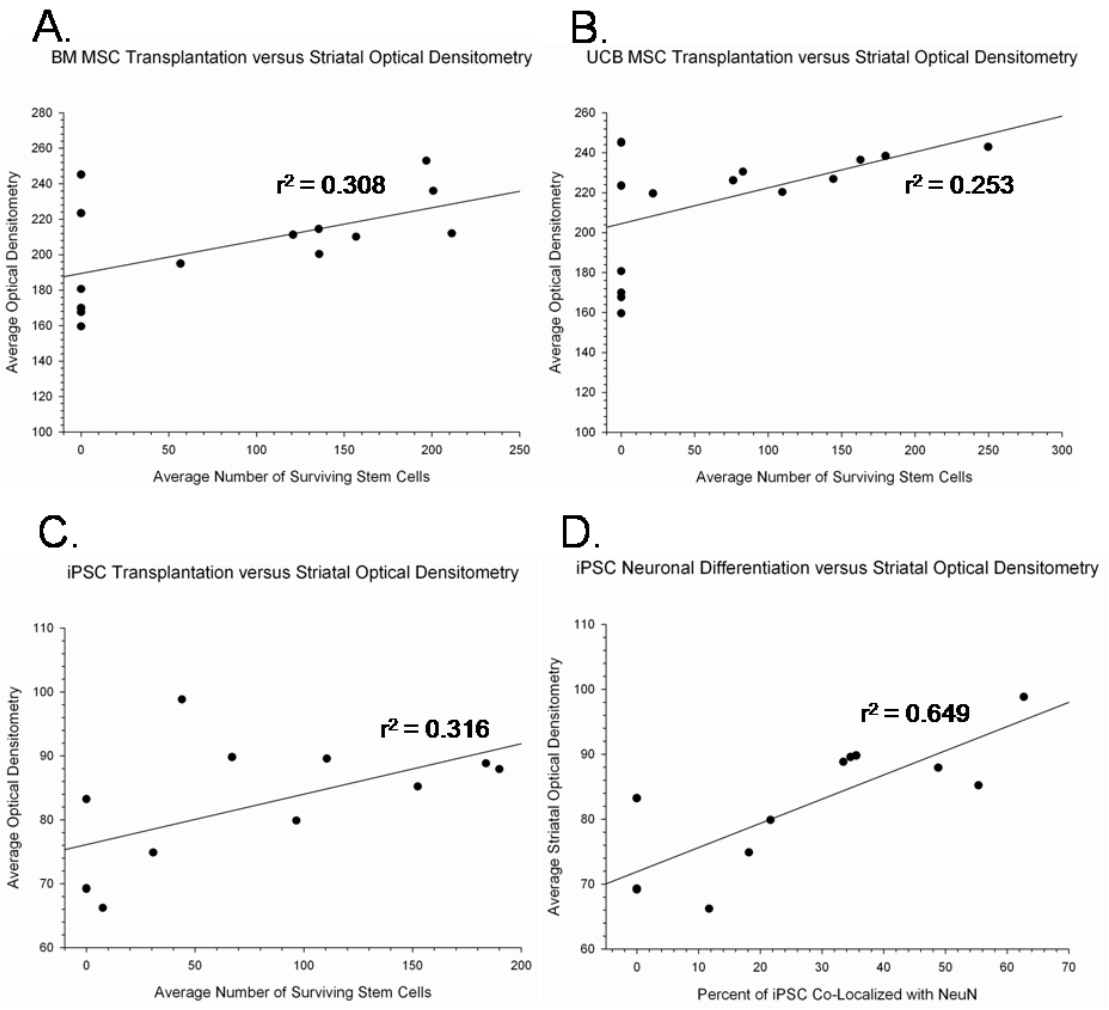

Figure 37. *Correlation between number of surviving stem cells and the optical density of CYO-labeled tissue in the striatum.*
A positive correlation was observed between the number of BM MSCs in the striatum and the optical densitometry in the striatum (A). A modest positive correlation was observed between the number of UCB MSCs in the striatum and the optical densitometry in the striatum (B). No correlation was observed between the number of iPSCs in the striatum and the optical densitometry in the striatum (C), however, a positive correlation was observed between the amount of iPSCs that were co-localized with NeuN, a mature neuronal marker, and the optical densitometry in the striatum (D).

Taken together, these experiments further support the contention that adult stem cells have significant potential for treating HD. New treatments for neurological diseases are needed. Stem cell therapies may offer one of the most promising avenues for treating a variety of disorders, not only in the central nervous system, but in other areas of the body as well. While data from this dissertation support the use of adult stem cells for the treatment of HD, specifically the use of iPSCs as a potential cell replacement therapy, many considerations need to be taken before this approach is tried clinically. A major hurdle that needs to be addressed is the timing of intervention with a biological agent, such as stem cells. Careful consideration needs to be taken to insure that the cells are implanted at the optimal time point to exert the maximal benefit as well as giving the cells the best chance to survive and integrate into the host. Data from this study indicate that transplantation of iPSCs is most effective prior to the onsetof motor symptoms and likely before the widespread neuronal loss in the striatum. While intervention at the late time point with iPSCs did partially restore motor deficits, the transplant were not able to restore the observed cell loss. This may be due to the lack of necessary cues for re-establishing synaptic connections and regenerating the lost striatal networks. However, transplantation of iPSCs at the late stage in this rat model of HD were able to significantly restore motor function, suggesting that even in lieu of neuronal restoration, some motor recovery is possible.

Currently, major drug companies are less driven to produce treatments for obscure neurological diseases as the development process is complex and expensive (it is thought to cost as much as 800 million dollars to develop a new drug). Only about 9% of new compounds that enter Phase 1 trials actually make it to the open market (Dutta et al., 2013). While much work is still needed before the widespread use of stem cells in therapeutic settings can be realized, this

mode of therapy may be better suited to treat neurological disorders than many others, because of the ability of stem cells to accurately mimic the normal cell repair and development process (Dutta et al., 2013). Although cell replacement therapies have been fraught with technical and political problems, there are early signs that this approach has considerable potential. Early work with Parkinson's Disease, where the first clinical trials were performed in the mid-1980's and a total of 300-400 patients have been treated subsequently with fetal cell transplantation and in the open label studies, has yielded evidence of some functional improvement [for review (Barker, 2012; Karussis et al., 2013)].

Clinical trials using MSCs are also now underway, and are still mainly focused on the safety of the cells. Currently, BM MSCs have been autologously transplanted into the subventricular zone in patients with advanced PD (Venkataramana et al., 2010), intravenously in patients that had suffered a stroke (Boncoraglio, Bersano, Candelise, Reynolds, & Parati, 2010; Lee et al., 2010), and UCB MSCs have been administered intravenously in children with cerebral palsy (Lee et al., 2012) with some clinical efficacy observed, and with no adverse side-effects from the cells.

As one of the fastest growing areas in cell research, iPSCs are already entering clinical studies in Japan (Cyranoski, 2013). The first planned clinical study will involve transplanting retinal cells, derived from iPSCs, and into six patients that have severe age-related macular degeneration. The initial aim of this study is to assess the safety of teh procedure, but the hope is to see the transplants slow the progression of the disease by repairing the pigment epithelium. Takahashi and colleagues plan to have approval in September of 2013 to transplant these cells within eight months (Cyranoski, 2013). While the field of iPSC transplantation is rapidly

growing, this technology provokes many of the same questions that surrounded questions of human embryonic tissue transplantation (Scott, 2013), so studies focused on the efficacy of these cells need to be performed cautiously. There are many safety concerns that need to be addressed prior to the full-scale clinical use of iPSCs, including which reprogramming method generates the best populations of pluripotent cell, their genomic stability, their capacity for proliferation following transplantation, and the potential immune response to the cells (Okano et al., 2013). All of these issues, along with the therapeutic efficacy of iPSCs need to be explored before this promising therapy can be used to treat neurodegenerative disorders.

REFERENCES

Abada, Y.-S. K., Nguyen, H. P., Schreiber, R., & Ellenbroek, B. (2013). Assessment of motor function, sensory motor gating and recognition memory in a novel BACHD transgenic rat model for huntington disease. *PloS one*, *8*(7), e68584. doi:10.1371/journal.pone.0068584

Adegani, F. J., Langroudi, L., Arefian, E., Shafiee, A., Dinarvand, P., & Soleimani, M. (2013). A comparison of pluripotency and differentiation status of four mesenchymal adult stem cells. *Molecular biology reports*, *40*(5), 3693–3703. doi:10.1007/s11033-012-2445-7

Ahmadbeigi, N., Soleimani, M., Gheisari, Y., Vasei, M., Amanpour, S., Bagherizadeh, I., … Nardi, N. B. (2011). Dormant phase and multinuclear cells: two key phenomena in early culture of murine bone marrow mesenchymal stem cells. *Stem cells and development*, *20*(8), 1337–1347. doi:10.1089/scd.2010.0266

Albin, R. L. (1995). Selective neurodegeneration in Huntington's disease. *Annals of neurology*, *38*(6), 835–836. doi:10.1002/ana.410380602

Albin, R. L. (2002). Fetal striatal transplantation in Huntington's disease: time for a pause. *Journal of neurology, neurosurgery, and psychiatry*, *73*(6), 612.

Albin, R. L., Reiner, A., Anderson, K. D., Dure, L. S., 4th, Handelin, B., Balfour, R., … Young, A. B. (1992). Preferential loss of striato-external pallidal projection neurons in presymptomatic Huntington's disease. *Annals of neurology*, *31*(4), 425–430. doi:10.1002/ana.410310412

Albin, R. L., Reiner, A., Anderson, K. D., Penney, J. B., & Young, A. B. (1990). Striatal and nigral neuron subpopulations in rigid Huntington's disease: implications for the functional anatomy of chorea and rigidity-akinesia. *Annals of neurology*, *27*(4), 357–365. doi:10.1002/ana.410270403

Albin, R. L., & Young, A. B. (1988). Somatosensory phenomena in Huntington's disease. *Movement disorders: official journal of the Movement Disorder Society*, *3*(4), 343–346. doi:10.1002/mds.870030411

Albin, R. L., Young, A. B., & Penney, J. B. (1989). The functional anatomy of basal ganglia disorders. *Trends in neurosciences*, *12*(10), 366–375.

Alvarez-Buylla, A., & Lois, C. (1995). Neuronal stem cells in the brain of adult vertebrates. *Stem cells (Dayton, Ohio)*, *13*(3), 263–272. doi:10.1002/stem.5530130307

Amin, E. M., Reza, B. A., Morteza, B. R., Maryam, M. M., Ali, M., & Zeinab, N. (2008). Microanatomical evidences for potential of mesenchymal stem cells in amelioration of striatal degeneration. *Neurological research*, *30*(10), 1086–1090. doi:10.1179/174313208X327955

Andressen, C. (2013). Neural stem cells: from neurobiology to clinical applications. *Current pharmaceutical biotechnology*, *14*(1), 20–28.

Aoi, T., Yae, K., Nakagawa, M., Ichisaka, T., Okita, K., Takahashi, K., … Yamanaka, S. (2008). Generation of pluripotent stem cells from adult mouse liver and stomach cells. *Science (New York, N.Y.)*, *321*(5889), 699–702. doi:10.1126/science.1154884

Araki, R., Uda, M., Hoki, Y., Sunayama, M., Nakamura, M., Ando, S., … Abe, M. (2013). Negligible immunogenicity of terminally differentiated cells derived from induced pluripotent or embryonic stem cells. *Nature*, *494*(7435), 100–104. doi:10.1038/nature11807

Armstrong, R. J., Watts, C., Svendsen, C. N., Dunnett, S. B., & Rosser, A. E. (2000). Survival, neuronal differentiation, and fiber outgrowth of propagated human neural precursor grafts in an animal model of Huntington's disease. *Cell transplantation*, *9*(1), 55–64.

Aubry, L., Bugi, A., Lefort, N., Rousseau, F., Peschanski, M., & Perrier, A. L. (2008). Striatal progenitors derived from human ES cells mature into DARPP32 neurons in vitro and in quinolinic acid-lesioned rats. *Proceedings of the National Academy of Sciences of the United States of America*, *105*(43), 16707–16712. doi:10.1073/pnas.0808488105

Ayalon, L., Doron, R., Weiner, I., & Joel, D. (2004). Amelioration of behavioral deficits in a rat model of Huntington's disease by an excitotoxic lesion to the globus pallidus. *Experimental neurology*, *186*(1), 46–58. doi:10.1016/S0014-4886(03)00312-1

Aylward, E. H., Rosenblatt, A., Field, K., Yallapragada, V., Kieburtz, K., McDermott, M., … Ross, C. A. (2003). Caudate volume as an outcome measure in clinical trials for Huntington's disease: a pilot study. *Brain research bulletin*, *62*(2), 137–141.

Bachoud-Lévi, A. C., Rémy, P., Nguyen, J. P., Brugières, P., Lefaucheur, J. P., Bourdet, C., … Peschanski, M. (2000). Motor and cognitive improvements in patients with Huntington's disease after neural transplantation. *Lancet*, *356*(9246), 1975–1979.

Bachoud-Lévi, A.-C. (2009). Neural grafts in Huntington's disease: viability after 10 years. *Lancet neurology*, *8*(11), 979–981. doi:10.1016/S1474-4422(09)70278-9

Bachoud-Lévi, A.-C., Gaura, V., Brugières, P., Lefaucheur, J.-P., Boissé, M.-F., Maison, P., … Peschanski, M. (2006). Effect of fetal neural transplants in patients with Huntington's disease 6 years after surgery: a long-term follow-up study. *Lancet neurology*, *5*(4), 303–309. doi:10.1016/S1474-4422(06)70381-7

Bae, K. S., Park, J. B., Kim, H. S., Kim, D. S., Park, D. J., & Kang, S. J. (2011). Neuron-like differentiation of bone marrow-derived mesenchymal stem cells. *Yonsei medical journal*, *52*(3), 401–412. doi:10.3349/ymj.2011.52.3.401

Bantubungi, K., Blum, D., Cuvelier, L., Wislet-Gendebien, S., Rogister, B., Brouillet, E., & Schiffmann, S. N. (2008). Stem cell factor and mesenchymal and neural stem cell transplantation in a rat model of Huntington's disease. *Molecular and cellular neurosciences*, *37*(3), 454–470. doi:10.1016/j.mcn.2007.11.001

Barker, R. A. (2012). Stem cells and neurodegenerative diseases: where is it all going? *Regenerative medicine*, *7*(6 Suppl), 26–31. doi:10.2217/rme.12.64

Barzilay, R., Ben-Zur, T., Bulvik, S., Melamed, E., & Offen, D. (2009). Lentiviral delivery of LMX1a enhances dopaminergic phenotype in differentiated human bone marrow mesenchymal stem cells. *Stem cells and development*, *18*(4), 591–601. doi:10.1089/scd.2008.0138

Barzilay, R., Kan, I., Ben-Zur, T., Bulvik, S., Melamed, E., & Offen, D. (2008). Induction of human mesenchymal stem cells into dopamine-producing cells with different differentiation protocols. *Stem cells and development*, *17*(3), 547–554. doi:10.1089/scd.2007.0172

Bauer, G., Dao, M. A., Case, S. S., Meyerrose, T., Wirthlin, L., Zhou, P., … Nolta, J. A. (2008). In vivo biosafety model to assess the risk of adverse events from retroviral and lentiviral vectors. *Molecular therapy: the journal of the American Society of Gene Therapy*, *16*(7), 1308–1315. doi:10.1038/mt.2008.93

Bazzett, T. J., Becker, J. B., Kaatz, K. W., & Albin, R. L. (1993). Chronic intrastriatal dialytic administration of quinolinic acid produces selective neural degeneration. *Experimental neurology*, *120*(2), 177–185. doi:10.1006/exnr.1993.1053

Bazzett, T., Legnard, E., Bauter, M. R., & Albin, R. L. (1999). Time-course analysis and comparison of acute and chronic intrastriatal quinolinic acid administration on forelimb reaching deficits in the rat. *Experimental neurology*, *158*(1), 126–134. doi:10.1006/exnr.1999.7070

Beal, M. F. (1994). Huntington's disease, energy, and excitotoxicity. *Neurobiology of aging*, *15*(2), 275–276.

Behrstock, S., Ebert, A. D., Klein, S., Schmitt, M., Moore, J. M., & Svendsen, C. N. (2008). Lesion-induced increase in survival and migration of human neural progenitor cells releasing GDNF. *Cell transplantation*, *17*(7), 753–762.

Bernreuther, C., Dihné, M., Johann, V., Schiefer, J., Cui, Y., Hargus, G., … Schachner, M. (2006). Neural cell adhesion molecule L1-transfected embryonic stem cells promote functional recovery after excitotoxic lesion of the mouse striatum. *The Journal of neuroscience: the official journal of the Society for Neuroscience*, *26*(45), 11532–11539. doi:10.1523/JNEUROSCI.2688-06.2006

Bertolo, A., Mehr, M., Janner-Jametti, T., Graumann, U., Aebli, N., Baur, M., … Stoyanov, J. V. (2013). An in vitro expansion score for tissue-engineering applications with human bone marrow-derived mesenchymal stem cells. *Journal of tissue engineering and regenerative medicine*. doi:10.1002/term.1734

Black, I. B., & Woodbury, D. (2001). Adult rat and human bone marrow stromal stem cells differentiate into neurons. *Blood cells, molecules & diseases*, *27*(3), 632–636. doi:10.1006/bcmd.2001.0423

Bohnen, N. I., Koeppe, R. A., Meyer, P., Ficaro, E., Wernette, K., Kilbourn, M. R., … Albin, R. L. (2000). Decreased striatal monoaminergic terminals in Huntington disease. *Neurology*, *54*(9), 1753–1759.

Boncoraglio, G. B., Bersano, A., Candelise, L., Reynolds, B. A., & Parati, E. A. (2010). Stem cell transplantation for ischemic stroke. *Cochrane database of systematic reviews (Online)*, (9), CD007231. doi:10.1002/14651858.CD007231.pub2

Bongso, A., & Fong, C.-Y. (2013). The Therapeutic Potential, Challenges and Future Clinical Directions of Stem Cells from the Wharton's Jelly of the Human Umbilical Cord. *Stem cell reviews*, *9*(2), 226–240. doi:10.1007/s12015-012-9418-z

Borovecki, F., Lovrecic, L., Zhou, J., Jeong, H., Then, F., Rosas, H. D., … Krainc, D. (2005). Genome-wide expression profiling of human blood reveals biomarkers for Huntington's disease. *Proceedings of the National Academy of Sciences of the United States of America*, *102*(31), 11023–11028. doi:10.1073/pnas.0504921102

Bosch, M., Pineda, J. R., Suñol, C., Petriz, J., Cattaneo, E., Alberch, J., & Canals, J. M. (2004). Induction of GABAergic phenotype in a neural stem cell line for transplantation in an excitotoxic model of Huntington's disease. *Experimental neurology*, *190*(1), 42–58. doi:10.1016/j.expneurol.2004.06.027

Boudreau, R. L., McBride, J. L., Martins, I., Shen, S., Xing, Y., Carter, B. J., & Davidson, B. L. (2009). Nonallele-specific silencing of mutant and wild-type huntingtin demonstrates therapeutic efficacy in Huntington's disease mice. *Molecular therapy: the journal of the American Society of Gene Therapy*, *17*(6), 1053–1063. doi:10.1038/mt.2009.17

Boyd, A. S., Rodrigues, N. P., Lui, K. O., Fu, X., & Xu, Y. (2012). Concise review: Immune recognition of induced pluripotent stem cells. *Stem cells (Dayton, Ohio)*, *30*(5), 797–803. doi:10.1002/stem.1066

Brazelton, T. R., Rossi, F. M., Keshet, G. I., & Blau, H. M. (2000). From marrow to brain: expression of neuronal phenotypes in adult mice. *Science (New York, N.Y.)*, *290*(5497), 1775–1779.

Brouillet, E., Guyot, M. C., Mittoux, V., Altairac, S., Condé, F., Palfi, S., & Hantraye, P. (1998). Partial inhibition of brain succinate dehydrogenase by 3-nitropropionic acid is sufficient to initiate striatal degeneration in rat. *Journal of neurochemistry*, *70*(2), 794–805.

Brundin, P., Barker, R. A., & Parmar, M. (2010). Neural grafting in Parkinson's disease Problems and possibilities. *Progress in brain research*, *184*, 265–294. doi:10.1016/S0079-6123(10)84014-2

Bugos, O., Bhide, M., & Zilka, N. (2009). Beyond the rat models of human neurodegenerative disorders. *Cellular and molecular neurobiology*, *29*(6-7), 859–869. doi:10.1007/s10571-009-9367-5

Burgdorf, J., Zhang, X., Weiss, C., Matthews, E., Disterhoft, J. F., Stanton, P. K., & Moskal, J. R. (2011). The N-methyl-D-aspartate receptor modulator GLYX-13 enhances learning and memory, in young adult and learning impaired aging rats. *Neurobiology of aging*, *32*(4), 698–706. doi:10.1016/j.neurobiolaging.2009.04.012

Cao, C., Temel, Y., Blokland, A., Ozen, H., Steinbusch, H. W. M., Vlamings, R., … Visser-Vandewalle, V. (2006). Progressive deterioration of reaction time performance and choreiform symptoms in a new Huntington's disease transgenic ratmodel. *Behavioural brain research*, *170*(2), 257–261. doi:10.1016/j.bbr.2006.02.028

Capetian, P., Knoth, R., Maciaczyk, J., Pantazis, G., Ditter, M., Bokla, L., … Nikkhah, G. (2009). Histological findings on fetal striatal grafts in a Huntington's disease patient early after transplantation. *Neuroscience*, *160*(3), 661–675. doi:10.1016/j.neuroscience.2009.02.035

Carey, B. W., Markoulaki, S., Hanna, J., Saha, K., Gao, Q., Mitalipova, M., & Jaenisch, R. (2009a). Reprogramming of murine and human somatic cells using a single polycistronic vector. *Proceedings of the National Academy of Sciences of the United States of America*, *106*(1), 157–162. doi:10.1073/pnas.0811426106

Carey, B. W., Markoulaki, S., Hanna, J., Saha, K., Gao, Q., Mitalipova, M., & Jaenisch, R. (2009b). Reprogramming of murine and human somatic cells using a single polycistronic vector. *Proceedings of the National Academy of Sciences of the United States of America*, *106*(1), 157–162. doi:10.1073/pnas.0811426106

Carlin, R., Davis, D., Weiss, M., Schultz, B., & Troyer, D. (2006). Expression of early transcription factors Oct-4, Sox-2 and Nanog by porcine umbilical cord (PUC) matrix cells. *Reproductive biology and endocrinology: RB&E*, *4*, 8. doi:10.1186/1477-7827-4-8

Chang, J., Lei, H., Liu, Q., Qin, S., Ma, K., Luo, S., … Xia, Y. (2012). Optimization of culture of mesenchymal stem cells: a comparison of conventional plate and microcarrier cultures. *Cell proliferation*, *45*(5), 430–437. doi:10.1111/j.1365-2184.2012.00836.x

Chang, M.-Y., Kim, D., Kim, C.-H., Kang, H.-C., Yang, E., Moon, J.-I., … Kim, K.-S. (2010). Direct reprogramming of rat neural precursor cells and fibroblasts into pluripotent stem cells. *PloS one*, *5*(3), e9838. doi:10.1371/journal.pone.0009838

Chin, M. H., Pellegrini, M., Plath, K., & Lowry, W. E. (2010). Molecular analyses of human induced pluripotent stem cells and embryonic stem cells. *Cell stem cell*, *7*(2), 263–269. doi:10.1016/j.stem.2010.06.019

Ciammola, A., Sassone, J., Cannella, M., Calza, S., Poletti, B., Frati, L., … Silani, V. (2007). Low brain-derived neurotrophic factor (BDNF) levels in serum of Huntington's disease patients. *American journal of medical genetics. Part B, Neuropsychiatric genetics: the official publication of the International Society of Psychiatric Genetics*, *144B*(4), 574–577. doi:10.1002/ajmg.b.30501

Cicchetti, F., Saporta, S., Hauser, R. A., Parent, M., Saint-Pierre, M., Sanberg, P. R., … Freeman, T. B. (2009). Neural transplants in patients with Huntington's disease undergo disease-like neuronal degeneration. *Proceedings of the National Academy of Sciences of the United States of America*, *106*(30), 12483–12488. doi:10.1073/pnas.0904239106

Cirillo, G., Maggio, N., Bianco, M. R., Vollono, C., Sellitti, S., & Papa, M. (2010). Discriminative behavioral assessment unveils remarkable reactive astrocytosis and early molecular correlates in basal ganglia of 3-nitropropionic acid subchronic treated rats. *Neurochemistry international*, *56*(1), 152–160. doi:10.1016/j.neuint.2009.09.013

Collier, T. J., Sortwell, C. E., Elsworth, J. D., Taylor, J. R., Roth, R. H., Sladek, J. R., Jr, & Redmond, D. E., Jr. (2002). Embryonic ventral mesencephalic grafts to the substantia nigra of MPTP-treated monkeys: feasibility relevant to multiple-target grafting as a therapy for Parkinson's disease. *The Journal of comparative neurology*, *442*(4), 320–330. doi:10.1002/cne.10108

Conforti, P., Ramos, C., Apostol, B. L., Simmons, D. A., Nguyen, H. P., Riess, O., … Cattaneo, E. (2008). Blood level of brain-derived neurotrophic factor mRNA is progressively reduced in rodent models of Huntington's disease: restoration by the neuroprotective compound CEP-1347. *Molecular and cellular neurosciences*, *39*(1), 1–7. doi:10.1016/j.mcn.2008.04.012

Coustasse, A., Pekar, A., Sikula, A., & Lurie, S. (2009). Ethical considerations of genetic presymptomatic testing for Huntington's disease. *Journal of hospital marketing & public relations*, *19*(2), 129–141. doi:10.1080/15390940903041583

Crane, A. T., Lowrance, S. A., Thibo, T. J., Fink, K. D., Hisscock, N., Tharp, M., … Dunbar, G. L. (In Preparation). Potential for treatment of cognitive deficits in early-stage 51 CAG transgenic Huntington's disease rats.

Croft, A. P., & Przyborski, S. A. (2006). Formation of neurons by non-neural adult stem cells: potential mechanism implicates an artifact of growth in culture. *Stem cells (Dayton, Ohio)*, *24*(8), 1841–1851. doi:10.1634/stemcells.2005-0609

Cyranoski, D. (2013). Stem cells cruise to clinic. *Nature*, *494*(7438), 413. doi:10.1038/494413a

Dey, N. D., Bombard, M. C., Roland, B. P., Davidson, S., Lu, M., Rossignol, J., … Dunbar, G. L. (2010). Genetically engineered mesenchymal stem cells reduce behavioral deficits in the YAC 128 mouse model of Huntington's disease. *Behavioural brain research*, *214*(2), 193–200. doi:10.1016/j.bbr.2010.05.023

DiFiglia, M., Sena-Esteves, M., Chase, K., Sapp, E., Pfister, E., Sass, M., … Aronin, N. (2007). Therapeutic silencing of mutant huntingtin with siRNA attenuates striatal and cortical neuropathology and behavioral deficits. *Proceedings of the National Academy of Sciences of the United States of America*, *104*(43), 17204–17209. doi:10.1073/pnas.0708285104

Ding, D.-C., Shyu, W.-C., Chiang, M.-F., Lin, S.-Z., Chang, Y.-C., Wang, H.-J., … Li, H. (2007). Enhancement of neuroplasticity through upregulation of beta1-integrin in human umbilical cord-derived stromal cell implanted stroke model. *Neurobiology of disease*, *27*(3), 339–353. doi:10.1016/j.nbd.2007.06.010

Dominici, M., Le Blanc, K., Mueller, I., Slaper-Cortenbach, I., Marini, F., Krause, D., … Horwitz, E. (2006). Minimal criteria for defining multipotent mesenchymal stromal cells. The International Society for Cellular Therapy position statement. *Cytotherapy*, *8*(4), 315–317. doi:10.1080/14653240600855905

Dunbar, G. L., Sandstrom, M. I., Rossignol, J., & Lescaudron, L. (2006). Neurotrophic enhancers as therapy for behavioral deficits in rodent models of Huntington's disease: use of gangliosides, substituted pyrimidines, and mesenchymal stem cells. *Behavioral and cognitive neuroscience reviews*, *5*(2), 63–79. doi:10.1177/1534582306289367

Dunnett, S. B., Carter, R. J., Watts, C., Torres, E. M., Mahal, A., Mangiarini, L., … Morton, A. J. (1998). Striatal transplantation in a transgenic mouse model of Huntington's disease. *Experimental neurology*, *154*(1), 31–40. doi:10.1006/exnr.1998.6926

Dunnett, S. B., & Rosser, A. E. (2011). Clinical translation of cell transplantation in the brain. *Current opinion in organ transplantation*, *16*(6), 632–639. doi:10.1097/MOT.0b013e32834c2356

Dutta, S., Singh, G., Sreejith, S., Mamidi, M. K., Husin, J. M., Datta, I., … Das, A. K. (2013). Cell therapy: the final frontier for treatment of neurological diseases. *CNS neuroscience & therapeutics*, *19*(1), 5–11. doi:10.1111/cns.12027

Dykxhoorn, D. M., & Lieberman, J. (2006). Running interference: prospects and obstacles to using small interfering RNAs as small molecule drugs. *Annual review of biomedical engineering*, *8*, 377–402. doi:10.1146/annurev.bioeng.8.061505.095848

Edalatmanesh, M.-A., Matin, M. M., Neshati, Z., Bahrami, A.-R., & Kheirabadi, M. (2010). Systemic transplantation of mesenchymal stem cells can reduce cognitive and motor deficits in rats with unilateral lesions of the neostriatum. *Neurological research*, *32*(2), 166–172. doi:10.1179/174313209X409025

El Massioui, N., Ouary, S., Chéruel, F., Hantraye, P., & Brouillet, E. (2001). Perseverative behavior underlying attentional set-shifting deficits in rats chronically treated with the neurotoxin 3-nitropropionic acid. *Experimental neurology*, *172*(1), 172–181. doi:10.1006/exnr.2001.7766

El-Akabawy, G., Rattray, I., Johansson, S. M., Gale, R., Bates, G., & Modo, M. (2012). Implantation of undifferentiated and pre-differentiated human neural stem cells in the R6/2 transgenic mouse model of Huntington's disease. *BMC neuroscience*, *13*, 97. doi:10.1186/1471-2202-13-97

Emerich, D. F., Cain, C. K., Greco, C., Saydoff, J. A., Hu, Z. Y., Liu, H., & Lindner, M. D. (1997). Cellular delivery of human CNTF prevents motor and cognitive dysfunction in a rodent model of Huntington's disease. *Cell transplantation*, *6*(3), 249–266.

Ende, N., & Chen, R. (2001). Human umbilical cord blood cells ameliorate Huntington's disease in transgenic mice. *Journal of medicine*, *32*(3-4), 231–240.

Estrada Sánchez, A. M., Mejía-Toiber, J., & Massieu, L. (2008). Excitotoxic neuronal death and the pathogenesis of Huntington's disease. *Archives of medical research*, *39*(3), 265–276. doi:10.1016/j.arcmed.2007.11.011

Evans, M. J., & Kaufman, M. H. (1981). Establishment in culture of pluripotential cells from mouse embryos. *Nature*, *292*(5819), 154–156.

Fändrich, F., Lin, X., Chai, G. X., Schulze, M., Ganten, D., Bader, M., … Binas, B. (2002). Preimplantation-stage stem cells induce long-term allogeneic graft acceptance without supplementary host conditioning. *Nature medicine*, *8*(2), 171–178. doi:10.1038/nm0202-171

Fink, K. D., Rossignol, J., Crane, A. T., Davis, K. K., Bavar, A. M., Dekorver, N. W., … Dunbar, G. L. (2012). Early cognitive dysfunction in the HD 51 CAG transgenic rat model of Huntington's disease. *Behavioral neuroscience*, *126*(3), 479–487. doi:10.1037/a0028028

Fink, K. D., Rossignol, J., Lu, M., Leveque, X., Hulse, T. D., Crane, A. T., … Dunbar, G. L. (In Revision). Survival and Differentiation of Adenovirus-Generated Induced Pluripotent Stem Cells Transplanted into the Rat Striatum. *Cell Transplantation*.

Fong, C. Y., Richards, M., Manasi, N., Biswas, A., & Bongso, A. (2007). Comparative growth behaviour and characterization of stem cells from human Wharton's jelly. *Reproductive biomedicine online*, *15*(6), 708–718.

Franich, N. R., Fitzsimons, H. L., Fong, D. M., Klugmann, M., During, M. J., & Young, D. (2008). AAV vector-mediated RNAi of mutant huntingtin expression is neuroprotective in a novel genetic rat model of Huntington's disease. *Molecular therapy: the journal of the American Society of Gene Therapy*, *16*(5), 947–956. doi:10.1038/mt.2008.50

Freeman, T. B., Cicchetti, F., Hauser, R. A., Deacon, T. W., Li, X. J., Hersch, S. M., … Isacson, O. (2000). Transplanted fetal striatum in Huntington's disease: phenotypic development and lack of pathology. *Proceedings of the National Academy of Sciences of the United States of America*, *97*(25), 13877–13882. doi:10.1073/pnas.97.25.13877

Friedenstein, A. J., Gorskaja, J. F., & Kulagina, N. N. (1976). Fibroblast precursors in normal and irradiated mouse hematopoietic organs. *Experimental hematology*, *4*(5), 267–274.

Fu, K.-Y., Dai, L.-G., Chiu, I.-M., Chen, J.-R., & Hsu, S. (2011). Sciatic nerve regeneration by microporous nerve conduits seeded with glial cell line-derived neurotrophic factor or brain-derived neurotrophic factor gene transfected neural stem cells. *Artificial organs*, *35*(4), 363–372. doi:10.1111/j.1525-1594.2010.01105.x

Fu, Y.-S., Cheng, Y.-C., Lin, M.-Y. A., Cheng, H., Chu, P.-M., Chou, S.-C., … Sung, M.-S. (2006). Conversion of human umbilical cord mesenchymal stem cells in Wharton's jelly to dopaminergic neurons in vitro: potential therapeutic application for Parkinsonism. *Stem cells (Dayton, Ohio)*, *24*(1), 115–124. doi:10.1634/stemcells.2005-0053

Fu, Y.-S., Shih, Y.-T., Cheng, Y.-C., & Min, M.-Y. (2004). Transformation of human umbilical mesenchymal cells into neurons in vitro. *Journal of biomedical science*, *11*(5), 652–660. doi:10.1159/000079678

Furtado, S., Sossi, V., Hauser, R. A., Samii, A., Schulzer, M., Murphy, C. B., … Stoessl, A. J. (2005). Positron emission tomography after fetal transplantation in Huntington's disease. *Annals of neurology*, *58*(2), 331–337. doi:10.1002/ana.20564

Gallina, P., Paganini, M., Lombardini, L., Mascalchi, M., Porfirio, B., Gadda, D., … Di Lorenzo, N. (2010). Human striatal neuroblasts develop and build a striatal-like structure into the brain of Huntington's disease patients after transplantation. *Experimental neurology*, *222*(1), 30–41. doi:10.1016/j.expneurol.2009.12.005

Giorgetti, A., Montserrat, N., Aasen, T., Gonzalez, F., Rodríguez-Pizà, I., Vassena, R., … Izpisua Belmonte, J. C. (2009). Generation of induced pluripotent stem cells from human cord blood using OCT4 and SOX2. *Cell stem cell*, *5*(4), 353–357. doi:10.1016/j.stem.2009.09.008

Gonzalez, F., Barragan Monasterio, M., Tiscornia, G., Montserrat Pulido, N., Vassena, R., Batlle Morera, L., … Izpisua Belmonte, J. C. (2009). Generation of mouse-induced pluripotent stem cells by transient expression of a single nonviral polycistronic vector. *Proceedings of the National Academy of Sciences of the United States of America*, *106*(22), 8918–8922. doi:10.1073/pnas.0901471106

Hardy, S. A., Maltman, D. J., & Przyborski, S. A. (2008). Mesenchymal stem cells as mediators of neural differentiation. *Current stem cell research & therapy*, *3*(1), 43–52.

Harper, S. Q., Staber, P. D., He, X., Eliason, S. L., Martins, I. H., Mao, Q., … Davidson, B. L. (2005). RNA interference improves motor and neuropathological abnormalities in a Huntington's disease mouse model. *Proceedings of the National Academy of Sciences of the United States of America*, *102*(16), 5820–5825. doi:10.1073/pnas.0501507102

Hauser, R. A., Furtado, S., Cimino, C. R., Delgado, H., Eichler, S., Schwartz, S., … Freeman, T. B. (2002). Bilateral human fetal striatal transplantation in Huntington's disease. *Neurology*, *58*(5), 687–695.

Heng, M. Y., Detloff, P. J., & Albin, R. L. (2008). Rodent genetic models of Huntington disease. *Neurobiology of disease*, *32*(1), 1–9. doi:10.1016/j.nbd.2008.06.005

Heng, M. Y., Detloff, P. J., Paulson, H. L., & Albin, R. L. (2010). Early alterations of autophagy in Huntington disease-like mice. *Autophagy*, *6*(8), 1206–1208.

Heng, M. Y., Detloff, P. J., Wang, P. L., Tsien, J. Z., & Albin, R. L. (2009). In vivo evidence for NMDA receptor-mediated excitotoxicity in a murine genetic model of Huntington disease. *The Journal of neuroscience: the official journal of the Society for Neuroscience*, *29*(10), 3200–3205. doi:10.1523/JNEUROSCI.5599-08.2009

Heng, M. Y., Duong, D. K., Albin, R. L., Tallaksen-Greene, S. J., Hunter, J. M., Lesort, M. J., … Detloff, P. J. (2010). Early autophagic response in a novel knock-in model of Huntington disease. *Human molecular genetics*, *19*(19), 3702–3720. doi:10.1093/hmg/ddq285

Ho, R., Chronis, C., & Plath, K. (2011). Mechanistic insights into reprogramming to induced pluripotency. *Journal of cellular physiology*, *226*(4), 868–878. doi:10.1002/jcp.22450

Huangfu, D., Osafune, K., Maehr, R., Guo, W., Eijkelenboom, A., Chen, S., … Melton, D. A. (2008). Induction of pluripotent stem cells from primary human fibroblasts with only Oct4 and Sox2. *Nature biotechnology*, *26*(11), 1269–1275. doi:10.1038/nbt.1502

Hung, S.-C., Cheng, H., Pan, C.-Y., Tsai, M. J., Kao, L.-S., & Ma, H.-L. (2002). In vitro differentiation of size-sieved stem cells into electrically active neural cells. *Stem cells (Dayton, Ohio)*, *20*(6), 522–529. doi:10.1634/stemcells.20-6-522

Huntington, G. (1872). On Chorea. *The Medical and Surgical Reporter: A Weekly Journal, 26*(15), 317–321.

Huntington, G. (2003). On chorea. George Huntington, M.D. *The Journal of neuropsychiatry and clinical neurosciences, 15*(1), 109–112.

Hurlbert, M. S., Gianani, R. I., Hutt, C., Freed, C. R., & Kaddis, F. G. (1999). Neural transplantation of hNT neurons for Huntington's disease. *Cell transplantation, 8*(1), 143–151.

Im, W., Ban, J., Lim, J., Lee, M., Lee, S.-T., Chu, K., & Kim, M. (2013). Extracts of Adipose Derived Stem Cells Slows Progression in the R6/2 Model of Huntington's Disease. *PloS one, 8*(4), e59438. doi:10.1371/journal.pone.0059438

Jia, F., Wilson, K. D., Sun, N., Gupta, D. M., Huang, M., Li, Z., … Wu, J. C. (2010). A nonviral minicircle vector for deriving human iPS cells. *Nature methods, 7*(3), 197–199. doi:10.1038/nmeth.1426

Jiang, Yuehua, Jahagirdar, B. N., Reinhardt, R. L., Schwartz, R. E., Keene, C. D., Ortiz-Gonzalez, X. R., … Verfaillie, C. M. (2002). Pluripotency of mesenchymal stem cells derived from adult marrow. *Nature, 418*(6893), 41–49. doi:10.1038/nature00870

Jiang, Yufeng, Lv, H., Huang, S., Tan, H., Zhang, Y., & Li, H. (2011). Bone marrow mesenchymal stem cells can improve the motor function of a Huntington's disease rat model. *Neurological research, 33*(3), 331–337. doi:10.1179/016164110X12816242542571

Johann, V., Schiefer, J., Sass, C., Mey, J., Brook, G., Krüttgen, A., … Kosinski, C. M. (2007). Time of transplantation and cell preparation determine neural stem cell survival in a mouse model of Huntington's disease. *Experimental brain research. Experimentelle Hirnforschung. Expérimentation cérébrale, 177*(4), 458–470. doi:10.1007/s00221-006-0689-y

Joyce, N., Annett, G., Wirthlin, L., Olson, S., Bauer, G., & Nolta, J. A. (2010). Mesenchymal stem cells for the treatment of neurodegenerative disease. *Regenerative medicine, 5*(6), 933–946. doi:10.2217/rme.10.72

Kaji, K., Norrby, K., Paca, A., Mileikovsky, M., Mohseni, P., & Woltjen, K. (2009). Virus-free induction of pluripotency and subsequent excision of reprogramming factors. *Nature, 458*(7239), 771–775. doi:10.1038/nature07864

Kallur, T., Darsalia, V., Lindvall, O., & Kokaia, Z. (2006). Human fetal cortical and striatal neural stem cells generate region-specific neurons in vitro and differentiate extensively to neurons after intrastriatal transplantation in neonatal rats. *Journal of neuroscience research, 84*(8), 1630–1644. doi:10.1002/jnr.21066

Kalonia, H., Kumar, P., Nehru, B., & Kumar, A. (2009). Neuroprotective effect of MK-801 against intra-striatal quinolinic acid induced behavioral, oxidative stress and cellular alterations in rats. *Indian journal of experimental biology*, *47*(11), 880–892.

Kántor, O., Temel, Y., Holzmann, C., Raber, K., Nguyen, H.-P., Cao, C., … Schmitz, C. (2006). Selective striatal neuron loss and alterations in behavior correlate with impaired striatal function in Huntington's disease transgenic rats. *Neurobiology of disease*, *22*(3), 538–547. doi:10.1016/j.nbd.2005.12.014

Karahuseyinoglu, S., Cinar, O., Kilic, E., Kara, F., Akay, G. G., Demiralp, D. O., … Can, A. (2007). Biology of stem cells in human umbilical cord stroma: in situ and in vitro surveys. *Stem cells (Dayton, Ohio)*, *25*(2), 319–331. doi:10.1634/stemcells.2006-0286

Karussis, D., Petrou, P., & Kassis, I. (2013). Clinical experience with stem cells and other cell therapies in neurological diseases. *Journal of the neurological sciences*, *324*(1-2), 1–9. doi:10.1016/j.jns.2012.09.031

Kawakami, M., Yoshimoto, T., Nakagata, N., Yamamura, K.-I., & Siesjo, B. K. (2011). Effects of cyclosporin A administration on gene expression in rat brain. *Brain injury: [BI]*, *25*(6), 614–623. doi:10.3109/02699052.2011.571229

Keene, C D, Sonnen, J. A., Swanson, P. D., Kopyov, O., Leverenz, J. B., Bird, T. D., & Montine, T. J. (2007). Neural transplantation in Huntington disease: long-term grafts in two patients. *Neurology*, *68*(24), 2093–2098. doi:10.1212/01.wnl.0000264504.14301.f5

Keene, C Dirk, Chang, R. C., Leverenz, J. B., Kopyov, O., Perlman, S., Hevner, R. F., … Montine, T. J. (2009). A patient with Huntington's disease and long-surviving fetal neural transplants that developed mass lesions. *Acta neuropathologica*, *117*(3), 329–338. doi:10.1007/s00401-008-0465-0

Kenney, C., Hunter, C., & Jankovic, J. (2007). Long-term tolerability of tetrabenazine in the treatment of hyperkinetic movement disorders. *Movement disorders: official journal of the Movement Disorder Society*, *22*(2), 193–197. doi:10.1002/mds.21222

Kim, J. B., Zaehres, H., Wu, G., Gentile, L., Ko, K., Sebastiano, V., … Schöler, H. R. (2008). Pluripotent stem cells induced from adult neural stem cells by reprogramming with two factors. *Nature*, *454*(7204), 646–650. doi:10.1038/nature07061

Klempír, J., Klempírová, O., Stochl, J., Spacková, N., & Roth, J. (2009). The relationship between impairment of voluntary movements and cognitive impairment in Huntington's disease. *Journal of neurology*, *256*(10), 1629–1633. doi:10.1007/s00415-009-5164-9

Koh, S.-H., Kim, K. S., Choi, M. R., Jung, K. H., Park, K. S., Chai, Y. G., … Kim, S. H. (2008). Implantation of human umbilical cord-derived mesenchymal stem cells as a neuroprotective therapy for ischemic stroke in rats. *Brain research*, *1229*, 233–248. doi:10.1016/j.brainres.2008.06.087

Kopen, G. C., Prockop, D. J., & Phinney, D. G. (1999). Marrow stromal cells migrate throughout forebrain and cerebellum, and they differentiate into astrocytes after injection into neonatal mouse brains. *Proceedings of the National Academy of Sciences of the United States of America*, *96*(19), 10711–10716.

Kopyov, O. V., Jacques, S., Lieberman, A., Duma, C. M., & Eagle, K. S. (1998). Safety of intrastriatal neurotransplantation for Huntington's disease patients. *Experimental neurology*, *149*(1), 97–108. doi:10.1006/exnr.1997.6685

Kordower, J H, Chen, E. Y., Winkler, C., Fricker, R., Charles, V., Messing, A., … Carpenter, M. K. (1997). Grafts of EGF-responsive neural stem cells derived from GFAP-hNGF transgenic mice: trophic and tropic effects in a rodent model of Huntington's disease. *The Journal of comparative neurology*, *387*(1), 96–113.

Kordower, Jeffrey H, Dodiya, H. B., Kordower, A. M., Terpstra, B., Paumier, K., Madhavan, L., … Collier, T. J. (2011). Transfer of host-derived α synuclein to grafted dopaminergic neurons in rat. *Neurobiology of disease*, *43*(3), 552–557. doi:10.1016/j.nbd.2011.05.001

Krystkowiak, P., Gaura, V., Labalette, M., Rialland, A., Remy, P., Peschanski, M., & Bachoud-Lévi, A.-C. (2007). Alloimmunisation to donor antigens and immune rejection following foetal neural grafts to the brain in patients with Huntington's disease. *PloS one*, *2*(1), e166. doi:10.1371/journal.pone.0000166

Kumar, P., & Kumar, A. (2009). Neuroprotective effect of cyclosporine and FK506 against 3-nitropropionic acid induced cognitive dysfunction and glutathione redox in rat: possible role of nitric oxide. *Neuroscience research*, *63*(4), 302–314.

Kurtzberg, J., Lyerly, A. D., & Sugarman, J. (2005). Untying the Gordian knot: policies, practices, and ethical issues related to banking of umbilical cord blood. *The Journal of clinical investigation*, *115*(10), 2592–2597. doi:10.1172/JCI26690

Labandeira-Garcia, J. L., Wictorin, K., Cunningham, E. T., Jr, & Björklund, A. (1991). Development of intrastriatal striatal grafts and their afferent innervation from the host. *Neuroscience*, *42*(2), 407–426.

Lalonde, R., & Strazielle, C. (2011). Brain regions and genes affecting limb-clasping responses. *Brain research reviews*, *67*(1-2), 252–259. doi:10.1016/j.brainresrev.2011.02.005

Laughlin, M. J., Barker, J., Bambach, B., Koc, O. N., Rizzieri, D. A., Wagner, J. E., … Kurtzberg, J. (2001). Hematopoietic engraftment and survival in adult recipients of umbilical-cord blood from unrelated donors. *The New England journal of medicine, 344*(24), 1815–1822. doi:10.1056/NEJM200106143442402

Lee, C. Y. D., Cantle, J. P., & Yang, X. W. (2013). Genetic manipulations of mutant huntingtin in mice: new insights into Huntington's disease pathogenesis. *The FEBS journal, 280*(18), 4382–4394. doi:10.1111/febs.12418

Lee, J., Hwang, Y. J., Kim, K. Y., Kowall, N. W., & Ryu, H. (2013). Epigenetic Mechanisms of Neurodegeneration in Huntington's Disease. *Neurotherapeutics: the journal of the American Society for Experimental NeuroTherapeutics*. doi:10.1007/s13311-013-0206-5

Lee, J. S., Hong, J. M., Moon, G. J., Lee, P. H., Ahn, Y. H., Bang, O. Y., & STARTING collaborators. (2010). A long-term follow-up study of intravenous autologous mesenchymal stem cell transplantation in patients with ischemic stroke. *Stem cells (Dayton, Ohio), 28*(6), 1099–1106. doi:10.1002/stem.430

Lee, S.-T., Chu, K., Jung, K.-H., Im, W.-S., Park, J.-E., Lim, H.-C., … Roh, J.-K. (2009). Slowed progression in models of Huntington disease by adipose stem cell transplantation. *Annals of neurology, 66*(5), 671–681. doi:10.1002/ana.21788

Lee, S.-T., Chu, K., Park, J.-E., Lee, K., Kang, L., Kim, S. U., & Kim, M. (2005). Intravenous administration of human neural stem cells induces functional recovery in Huntington's disease rat model. *Neuroscience research, 52*(3), 243–249. doi:10.1016/j.neures.2005.03.016

Lee, S.-T., Park, J.-E., Lee, K., Kang, L., Chu, K., Kim, S. U., … Roh, J.-K. (2006). Noninvasive method of immortalized neural stem-like cell transplantation in an experimental model of Huntington's disease. *Journal of neuroscience methods, 152*(1-2), 250–254. doi:10.1016/j.jneumeth.2005.09.013

Lee, Y.-H., Choi, K. V., Moon, J. H., Jun, H.-J., Kang, H.-R., Oh, S.-I., … Yang, Y.-S. (2012). Safety and feasibility of countering neurological impairment by intravenous administration of autologous cord blood in cerebral palsy. *Journal of translational medicine, 10*, 58. doi:10.1186/1479-5876-10-58

Lennon, D. P., Schluchter, M. D., & Caplan, A. I. (2012). The effect of extended first passage culture on the proliferation and differentiation of human marrow-derived mesenchymal stem cells. *Stem cells translational medicine, 1*(4), 279–288. doi:10.5966/sctm.2011-0011

Lescaudron, L., Boyer, C., Bonnamain, V., Fink, K. D., Lévêque, X., Rossignol, J., … Dunbar, G. L. (2012). Assessing the potential clinical utility of transplantations of neural and mesenchymal stem cells for treating neurodegenerative diseases. *Methods in molecular biology (Clifton, N.J.), 879*, 147–164. doi:10.1007/978-1-61779-815-3_10

Lescaudron, L., Unni, D., & Dunbar, G. L. (2003). Autologous adult bone marrow stem cell transplantation in an animal model of huntington's disease: behavioral and morphological outcomes. *The International journal of neuroscience*, *113*(7), 945–956. doi:DOI: 10.1080/00207450390207759

Li, W., Wei, W., Zhu, S., Zhu, J., Shi, Y., Lin, T., … Ding, S. (2009). Generation of rat and human induced pluripotent stem cells by combining genetic reprogramming and chemical inhibitors. *Cell stem cell*, *4*(1), 16–19. doi:10.1016/j.stem.2008.11.014

Li, X.-Y., Ding, J., Zheng, Z.-H., Li, X.-Y., Wu, Z.-B., & Zhu, P. (2012). Long-term culture in vitro impairs the immunosuppressive activity of mesenchymal stem cells on T cells. *Molecular medicine reports*, *6*(5), 1183–1189. doi:10.3892/mmr.2012.1039

Lim, H.-C., Lee, S.-T., Chu, K., Joo, K. M., Kang, L., Im, W.-S., … Cha, C.-I. (2008). Neuroprotective effect of neural stem cell-conditioned media in in vitro model of Huntington's disease. *Neuroscience letters*, *435*(3), 175–180. doi:10.1016/j.neulet.2008.02.035

Lin, C. H., Tallaksen-Greene, S., Chien, W. M., Cearley, J. A., Jackson, W. S., Crouse, A. B., … Detloff, P. J. (2001). Neurological abnormalities in a knock-in mouse model of Huntington's disease. *Human molecular genetics*, *10*(2), 137–144.

Lin, Y.-T., Chern, Y., Shen, C.-K. J., Wen, H.-L., Chang, Y.-C., Li, H., … Hsieh-Li, H. M. (2011). Human mesenchymal stem cells prolong survival and ameliorate motor deficit through trophic support in Huntington's disease mouse models. *PloS one*, *6*(8), e22924. doi:10.1371/journal.pone.0022924

Lindvall, O., Barker, R. A., Brüstle, O., Isacson, O., & Svendsen, C. N. (2012). Clinical translation of stem cells in neurodegenerative disorders. *Cell stem cell*, *10*(2), 151–155. doi:10.1016/j.stem.2012.01.009

Lister, R., Pelizzola, M., Kida, Y. S., Hawkins, R. D., Nery, J. R., Hon, G., … Ecker, J. R. (2011). Hotspots of aberrant epigenomic reprogramming in human induced pluripotent stem cells. *Nature*, *471*(7336), 68–73. doi:10.1038/nature09798

Lorincz, M. T., Detloff, P. J., Albin, R. L., & O'Shea, K. S. (2004). Embryonic stem cells expressing expanded CAG repeats undergo aberrant neuronal differentiation and have persistent Oct-4 and REST/NRSF expression. *Molecular and cellular neurosciences*, *26*(1), 135–143. doi:10.1016/j.mcn.2004.01.016

Lowry, W. E., Richter, L., Yachechko, R., Pyle, A. D., Tchieu, J., Sridharan, R., … Plath, K. (2008). Generation of human induced pluripotent stem cells from dermal fibroblasts. *Proceedings of the National Academy of Sciences of the United States of America*, *105*(8), 2883–2888. doi:10.1073/pnas.0711983105

Lukács, A., Szabó, A., Papp, A., & Vezér, T. (2009). Altered open field behavior in rats induced by acute administration of 3-nitropropionic acid: possible glutamatergic and dopaminergic involvement. *Acta biologica Hungarica*, *60*(4), 359–367. doi:10.1556/ABiol.60.2009.4.3

Ma, L., Hu, B., Liu, Y., Vermilyea, S. C., Liu, H., Gao, L., … Zhang, S.-C. (2012). Human embryonic stem cell-derived GABA neurons correct locomotion deficits in quinolinic acid-lesioned mice. *Cell stem cell*, *10*(4), 455–464. doi:10.1016/j.stem.2012.01.021

Ma, L., Liu, Y., & Zhang, S.-C. (2011). Directed differentiation of dopamine neurons from human pluripotent stem cells. *Methods in molecular biology (Clifton, N.J.)*, *767*, 411–418. doi:10.1007/978-1-61779-201-4_30

Madhavan, L., & Collier, T. J. (2010). A synergistic approach for neural repair: cell transplantation and induction of endogenous precursor cell activity. *Neuropharmacology*, *58*(6), 835–844. doi:10.1016/j.neuropharm.2009.10.005

Madhavan, L., Daley, B. F., Paumier, K. L., & Collier, T. J. (2009). Transplantation of subventricular zone neural precursors induces an endogenous precursor cell response in a rat model of Parkinson's disease. *The Journal of comparative neurology*, *515*(1), 102–115. doi:10.1002/cne.22033

Madhavan, L., Daley, B. F., Sortwell, C. E., & Collier, T. J. (2012). Endogenous neural precursors influence grafted neural stem cells and contribute to neuroprotection in the parkinsonian rat. *The European journal of neuroscience*, *35*(6), 883–895. doi:10.1111/j.1460-9568.2012.08019.x

Madrazo, I., Franco-Bourland, R. E., Castrejon, H., Cuevas, C., & Ostrosky-Solis, F. (1995). Fetal striatal homotransplantation for Huntington's disease: first two case reports. *Neurological research*, *17*(4), 312–315.

Manca, M. F., Zwart, I., Beo, J., Palasingham, R., Jen, L.-S., Navarrete, R., … Navarrete, C. V. (2008). Characterization of mesenchymal stromal cells derived from full-term umbilical cord blood. *Cytotherapy*, *10*(1), 54–68. doi:10.1080/14653240701732763

Mathews, D. J. H., Sugarman, J., Bok, H., Blass, D. M., Coyle, J. T., Duggan, P., … Faden, R. (2008). Cell-based interventions for neurologic conditions: ethical challenges for early human trials. *Neurology*, *71*(4), 288–293. doi:10.1212/01.wnl.0000316436.13659.80

McBride, J. L., Behrstock, S. P., Chen, E.-Y., Jakel, R. J., Siegel, I., Svendsen, C. N., & Kordower, J. H. (2004). Human neural stem cell transplants improve motor function in a rat model of Huntington's disease. *The Journal of comparative neurology*, *475*(2), 211–219. doi:10.1002/cne.20176

McBride, J. L., Ramaswamy, S., Gasmi, M., Bartus, R. T., Herzog, C. D., Brandon, E. P., … Kordower, J. H. (2006). Viral delivery of glial cell line-derived neurotrophic factor improves behavior and protects striatal neurons in a mouse model of Huntington's disease. *Proceedings of the National Academy of Sciences of the United States of America*, *103*(24), 9345–9350. doi:10.1073/pnas.0508875103

Medicetty, S., Bledsoe, A. R., Fahrenholtz, C. B., Troyer, D., & Weiss, M. L. (2004). Transplantation of pig stem cells into rat brain: proliferation during the first 8 weeks. *Experimental neurology*, *190*(1), 32–41. doi:10.1016/j.expneurol.2004.06.023

Meyerrose, T., Olson, S., Pontow, S., Kalomoiris, S., Yunjoon Jung, Annett, G., … Nolta, J. A. (2010). Mesenchymal stem cells for the sustained in vivo delivery of bioactive factors. *Advanced drug delivery reviews*, *62*(12), 1167–1174. doi:10.1016/j.addr.2010.09.013

Mezey, E., Chandross, K. J., Harta, G., Maki, R. A., & McKercher, S. R. (2000). Turning blood into brain: cells bearing neuronal antigens generated in vivo from bone marrow. *Science (New York, N.Y.)*, *290*(5497), 1779–1782.

Mitchell, K. E., Weiss, M. L., Mitchell, B. M., Martin, P., Davis, D., Morales, L., … Medicetty, S. (2003). Matrix cells from Wharton's jelly form neurons and glia. *Stem cells (Dayton, Ohio)*, *21*(1), 50–60. doi:10.1634/stemcells.21-1-50

Moraes, L., Vasconcelos-dos-Santos, A., Santana, F. C., Godoy, M. A., Rosado-de-Castro, P. H., Jasmin, … Mendez-Otero, R. (2012). Neuroprotective effects and magnetic resonance imaging of mesenchymal stem cells labeled with SPION in a rat model of Huntington's disease. *Stem cell research*, *9*(2), 143–155. doi:10.1016/j.scr.2012.05.005

Morton, A. J., Hunt, M. J., Hodges, A. K., Lewis, P. D., Redfern, A. J., Dunnett, S. B., & Jones, L. (2005). A combination drug therapy improves cognition and reverses gene expression changes in a mouse model of Huntington's disease. *The European journal of neuroscience*, *21*(4), 855–870. doi:10.1111/j.1460-9568.2005.03895.x

Muñoz-Elias, G., Marcus, A. J., Coyne, T. M., Woodbury, D., & Black, I. B. (2004). Adult bone marrow stromal cells in the embryonic brain: engraftment, migration, differentiation, and long-term survival. *The Journal of neuroscience: the official journal of the Society for Neuroscience*, *24*(19), 4585–4595. doi:10.1523/JNEUROSCI.5060-03.2004

Murphy, K. P., Carter, R. J., Lione, L. A., Mangiarini, L., Mahal, A., Bates, G. P., … Morton, A. J. (2000). Abnormal synaptic plasticity and impaired spatial cognition in mice transgenic for exon 1 of the human Huntington's disease mutation. *The Journal of neuroscience: the official journal of the Society for Neuroscience*, *20*(13), 5115–5123.

Nadeau, S., & Rivest, S. (1999). Regulation of the gene encoding tumor necrosis factor alpha (TNF-alpha) in the rat brain and pituitary in response in different models of systemic immune challenge. *Journal of neuropathology and experimental neurology*, *58*(1), 61–77.

Nakagawa, M., Koyanagi, M., Tanabe, K., Takahashi, K., Ichisaka, T., Aoi, T., … Yamanaka, S. (2008). Generation of induced pluripotent stem cells without Myc from mouse and human fibroblasts. *Nature biotechnology*, *26*(1), 101–106. doi:10.1038/nbt1374

Nguyen, H. P., Kobbe, P., Rahne, H., Wörpel, T., Jäger, B., Stephan, M., … von Hörsten, S. (2006). Behavioral abnormalities precede neuropathological markers in rats transgenic for Huntington's disease. *Human molecular genetics*, *15*(21), 3177–3194. doi:10.1093/hmg/ddl394

Nguyen, T. H., Bellodi-Privato, M., Aubert, D., Pichard, V., Myara, A., Trono, D., & Ferry, N. (2005). Therapeutic lentivirus-mediated neonatal in vivo gene therapy in hyperbilirubinemic Gunn rats. *Molecular therapy: the journal of the American Society of Gene Therapy*, *12*(5), 852–859. doi:10.1016/j.ymthe.2005.06.482

Nicoleau, C., Viegas, P., Peschanski, M., & Perrier, A. L. (2011). Human pluripotent stem cell therapy for Huntington's disease: technical, immunological, and safety challenges human pluripotent stem cell therapy for Huntington's disease: technical, immunological, and safety challenges. *Neurotherapeutics: the journal of the American Society for Experimental NeuroTherapeutics*, *8*(4), 562–576. doi:10.1007/s13311-011-0079-4

Niibe, K., Kawamura, Y., Araki, D., Morikawa, S., Miura, K., Suzuki, S., … Matsuzaki, Y. (2011). Purified mesenchymal stem cells are an efficient source for iPS cell induction. *PloS one*, *6*(3), e17610. doi:10.1371/journal.pone.0017610

Nussbaum, J., Minami, E., Laflamme, M. A., Virag, J. A. I., Ware, C. B., Masino, A., … Murry, C. E. (2007). Transplantation of undifferentiated murine embryonic stem cells in the heart: teratoma formation and immune response. *FASEB journal: official publication of the Federation of American Societies for Experimental Biology*, *21*(7), 1345–1357. doi:10.1096/fj.06-6769com

O'Keeffe, G. C., Michell, A. W., & Barker, R. A. (2009). Biomarkers in Huntington's and Parkinson's Disease. *Annals of the New York Academy of Sciences*, *1180*, 97–110. doi:10.1111/j.1749-6632.2009.04943.x

Ohnuki, M., Takahashi, K., & Yamanaka, S. (2009). Generation and characterization of human induced pluripotent stem cells. *Current protocols in stem cell biology*, *Chapter 4*, Unit 4A.2. doi:10.1002/9780470151808.sc04a02s9

Okano, H., Nakamura, M., Yoshida, K., Okada, Y., Tsuji, O., Nori, S., … Miura, K. (2013). Steps toward safe cell therapy using induced pluripotent stem cells. *Circulation research*, *112*(3), 523–533. doi:10.1161/CIRCRESAHA.111.256149

Okita, K., Ichisaka, T., & Yamanaka, S. (2007). Generation of germline-competent induced pluripotent stem cells. *Nature*, *448*(7151), 313–317. doi:10.1038/nature05934

Okita, K., Nakagawa, M., Hyenjong, H., Ichisaka, T., & Yamanaka, S. (2008). Generation of mouse induced pluripotent stem cells without viral vectors. *Science (New York, N.Y.)*, *322*(5903), 949–953. doi:10.1126/science.1164270

Olson, S. D., Kambal, A., Pollock, K., Mitchell, G.-M., Stewart, H., Kalomoiris, S., … Nolta, J. A. (2012). Examination of mesenchymal stem cell-mediated RNAi transfer to Huntington's disease affected neuronal cells for reduction of huntingtin. *Molecular and cellular neurosciences*, *49*(3), 271–281. doi:10.1016/j.mcn.2011.12.001

Pearl, J. I., Kean, L. S., Davis, M. M., & Wu, J. C. (2012). Pluripotent stem cells: immune to the immune system? *Science translational medicine*, *4*(164), 164ps25. doi:10.1126/scitranslmed.3005090

Perry, G. M., Tallaksen-Greene, S., Kumar, A., Heng, M. Y., Kneynsberg, A., van Groen, T., … Lesort, M. (2010). Mitochondrial calcium uptake capacity as a therapeutic target in the R6/2 mouse model of Huntington's disease. *Human molecular genetics*, *19*(17), 3354–3371. doi:10.1093/hmg/ddq247

Philpott, L. M., Kopyov, O. V., Lee, A. J., Jacques, S., Duma, C. M., Caine, S., … Eagle, K. S. (1997). Neuropsychological functioning following fetal striatal transplantation in Huntington's chorea: three case presentations. *Cell transplantation*, *6*(3), 203–212.

Pineda, J. R., Rubio, N., Akerud, P., Urbán, N., Badimon, L., Arenas, E., … Canals, J. M. (2007). Neuroprotection by GDNF-secreting stem cells in a Huntington's disease model: optical neuroimage tracking of brain-grafted cells. *Gene therapy*, *14*(2), 118–128. doi:10.1038/sj.gt.3302847

Pittenger, M. F., Mackay, A. M., Beck, S. C., Jaiswal, R. K., Douglas, R., Mosca, J. D., … Marshak, D. R. (1999). Multilineage potential of adult human mesenchymal stem cells. *Science (New York, N.Y.)*, *284*(5411), 143–147.

Powers, W. J., Videen, T. O., Markham, J., McGee-Minnich, L., Antenor-Dorsey, J. V., Hershey, T., & Perlmutter, J. S. (2007). Selective defect of in vivo glycolysis in early Huntington's disease striatum. *Proceedings of the National Academy of Sciences of the United States of America*, *104*(8), 2945–2949. doi:10.1073/pnas.0609833104

Pullicino, P. M., & Burke, W. J. (2009). Cell-based interventions for neurologic conditions: ethical challenges for early human trials. *Neurology*, *72*(19), 1709; author reply 1709. doi:10.1212/01.wnl.0000346753.90198.a6

Purves, D., Augustine, G., & Fitzpatrick, D. (2001). *Circuits within the Basal Ganglia System* (2nd ed.).

Redmond, D. E., Jr, Elsworth, J. D., Roth, R. H., Leranth, C., Collier, T. J., Blanchard, B., … Sladek, J. R., Jr. (2009). Embryonic substantia nigra grafts in the mesencephalon send neurites to the host striatum in non-human primate after overexpression of GDNF. *The Journal of comparative neurology*, *515*(1), 31–40. doi:10.1002/cne.22028

Redmond, D. E., Jr, Weiss, S., Elsworth, J. D., Roth, R. H., Wakeman, D. R., Bjugstad, K. B., … Sladek, J. R., Jr. (2010). Cellular repair in the parkinsonian nonhuman primate brain. *Rejuvenation research*, *13*(2-3), 188–194. doi:10.1089/rej.2009.0960

Rehman, J., Traktuev, D., Li, J., Merfeld-Clauss, S., Temm-Grove, C. J., Bovenkerk, J. E., … March, K. L. (2004). Secretion of angiogenic and antiapoptotic factors by human adipose stromal cells. *Circulation*, *109*(10), 1292–1298. doi:10.1161/01.CIR.0000121425.42966.F1

Reiner, A., Albin, R. L., Anderson, K. D., D'Amato, C. J., Penney, J. B., & Young, A. B. (1988). Differential loss of striatal projection neurons in Huntington disease. *Proceedings of the National Academy of Sciences of the United States of America*, *85*(15), 5733–5737.

Reuter, I., Tai, Y. F., Pavese, N., Chaudhuri, K. R., Mason, S., Polkey, C. E., … Piccini, P. (2008). Long-term clinical and positron emission tomography outcome of fetal striatal transplantation in Huntington's disease. *Journal of neurology, neurosurgery, and psychiatry*, *79*(8), 948–951. doi:10.1136/jnnp.2007.142380

Reynolds, B. A., & Weiss, S. (1992). Generation of neurons and astrocytes from isolated cells of the adult mammalian central nervous system. *Science (New York, N.Y.)*, *255*(5052), 1707–1710.

Roberts, T. J., Price, J., Williams, S. C. R., & Modo, M. (2006). Preservation of striatal tissue and behavioral function after neural stem cell transplantation in a rat model of Huntington's disease. *Neuroscience*, *139*(4), 1187–1199. doi:10.1016/j.neuroscience.2006.01.025

Ronaghi, M., Erceg, S., Moreno-Manzano, V., & Stojkovic, M. (2010). Challenges of stem cell therapy for spinal cord injury: human embryonic stem cells, endogenous neural stem cells, or induced pluripotent stem cells? *Stem cells (Dayton, Ohio)*, *28*(1), 93–99. doi:10.1002/stem.253

Roos, R. A., Pruyt, J. F., de Vries, J., & Bots, G. T. (1985). Neuronal distribution in the putamen in Huntington's disease. *Journal of neurology, neurosurgery, and psychiatry*, *48*(5), 422–425.

Rosas, H. D., Koroshetz, W. J., Jenkins, B. G., Chen, Y. I., Hayden, D. L., Beal, M. F., & Cudkowicz, M. E. (1999). Riluzole therapy in Huntington's disease (HD). *Movement disorders: official journal of the Movement Disorder Society*, *14*(2), 326–330.

Rosser, A. E., Barker, R. A., Harrower, T., Watts, C., Farrington, M., Ho, A. K., … Dunnett, S. B. (2002). Unilateral transplantation of human primary fetal tissue in four patients with Huntington's disease: NEST-UK safety report ISRCTN no 36485475. *Journal of neurology, neurosurgery, and psychiatry*, *73*(6), 678–685.

Rossignol, J., Boyer, C., Lévèque, X., Fink, K. D., Thinard, R., Blanchard, F., … Lescaudron, L. (2011). Mesenchymal stem cell transplantation and DMEM administration in a 3NP rat model of Huntington's disease: morphological and behavioral outcomes. *Behavioural brain research*, *217*(2), 369–378. doi:10.1016/j.bbr.2010.11.006

Rossignol, J., Boyer, C., Thinard, R., Remy, S., Dugast, A.-S., Dubayle, D., … Lescaudron, L. (2009). Mesenchymal stem cells induce a weak immune response in the rat striatum after allo or xenotransplantation. *Journal of cellular and molecular medicine*, *13*(8B), 2547–2558. doi:10.1111/j.1582-4934.2009.00657.x

Rossignol, J., Fink, K. D., Crane, A. T., Davis, K. K., Bombard, M. C., Clerc, S., … Dunbar, G. L. (In Review). Behavioral and Neurolopathological Sparing in the R6/2 Mouse Model of Huntington's disease following Transplantation of Bone-Marrow-Derived Mesenchymal Stem Cells is Dependent on Passage Number. *Stem Cells and Development*.

Rossignol, J., Fink, K. D., Davis, K. K., Clerc, S., Crane, A. T., Matchynski, J., … Dunbar, G. L. (In Revision). Transplants of adult mesenchymal and neural stem cells provide neuroprotection and behavioral sparing in a transgenic rat model of Huntington's disease. *Stem Cells*.

Ryu, J. K., Kim, J., Cho, S. J., Hatori, K., Nagai, A., Choi, H. B., … Kim, S. U. (2004). Proactive transplantation of human neural stem cells prevents degeneration of striatal neurons in a rat model of Huntington disease. *Neurobiology of disease*, *16*(1), 68–77. doi:10.1016/j.nbd.2004.01.016

Sadan, O, Shemesh, N., Barzilay, R., Dadon-Nahum, M., Blumenfeld-Katzir, T., Assaf, Y., … Offen, D. (2012). Mesenchymal stem cells induced to secrete neurotrophic factors attenuate quinolinic acid toxicity: a potential therapy for Huntington's disease. *Experimental neurology*, *234*(2), 417–427. doi:10.1016/j.expneurol.2011.12.045

Sadan, Ofer, Shemesh, N., Barzilay, R., Bahat-Stromza, M., Melamed, E., Cohen, Y., & Offen, D. (2008). Migration of neurotrophic factors-secreting mesenchymal stem cells toward a quinolinic acid lesion as viewed by magnetic resonance imaging. *Stem cells (Dayton, Ohio)*, *26*(10), 2542–2551. doi:10.1634/stemcells.2008-0240

Samadi, P., Boutet, A., Rymar, V. V., Rawal, K., Maheux, J., Kvann, J.-C., … Sadikot, A. F. (2013). Relationship between BDNF expression in major striatal afferents, striatum morphology and motor behavior in the R6/2 mouse model of Huntington's disease. *Genes, brain, and behavior*, *12*(1), 108–124. doi:10.1111/j.1601-183X.2012.00858.x

Sanchez-Ramos, J., Song, S., Cardozo-Pelaez, F., Hazzi, C., Stedeford, T., Willing, A., … Sanberg, P. R. (2000). Adult bone marrow stromal cells differentiate into neural cells in vitro. *Experimental neurology*, *164*(2), 247–256. doi:10.1006/exnr.2000.7389

Sari, Y. (2011). Potential drugs and methods for preventing or delaying the progression of Huntington's disease. *Recent patents on CNS drug discovery*, *6*(2), 80–90.

Sawamoto, K., Nakao, N., Kakishita, K., Ogawa, Y., Toyama, Y., Yamamoto, A., … Okano, H. (2001). Generation of dopaminergic neurons in the adult brain from mesencephalic precursor cells labeled with a nestin-GFP transgene. *The Journal of neuroscience: the official journal of the Society for Neuroscience*, *21*(11), 3895–3903.

Scott, C. (2013). Two watershed stem cell experiments: a look back. *The American journal of bioethics: AJOB*, *13*(1), 17–18. doi:10.1080/15265161.2013.747371

Semaka, A., Kay, C., Doty, C., Collins, J. A., Bijlsma, E. K., Richards, F., … Hayden, M. R. (2013). CAG size-specific risk estimates for intermediate allele repeat instability in Huntington disease. *Journal of medical genetics*, *50*(10), 696–703. doi:10.1136/jmedgenet-2013-101796

Shear, D. A., Dong, J., Haik-Creguer, K. L., Bazzett, T. J., Albin, R. L., & Dunbar, G. L. (1998). Chronic administration of quinolinic acid in the rat striatum causes spatial learning deficits in a radial arm water maze task. *Experimental neurology*, *150*(2), 305–311. doi:10.1006/exnr.1998.6767

Shear, D. A., Haik, K. L., & Dunbar, G. L. (2000). Creatine reduces 3-nitropropionic-acid-induced cognitive and motor abnormalities in rats. *Neuroreport*, *11*(9), 1833–1837.

Shin, E., Palmer, M. J., Li, M., & Fricker, R. A. (2012). GABAergic neurons from mouse embryonic stem cells possess functional properties of striatal neurons in vitro, and develop into striatal neurons in vivo in a mouse model of Huntington's disease. *Stem cell reviews*, *8*(2), 513–531. doi:10.1007/s12015-011-9290-2

Shoulson, I., & Young, A. B. (2011). Milestones in huntington disease. *Movement disorders: official journal of the Movement Disorder Society*, *26*(6), 1127–1133. doi:10.1002/mds.23685

Slow, E. J., van Raamsdonk, J., Rogers, D., Coleman, S. H., Graham, R. K., Deng, Y., … Hayden, M. R. (2003). Selective striatal neuronal loss in a YAC128 mouse model of Huntington disease. *Human molecular genetics*, *12*(13), 1555–1567.

Snyder, B. R., Chiu, A. M., Prockop, D. J., & Chan, A. W. S. (2010). Human multipotent stromal cells (MSCs) increase neurogenesis and decrease atrophy of the striatum in a transgenic mouse model for Huntington's disease. *PloS one*, *5*(2), e9347. doi:10.1371/journal.pone.0009347

Soderstrom, K. E., Meredith, G., Freeman, T. B., McGuire, S. O., Collier, T. J., Sortwell, C. E., … Steece-Collier, K. (2008). The synaptic impact of the host immune response in a parkinsonian allograft rat model: Influence on graft-derived aberrant behaviors. *Neurobiology of disease*, *32*(2), 229–242. doi:10.1016/j.nbd.2008.06.018

Soderstrom, K., O'Malley, J., Steece-Collier, K., & Kordower, J. H. (2006). Neural repair strategies for Parkinson's disease: insights from primate models. *Cell transplantation*, *15*(3), 251–265.

Sommer, C. A., Stadtfeld, M., Murphy, G. J., Hochedlinger, K., Kotton, D. N., & Mostoslavsky, G. (2009). Induced pluripotent stem cell generation using a single lentiviral stem cell cassette. *Stem cells (Dayton, Ohio)*, *27*(3), 543–549. doi:10.1634/stemcells.2008-1075

Song, J., Lee, S.-T., Kang, W., Park, J.-E., Chu, K., Lee, S., … Kim, M. (2007). Human embryonic stem cell-derived neural precursor transplants attenuate apomorphine-induced rotational behavior in rats with unilateral quinolinic acid lesions. *Neuroscience letters*, *423*(1), 58–61. doi:10.1016/j.neulet.2007.05.066

Sortwell, C. E., Collier, T. J., & Sladek, J. R., Jr. (1998). Co-grafted embryonic striatum increases the survival of grafted embryonic dopamine neurons. *The Journal of comparative neurology*, *399*(4), 530–540.

Southwell, A. L., Ko, J., & Patterson, P. H. (2009). Intrabody gene therapy ameliorates motor, cognitive, and neuropathological symptoms in multiple mouse models of Huntington's disease. *The Journal of neuroscience: the official journal of the Society for Neuroscience*, *29*(43), 13589–13602. doi:10.1523/JNEUROSCI.4286-09.2009

Spieles-Engemann, A. L., Steece-Collier, K., Behbehani, M. M., Collier, T. J., Wohlgenant, S. L., Kemp, C. J., … Sortwell, C. E. (2011). Subthalamic Nucleus Stimulation Increases Brain Derived Neurotrophic Factor in the Nigrostriatal System and Primary Motor Cortex. *Journal of Parkinson's disease*, *1*(1), 123–136.

Stadtfeld, M., Apostolou, E., Akutsu, H., Fukuda, A., Follett, P., Natesan, S., … Hochedlinger, K. (2010). Aberrant silencing of imprinted genes on chromosome 12qF1 in mouse induced pluripotent stem cells. *Nature*, *465*(7295), 175–181. doi:10.1038/nature09017

Stadtfeld, M., Nagaya, M., Utikal, J., Weir, G., & Hochedlinger, K. (2008). Induced pluripotent stem cells generated without viral integration. *Science (New York, N.Y.)*, *322*(5903), 945–949. doi:10.1126/science.1162494

Stanton, P. K., Potter, P. E., Aguilar, J., Decandia, M., & Moskal, J. R. (2009). Neuroprotection by a novel NMDAR functional glycine site partial agonist, GLYX-13. *Neuroreport*, *20*(13), 1193–1197. doi:10.1097/WNR.0b013e32832f5130

Steece-Collier, K., Collier, T. J., Danielson, P. D., Kurlan, R., Yurek, D. M., & Sladek, J. R., Jr. (2003). Embryonic mesencephalic grafts increase levodopa-induced forelimb hyperkinesia in parkinsonian rats. *Movement disorders: official journal of the Movement Disorder Society*, *18*(12), 1442–1454. doi:10.1002/mds.10588

Steece-Collier, K., Soderstrom, K. E., Collier, T. J., Sortwell, C. E., & Maries-Lad, E. (2009). Effect of levodopa priming on dopamine neuron transplant efficacy and induction of abnormal involuntary movements in parkinsonian rats. *The Journal of comparative neurology*, *515*(1), 15–30. doi:10.1002/cne.22037

Stout, J. C., Weaver, M., Solomon, A. C., Queller, S., Hui, S., Johnson, S. A., … Foroud, T. (2007). Are cognitive changes progressive in prediagnostic HD? *Cognitive and behavioral neurology: official journal of the Society for Behavioral and Cognitive Neurology*, *20*(4), 212–218. doi:10.1097/WNN.0b013e31815cfef8

Suzuki, M., Desmond, T. J., Albin, R. L., & Frey, K. A. (2001). Vesicular neurotransmitter transporters in Huntington's disease: initial observations and comparison with traditional synaptic markers. *Synapse (New York, N.Y.)*, *41*(4), 329–336. doi:10.1002/syn.1089

Tabrizi, S. J., Langbehn, D. R., Leavitt, B. R., Roos, R. A., Durr, A., Craufurd, D., … Stout, J. C. (2009). Biological and clinical manifestations of Huntington's disease in the longitudinal TRACK-HD study: cross-sectional analysis of baseline data. *Lancet neurology*, *8*(9), 791–801. doi:10.1016/S1474-4422(09)70170-X

Takahashi, K., & Yamanaka, S. (2006). Induction of pluripotent stem cells from mouse embryonic and adult fibroblast cultures by defined factors. *Cell*, *126*(4), 663–676. doi:10.1016/j.cell.2006.07.024

Tallaksen-Greene, S. J., & Albin, R. L. (2011). Treating mouse models of Huntington disease. *Neuropsychopharmacology: official publication of the American College of Neuropsychopharmacology*, *36*(12), 2373–2374. doi:10.1038/npp.2011.158

Tallaksen-Greene, S. J., Janiszewska, A., Benton, K., Hou, G., Dick, R., Brewer, G. J., & Albin, R. L. (2009). Evaluation of tetrathiomolybdate in the R6/2 model of Huntington disease. *Neuroscience letters*, *452*(1), 60–62. doi:10.1016/j.neulet.2009.01.040

Tallaksen-Greene, S. J., Janiszewska, A., Benton, K., Ruprecht, L., & Albin, R. L. (2010). Lack of efficacy of NMDA receptor-NR2B selective antagonists in the R6/2 model of Huntington disease. *Experimental neurology*, *225*(2), 402–407. doi:10.1016/j.expneurol.2010.07.015

Tan, K. Y., Eminli, S., Hettmer, S., Hochedlinger, K., & Wagers, A. J. (2011). Efficient generation of iPS cells from skeletal muscle stem cells. *PloS one*, *6*(10), e26406. doi:10.1371/journal.pone.0026406

The Huntington's Collaborative Research Group. (1993). A novel gene containing a trinucleotide repeat that is expanded and unstable on Huntington's disease chromosomes. The Huntington's Disease Collaborative Research Group. *Cell*, *72*(6), 971–983.

The Huntington's Collaborative Research Group. (2006). Tetrabenazine as antichorea therapy in Huntington disease: a randomized controlled trial. *Neurology*, *66*(3), 366–372. doi:10.1212/01.wnl.0000198586.85250.13

Túnez, I., Tasset, I., Pérez-De La Cruz, V., & Santamaría, A. (2010). 3-Nitropropionic acid as a tool to study the mechanisms involved in Huntington's disease: past, present and future.

Molecules (Basel, Switzerland), *15*(2), 878–916. doi:10.3390/molecules15020878

Van Raamsdonk, J. M., Pearson, J., Slow, E. J., Hossain, S. M., Leavitt, B. R., & Hayden, M. R. (2005). Cognitive dysfunction precedes neuropathology and motor abnormalities in the YAC128 mouse model of Huntington's disease. *The Journal of neuroscience: the official journal of the Society for Neuroscience*, *25*(16), 4169–4180. doi:10.1523/JNEUROSCI.0590-05.2005

Vazey, E. M., Chen, K., Hughes, S. M., & Connor, B. (2006). Transplanted adult neural progenitor cells survive, differentiate and reduce motor function impairment in a rodent model of Huntington's disease. *Experimental neurology*, *199*(2), 384–396. doi:10.1016/j.expneurol.2006.01.034

Velloso, N. A., Dalmolin, G. D., Gomes, G. M., Rubin, M. A., Canas, P. M., Cunha, R. A., & Mello, C. F. (2009). Spermine improves recognition memory deficit in a rodent model of Huntington's disease. *Neurobiology of learning and memory*, *92*(4), 574–580. doi:10.1016/j.nlm.2009.07.006

Venkataramana, N. K., Kumar, S. K. V., Balaraju, S., Radhakrishnan, R. C., Bansal, A., Dixit, A., … Totey, S. M. (2010). Open-labeled study of unilateral autologous bone-marrow-derived mesenchymal stem cell transplantation in Parkinson's disease. *Translational research: the journal of laboratory and clinical medicine*, *155*(2), 62–70. doi:10.1016/j.trsl.2009.07.006

Venuto, C. S., McGarry, A., Ma, Q., & Kieburtz, K. (2012). Pharmacologic approaches to the treatment of Huntington's disease. *Movement disorders: official journal of the Movement Disorder Society*, *27*(1), 31–41. doi:10.1002/mds.23953

Verfaillie, C. (2009). Pluripotent stem cells. *Transfusion clinique et biologique: journal de la Société française de transfusion sanguine*, *16*(2), 65–69. doi:10.1016/j.tracli.2009.04.006

Visnyei, K., Tatsukawa, K. J., Erickson, R. I., Simonian, S., Oknaian, N., Carmichael, S. T., & Kornblum, H. I. (2006). Neural progenitor implantation restores metabolic deficits in the brain following striatal quinolinic acid lesion. *Experimental neurology*, *197*(2), 465–474. doi:10.1016/j.expneurol.2005.10.023

Von Hörsten, S., Schmitt, I., Nguyen, H. P., Holzmann, C., Schmidt, T., Walther, T., … Riess, O. (2003). Transgenic rat model of Huntington's disease. *Human molecular genetics*, *12*(6), 617–624.

Wang, H.-S., Hung, S.-C., Peng, S.-T., Huang, C.-C., Wei, H.-M., Guo, Y.-J., … Chen, C.-C. (2004). Mesenchymal stem cells in the Wharton's jelly of the human umbilical cord. *Stem cells (Dayton, Ohio)*, *22*(7), 1330–1337. doi:10.1634/stemcells.2004-0013

Wang, M., Crisostomo, P. R., Herring, C., Meldrum, K. K., & Meldrum, D. R. (2006). Human progenitor cells from bone marrow or adipose tissue produce VEGF, HGF, and IGF-I in response to TNF by a p38 MAPK-dependent mechanism. *American journal of physiology. Regulatory*,

integrative and comparative physiology, *291*(4), R880–884. doi:10.1152/ajpregu.00280.2006

Wegner, F., Kraft, R., Busse, K., Härtig, W., Schaarschmidt, G., Schwarz, S. C., … Hevers, W. (2008). Functional and molecular analysis of GABA receptors in human midbrain-derived neural progenitor cells. *Journal of neurochemistry*, *107*(4), 1056–1069. doi:10.1111/j.1471-4159.2008.05688.x

Weiss, M. L., & Troyer, D. L. (2006). Stem cells in the umbilical cord. *Stem cell reviews*, *2*(2), 155–162. doi:10.1007/s12015-006-0022-y

Wernig, M., Lengner, C. J., Hanna, J., Lodato, M. A., Steine, E., Foreman, R., … Jaenisch, R. (2008). A drug-inducible transgenic system for direct reprogramming of multiple somatic cell types. *Nature biotechnology*, *26*(8), 916–924. doi:10.1038/nbt1483

Wernig, M., Meissner, A., Foreman, R., Brambrink, T., Ku, M., Hochedlinger, K., … Jaenisch, R. (2007). In vitro reprogramming of fibroblasts into a pluripotent ES-cell-like state. *Nature*, *448*(7151), 318–324. doi:10.1038/nature05944

Woodbury, D., Schwarz, E. J., Prockop, D. J., & Black, I. B. (2000). Adult rat and human bone marrow stromal cells differentiate into neurons. *Journal of neuroscience research*, *61*(4), 364–370.

Yamanaka, S., & Blau, H. M. (2010). Nuclear reprogramming to a pluripotent state by three approaches. *Nature*, *465*(7299), 704–712. doi:10.1038/nature09229

Yang, C.-R., & Yu, R. K. (2009). Intracerebral transplantation of neural stem cells combined with trehalose ingestion alleviates pathology in a mouse model of Huntington's disease. *Journal of neuroscience research*, *87*(1), 26–33. doi:10.1002/jnr.21817

Yu-Taeger, L., Petrasch-Parwez, E., Osmand, A. P., Redensek, A., Metzger, S., Clemens, L. E., … Nguyen, H. P. (2012). A novel BACHD transgenic rat exhibits characteristic neuropathological features of Huntington disease. *The Journal of neuroscience: the official journal of the Society for Neuroscience*, *32*(44), 15426–15438. doi:10.1523/JNEUROSCI.1148-12.2012

Zhang, L., Li, Y., Zhang, C., Chopp, M., Gosiewska, A., & Hong, K. (2011). Delayed administration of human umbilical tissue-derived cells improved neurological functional recovery in a rodent model of focal ischemia. *Stroke; a journal of cerebral circulation*, *42*(5), 1437–1444. doi:10.1161/STROKEAHA.110.593129

Zhang, Y., Yao, L., Yu, X., Ou, J., Hui, N., & Liu, S. (2012). A poor imitation of a natural process: a call to reconsider the iPSC engineering technique. *Cell cycle (Georgetown, Tex.)*, *11*(24), 4536–4544. doi:10.4161/cc.22575

Zuccato, C., Ciammola, A., Rigamonti, D., Leavitt, B. R., Goffredo, D., Conti, L., … Cattaneo,

E. (2001). Loss of huntingtin-mediated BDNF gene transcription in Huntington's disease. *Science (New York, N.Y.), 293*(5529), 493–498. doi:10.1126/science.1059581

Zuccato, C., Marullo, M., Vitali, B., Tarditi, A., Mariotti, C., Valenza, M., … Cattaneo, E. (2011). Brain-derived neurotrophic factor in patients with Huntington's disease. *PloS one*, *6*(8), e22966. doi:10.1371/journal.pone.0022966

l'université nantes angers le mans
PÔLE DE RECHERCHE ET D'ENSEIGNEMENT SUPÉRIEUR

UNIVERSITÉ DE NANTES

Thèse de Doctorat

Kyle D. FINK

Potentiel thérapeutique des cellules souches adultes pour le traitement de la maladie de Huntington
Therapeutic potential adult stem cells for the treatment of Huntington's disease

Résumé

L'objectif de ce travail de thèse dans le domaine de la Médecine Régénératrice a été d'étudier les effets d'une transplantation de 2 types de cellules souches adultes dans des deux modèles rongeurs de la maladie de Huntington. Pour se faire, des techniques de culture cellulaire et de biologie cellulaire et moléculaire ainsi que différents test comportementaux ont été mis en œuvre. Les résultats ont révélé que les cellules souches mésenchymateuses (MSCs) obtenues à partir de moelle osseuse, ou de cordon ombilical (mais dans une moindre mesure), ont permis d'améliorer les déficits comportementaux et neuropathologiques observés chez des souris transgéniques modèle de la maladie de Huntington par rapport aux animaux non traités. Cependant, les effets bénéfiques des MSCs semblent plutôt être attribués à leur sécrétion de facteurs neurotrophiques dans l'environnement lésé qu'à leur trans-différenciation neuronale. Parallèlement, l'utilisation des cellules souches pluripotentes induites (iPSCs) dans le cadre d'une intervention thérapeutique dans un modèle de lésion toxique de la maladie de Huntington (3-NP) a également été étudiée chez le rat. Ainsi, après transplantation d'iPSCs, les animaux ont présenté une amélioration comportementale et neuropathologique significative. Le mécanisme de récupération de ces animaux après transplantation d'iPSC a été, cette fois-ci, attribué à la différenciation neuronale des cellules implantées, et non à leur production de facteurs neurotrophiques. Les résultats de ces deux études suggèrent de manière encourageante que les cellules souches adultes pourraient être utilisées comme traitement de la maladie de Huntington dans le futur.

Mots clés
Maladie de Huntington, Médecine régénératrice, Transplantation, Cellule souche mésenchymateuse, Cellule souche pluripotentes induite

Abstract

The goal of this doctoral dissertation was to compare the potential therapeutic effects of transplanting various types of adult stem cells into the striata of R6/2 transgenic mice or rats given 3-nitropropionic acid (3-NP), which are commonly-used rodent models of Huntington's disease (HD). It was observed that transplants of mesenchymal stem cells (MSCs), isolated from bone-marrow and, to a more limited extent, umbilical cord blood, reduced behavioral and neuropathological deficits in R6/2 mice. It was hypothesized that these stem cell transplants exerted their beneficial effects through the release of neurotrophic factors and/or anti-inflammatory cytokines, rather than via cell replacement. In addition, it was found that intrastriatal transplants of induced pluripotent stem cells (iPSCs) reduced behavioral and neuropathological deficits in 3-NP-treated rats. In this latter study, it was observed that the iPSCs were able to differentiate into cells with region-specific neuronal phenotypes. It was hypothesized that mechanisms, other than primarily providing trophic support, may underlie the recovery observed in this second group of studies. Taken together, the results from these five studies suggest that adult stem cells hold significant therapeutic potential for reducing behavioral deficits in HD.

Key Words
Huntington's disease, Regenerative medicine, Transplantation, Mesenchymal Stem Cell, Induced Pluripotent Stem Cell

L'Université Nantes Angers Le Mans